

**Applications of mass spectrometry in natural product drug discovery for malaria:  
Targeting *Plasmodium falciparum* thioredoxin reductase**

by

Ranjith K. Munigunti

A dissertation submitted to the Graduate Faculty of  
Auburn University  
in partial fulfillment of the  
requirements for the Degree of  
Doctor of Philosophy

Auburn, Alabama  
May 5, 2013

Keywords: Chromatography, mass spectrometry, malaria,  
*Plasmodium falciparum*, thioredoxin reductase, thioredoxin

Copyright 2013 by Ranjith K. Munigunti

Approved by

Angela I. Calderón, Chair, Assistant Professor of Pharmacal Sciences  
C. Randall Clark, Professor of Pharmacal Sciences  
Jack DeRuiter, Professor of Pharmacal Sciences  
Forrest Smith, Associate Professor of Pharmacal Sciences  
Orlando Acevedo, Associate Professor of Chemistry and Biochemistry

## Abstract

Malaria is considered to be the dominant cause of death in low income countries especially in Africa. Malaria caused by *Plasmodium falciparum* is a most lethal form of the disease because of its rapid spread and the development of drug resistance. The main problem in the treatment of malaria is the emergence of drug resistant malaria parasites. Over the years/decades, natural products have been used for the treatment or prevention of number of diseases. They can serve as compounds of interest both in their natural form and as templates for synthetic modification. Nature has provided a wide variety of compounds that inspired the development of potential therapeutics such as quinine, artemisinin and lapachol as antimalarial agents. As the resistance to known antimalarials is increasing, there is a need to expand the antimalarial drug discovery efforts for new classes of molecules to combat malaria. This research work focuses on the applications of ultrafiltration, mass spectrometry and molecular modeling based approaches to identify inhibitors of *Plasmodium falciparum* thioredoxin reductase (*PfTrxR*), our main target and *Plasmodium falciparum* glutathione reductase (*PfGR*) as an alternative target for malaria drug discovery.

In our first approach, we used an ultrafiltration and liquid chromatography mass spectrometry based approach to screen one hundred and thirty three structurally diverse natural compounds to determine their binding affinity towards *PfTrxR*. Along with the set of natural products, different plant extracts were also subject to binding experiments to identify ligands of

*PfTrxR* followed by identification and structure elucidation of identified ligands using mass spectrometry.

In our second approach, we had developed an LC-MS based functional assay to identify inhibitors of *PfTrxR* by quantifying the reduced thioredoxin ( $\text{Trx}-(\text{SH})_2$ ), the product formed in the enzymatic reaction. Thioredoxin is a 11.7 kDa protein. To validate the developed functional assay we have screened reference compounds 2,4-dinitrophenyl sulfide (2,4-DNPS), 4-nitrobenzothiadiazole (4-NBT) and 3-(dimethylamino)-propiophenone (3-DAP) for their *PfTrxR* inhibitory activity and ten natural compounds (at 10 mM) which were earlier identified as ligands of *PfTrxR* by a UF-LC-MS based binding assay.

In the third approach, our goal was to identify natural products which can selectively target *Plasmodium falciparum* thioredoxin reductase (*PfTrxR*), *Plasmodium falciparum* glutathione reductase (*PfGR*) enzymes of the parasite distinct from the host enzymes. In our study, the binding affinities of natural products towards *PfTrxR*, *PfGR*, human TrxR and human GR were determined using a mass spectrometry based ligand binding assay. The *in vitro* antimalarial activity ( $\text{IC}_{50}$ ) and cytotoxicity of these ligands were also determined. *In silico* molecular modeling was used to ascertain and further confirm the binding affinities and key interactions of these ligands towards *PfTrxR*, *PfGR* and human isoforms of these enzymes.

## Acknowledgements

Firstly I want to praise and extend my thanks to God, Sai Baba for giving me strength, patience, knowledge, oppurtunities whenever needed and for guiding me through struggles to accomplish my tasks. I would like to dedicate my work to my parents, my brothers Ashok, Praveen and to Mr & Mrs. Pendyala Ravinder Reddy. It is because of their unconditional love, care, motivation and moral support; I have been able to quench my desire for higher studies.

I express my sincere gratitude to my advisor Dr. Angela Calderón, for giving me opportunity, for guiding and motivating me in accomplishing my research goals successfully. I am glad to be her first PhD student. I am especially indebted to my thesis committee members Professor Randall Clark for his support, guidance and lectures on chromatography and mass spectrometry which are invaluable, Professor Jack DeRuiter for helping me understand drug designing through his DAD courses and Dr. Forrest Smith for his outstanding lectures in organic synthesis enabled me to have strong background in synthesis which helps to pursue my career in medicinal chemistry. Thanks to the committee members for their insightful comments, hard questions and encouragement.

I want to thank Dr. Katja Becker from the Justus-Liebig University, Germany for supplying the two enzymes *PfTrxR* and *PfGR* and for testing compounds for *PfGR* inhibitory activity. I am grateful to all my collaborators Dr. Babu Tekwani from National Natural Products Research Center from the University of Mississippi, and Dr. Reto Brun from Swiss Tropical Institute of

Hygiene, Switzerland for carrying out the antimalarial and cytotoxicity assays of my compounds and their support to carry out my work and valuable scientific inputs to accomplish my research successfully. I would like to thank Dr. Orlando Acevedo from the department of Chemistry and Biochemistry from Auburn University for helping us with the docking studies and for accepting to serve as an outside reader for my dissertation. My special thanks to Dr. Carol Honey Ball, Agilent Technologies, for excellent technical assistance for intact protein analysis. I want to thank Dr. Mahabir P. Gupta for supplying the plant extracts studied in this work. I am thankful to Dr. G. V. Subbaraju, AptuitLauras, Hyderabad, India for providing us the three hispolone analogs. Thanks are also due to Symon Gathiaka, a graduate student from Dr. Acevedo's lab for carrying out the docking studies and corresponding data analysis. I would like to thank Dr. Yonnie Wu, director of MS facility at the department of chemistry and biochemistry for his valuable technical inputs on LC-MS applications.

The work was supported by start-up funding from Harrison School of Pharmacy and a Research Starter Grant from the American Society of Pharmacognosy to Dr. A. I. Calderón. I am also grateful to the Department of Pharmacal Sciences for providing me graduate assistantship which helped me to carry out my studies at Auburn University.

I am grateful also to Dr. Jayachandra Babu, Dr. Daniel Parsons, Dr. Vishnu Suppiramaniam, Dr. Murali Dhanasekaran and Dr. Rajesh Amin for extending timely help, support and guidance throughout my stay in the department.

I want to thank my lab members Dr. Vanisree Mulabagal, Johayra Simithy Williams, Cole Sterling, Nathan Reeve, Neil Tiwari, Mary Smith for their assistance and creating joyful environment in the laboratory. My time in Department of Pharmacal Sciences was made

enjoyable due to colleagues Dr. Sheriff Hammad, Dr. Karim Hafiz, Gayani, Kariharan, Kasturi, Manuj Ahuja, Wanshu Ma and faculty and staff.

My sincere thanks to Dr. Vanisree Mulabagal for her support, guidance and insights in research during my PhD. Her enthusiasm and love for research are admirable. My special thanks to Mr & Mrs. Ravi Satya, Mr & Mrs Dr. Sateesh Sathigari for their moral support, encouragement and for memorable and joyful moments we had during my stay in Auburn.

I want to extend my thanks and regards to all my friends Dr. Ramesh Pallapolu, Dr. Susilpa Bommareddy, Dr. Divya Repala, Nataraju Gokeda, Manuj Ahuja and Kavitha for making my stay in Auburn memorable, joyful and comfortable.

I would like to thank my dear friends Praveen Alugoju, Dilip Bandi, Shilpa Vootla, Kiran Kanukuntla, Dr. Preethi Vennam, Dr. Sateesh Sathigari, Ravi Satya for their unconditional love, support and encouragement.

Last but not the least, I want to thank my dearest wife Srujana, who never stopped believing in me, for her love, continuous support and patience without which I would not have accomplished this task.

## Table of Contents

Abstract .....	iii
Acknowledgements .....	iv
List of Abbreviations .....	xiv
1. Literature review .....	1
1.1 Introduction .....	1
1.2 <i>Plasmodium falciparum</i> thioredoxin reductase and glutathione reductase .....	4
1.3 Rapid resolution liquid chromatography .....	8
1.4 Quadrupole time of flight mass spectrometry .....	11
1.5 Electrospray ionization .....	14
1.6 Project rationale .....	18
1.7 Objectives of Research .....	19
1.8 References .....	22
2. Screening of natural compounds for ligands to <i>PfTrxR</i> by ultrafiltration and LC-MS based binding assay .....	26
2.1 Abstract .....	26
2.2 Introduction .....	26
2.2.1 <i>PfTrxR</i> and <i>PfGR</i> enzymes binding assay using ultrafiltration (UF) and liquid chromatography mass spectrometry .....	27
2.3 Materials and methods .....	29
2.3.1 Chemicals and enzymes .....	29
2.3.2 UF-LC-MS binding assay .....	30

2.3.3 LC-MS analysis .....	30
2.3.3.1 LC-MS analysis of ligands 1, 2, 3, 5, 6, 7, 8 and 9 in equimolar mixture of 1 $\mu$ M ..	31
2.4 Results and Discussion .....	39
2.5 Conclusions .....	45
2.6 References .....	46
3. LC-MS based identification and structure elucidation of oleamide as a ligand of <i>Plasmodium falciparum</i> thioredoxin reductase in <i>Guatteria recurvisepala</i> .....	49
3.1 Abstract.....	49
3.2 Introduction .....	50
3.2.1 Mass spectrometry for identification and structure elucidation of natural products ....	51
3.2.2 Dereplication of natural products by mass spectrometry .....	53
3.3 Materials and Methods .....	55
3.3.1 Chemicals and enzymes.....	55
3.3.2 Plant material .....	56
3.3.3 Extraction and isolation .....	57
3.4 Antiplasmodial assays .....	57
3.4.1 Antiplasmodial screening of plant extracts .....	57
3.4.2 Antiplasmodial activity and IC <sub>50</sub> value of oleamide .....	58
3.5 <i>Pf</i> TrxR enzyme binding assay using ultrafiltration (UF) and LC-MS .....	58
3.6 LC-MS and tandem MS analysis.....	59
3.7 Results and Discussion .....	60
3.8 Conclusions .....	63
3.9 References .....	64
4. Development of liquid chromatography/mass spectrometry based screening assay for <i>Pf</i> TrxR inhibitors using relative quantitation of intact thioredoxin. ....	67
4.1 Abstract.....	67

4.2 Introduction .....	68
4.2.1 Role of mass spectrometry for detection of enzyme inhibition.....	69
4.2.2 Identification and quantitation of intact proteins.....	72
4.3 Experimental.....	73
4.3.1 Chemicals and reagents .....	73
4.3.2 Functional assay .....	74
4.3.3 Sample preparation.....	75
4.3.4 Trx-(SH) <sub>2</sub> calibration curve .....	75
4.3.5 LC-MS analysis of intact thioredoxin .....	76
4.3.6 Data Analysis.....	76
4.4 Results and Discussion .....	80
4.5 Conclusions .....	84
4.6 References .....	85
5. Characterization of <i>Pf</i> TrxR inhibitors using mass spectrometry and <i>in silico</i> molecular modeling.....	88
5.1 Abstract.....	88
5.2 Introduction .....	89
5.2.1 Selective tools for identifying inhibitors of <i>Pf</i> TrxR and <i>Pf</i> GR.....	90
5.2.2 Key differences in active sites between parasite and human enzymes.....	91
5.3 Materials and Methods .....	94
5.3.1 Chemicals and enzymes.....	94
5.3.2 Protocols of experiments .....	95
5.3.2.1. <i>Pf</i> TrxR enzyme binding assay using ultrafiltration and liquid chromatography-mass spectrometry .....	95
5.3.2.2. LC-MS based <i>Pf</i> TrxR functional assay .....	95

5.3.2.3. Antiplasmodial activity and cytotoxicity against L6 cells of tested natural products .....	96
5.3.2.4. Assays for <i>in vitro</i> antimalarial activity and cytotoxicity of known <i>PfTrxR</i> inhibitors .....	97
5.3.2.5 ROS assay .....	98
5.3.2.6 Computational methods .....	99
5.3.2.7 AutoDockVina details .....	99
5.4. Results and Discussion .....	100
5.4.1. Evaluation of known inhibitors of <i>PfTrxR</i> .....	100
5.4.2 Evaluation of natural products as inhibitors of <i>PfTrxR</i> and <i>PfGR</i> .....	107
5.4.2.1 Curcumin and demethoxycurcumin (DMC).....	107
5.4.2.2 Subset of <i>PfTrxR</i> natural product ligands .....	111
5.5 Conclusions .....	114
5.7 References .....	115

## List of Figures

<b>Figure 1.1</b> Development of leads from natural products. ....	4
<b>Figure 1.2</b> A general scheme showing the various biochemical processes of antioxidant defense in <i>Plasmodium falciparum</i> .....	6
<b>Figure 1.3</b> van Deemter plot, illustrating the evolution of particle sizes over the last three decades.....	10
<b>Figure 1.4</b> Schematic diagram of the tandem QqTOF mass spectrometer. ....	14
<b>Figure 1.5</b> Schematic of the electrospray ionization process and the general MS instrument. ...	16
<b>Figure 1.6</b> Droplet production in the electrospray interface. ....	17
<b>Figure 2.1</b> Structures of active compounds screened for <i>PfTrxR</i> .....	40
<b>Figure 2.2</b> UF and LC-MS screening of equimolar mixture of compounds 1, 2, 3, 5, 6, 7, 8 and 9 incubated with 1 $\mu$ M <i>PfTrxR</i> .....	44
<b>Figure 3.1</b> Representation of the CID process in tandem mass spectrometry (MS/MS).....	53
<b>Figure 3.2</b> UF-LC-MS based binding experiment of <i>Guatteria recurvisepala</i> plant extract incubated with 1 $\mu$ M <i>PfTrxR</i> .....	61
<b>Figure 3.3</b> MS and MS/MS analysis of oleamide in plant extract and standard oleamide.....	62
<b>Figure 4.1</b> The principles of MS-based screening. ....	71
<b>Figure 4.2</b> Structures of reference compounds 1, 2 and 3.....	74
<b>Figure 4.3</b> Calibration curve of intact Trx—(SH) <sub>2</sub> .....	75
<b>Figure 4.4</b> LC-MS analysis of thioredoxin. ....	77

<b>Figure 4.5</b> Deconvoluted MS spectra of Trx-(SH) <sub>2</sub> . .....	78
<b>Figure 4.6</b> Dose response curves of compounds 1, 2, 3 and 4 tested at 0.5 $\mu$ M <i>Pf</i> TrxR. ....	79
<b>Figure 5.1</b> Superposition of <i>h</i> TrxR with <i>Pf</i> TrxR. ....	91
<b>Figure 5.2</b> <i>Pf</i> TrxR in comparison with <i>h</i> TrxR. ....	92
<b>Figure 5.3</b> Molecular surfaces of the <i>Pf</i> TrxR and <i>h</i> TrxR cavities. ....	92
<b>Figure 5.4</b> Superposition of <i>h</i> GR with <i>Pf</i> GR. ....	93
<b>Figure 5.5</b> The dimer cavity of <i>h</i> GR. ....	93
<b>Figure 5.6</b> Molecular surfaces of the <i>Pf</i> GR and <i>h</i> GR cavities. ....	93
<b>Figure 5.7</b> <i>h</i> GR inhibitors xanthene and pyocyanin docked and compared to the experimental crystal structures. ....	100
<b>Figure 5.8</b> Structures of five known inhibitors of <i>Pf</i> TrxR. ....	101
<b>Figure 5.9</b> Formation of reactive oxygen species (ROS), as indicated by increase in fluorescence .....	102
<b>Figure 5.10</b> <i>Pf</i> TrxR/MD, <i>Pf</i> TrxR/4-NBT, and <i>Pf</i> TrxR/2, 4-DNPS complexes. ....	106
<b>Figure 5.11</b> The docking pose differences of 2, 4-DNPS and 4-NBT between the <i>Pf</i> - and <i>h</i> -TrxR. ....	107
<b>Figure 5.12</b> <i>Pf</i> TrxR/DMC and –Curcumin complexes. ....	109
<b>Figure 5.13</b> Structures of curcumin and demethoxycurcumin (DMC) .....	110
<b>Figure 5.14</b> The interactions between DMC and Curcumin with <i>Pf</i> TrxR. ....	110

## List of Tables

<b>Table 2.1</b> List of one hundred and thirty-three natural products from Analyticon Discovery library tested for binding to <i>PfTrxR</i> .....	32
<b>Table 2.2</b> LC-MS conditions for detection of the one hundred and thirty-three natural products.....	37
<b>Table 2.3</b> Relative binding affinities for ligands 1-10 tested UF-LC-MS screening against <i>PfTrxR</i> .....	41
<b>Table 3.1</b> Taxonomic information on the studied plants.....	56
<b>Table 4.1</b> IC <sub>50</sub> values of compounds 1 – 4 tested in duplicates and injected in triplicates.....	79
<b>Table 4.2</b> Trx–(SH) <sub>2</sub> time course study in control experiments tested in duplicates and injected in triplicates.....	83
<b>Table 5.1</b> Antiplasmodial activity and inhibition of <i>PfTrxR</i> by known inhibitors .....	104
<b>Table 5.2</b> Comparison between computed binding affinities (kcal/mol) at the dimer interface in <i>PfTrxR</i> and experimental IC <sub>50</sub> values (μM). .....	104
<b>Table 5.3</b> Comparison between computed binding affinities (kcal/mol) at the dimer interface and experimental IC <sub>50</sub> values (μM) selectivity values in <i>PfTrxR</i> and <i>hTrxR</i> . .....	106
<b>Table 5.4</b> Antiplasmodial activity and inhibition of <i>PfTrxR</i> by curcuminoids.....	108
<b>Table 5.5</b> Comparison between predicted binding affinities and experimental IC <sub>50</sub> values of curcuminoids. ....	111
<b>Table 5.6</b> UF-LC-MS based binding affinities of natural products for <i>PfTrxR</i> and <i>PfGR</i> .....	113
<b>Table 5.7</b> <i>PfTrxR</i> and <i>PfGR</i> inhibitory and antiplasmodial activities by selected natural products.....	114

### List of Abbreviations

$\mu\text{L}$	Micro liter
$\mu\text{M}$	Micromolar
$\mu\text{g}$	Microgram
$^{\circ}\text{C}$	Degree centigrade
DNPS	Dinitrophenyl sulfide
DMC	Demethoxycurcumin
Da	Dalton
DAP	Dimethylamino propionic acid
ESI	Electrospray ionization
FA	Formic acid
GR	Glutathione reductase
LC	Liquid chromatography
LC-MS	Liquid chromatography- mass spectrometry
m	Meter
min	Minute
mL	Milliliter

MD	Menadione
MS	Mass spectrometry
NQ	Naphthaquinone
NBT	Nitrobenzothiadiazole
ppm	Part per million
<i>Pf</i>	<i>Plasmodium falciparum</i>
QTOF	Quadrupole time of flight mass spectrometry
RT	Room temperature
ROS	Reactive oxygen species
RRLC	Rapid resolution liquid chromatography
TrxR	Thioredoxin reductase
TOF	Time of flight
UF	Ultrafiltration



## 1. Literature review

### 1.1 Introduction

Malaria affected 219 million people worldwide, causing an estimated 6.6 million deaths in 2010. Ninety percent of these deaths occur in sub-Saharan Africa, mostly among children younger than age five [1]. Malaria is endemic to over 100 nations and territories in Africa, Asia, Latin America, the Middle East, and the South Pacific. It is caused by a parasite that is transferred by the bite of an infected *Anopheles* mosquito. *Plasmodium falciparum* is by far the deadliest of the four human malarial species (*Plasmodium falciparum*, *malariae*, *ovale*, and *vivax*) [2]. In addition to being the deadliest form of malaria, *P. falciparum* destroys red blood cells, which can cause acute anemia. Also adherence to cells in certain tissues may cause problems within those organs, such as the lungs, kidneys and brain. A major complication of *P. falciparum*, cerebral malaria, can lead to coma, transient or permanent neurological effects, and death [3]. With no immediate prospect of a vaccine against the disease, drugs are the only choice for therapy. Quinine, an aminoquinoline alkaloid isolated from the bark of *Cinchona* species (Rubiaceae) in 1820 by Pelletier and Caventou, is one of the oldest and most important antimalarial drugs and is still used today. For almost three centuries, this alkaloid was the sole active principle effective against *Plasmodium falciparum*, and it has been considered the prototype, after the Second World War, for the development of synthetic antimalarial drugs

belonging to the classes of 4- and 8-aminoquinolines, such as chloroquine (CQ) in 1940 and primaquine in 1952, among others. Until recently, chloroquine was the only synthetic drug used for the treatment of malaria [4]. Artemisinin (ART) also known as qinghaosu is an endoperoxide sesquiterpene lactone. It was isolated from the leaves of *Artemisia annua* L. (Asteraceae), a plant species that has been used traditionally in China for treatment of fever for several millennia [5]. The discovery and use of ART has been a valuable addition for the treatment of malaria. Many derivatives of ART such as artemether, arteether, dihydroartemisinin, artesunate, artemisone and artelinate were prepared with improved antimalarial properties, killing CQ and Sulfadoxin-Pyrimethamine-resistant parasites. ART has a disadvantage that it has poor pharmacokinetic properties including short half-life which necessitated the use of ART for seven days resulting in poor compliance. Therefore artemisinin-based combination therapies (ACTs) such as artemether-lumifantrine (Coartem), artesunate-mefloquine, artesunate-amodiaquine and artesunate-sulfadoxine/pyrimethamine have been developed as the front line treatment for malaria disease [6]. The main challenge to the effective management of diagnosed malaria cases has been, and continues to be, the development of resistance by the causative microorganisms to known antimalarials. Disease condition is alarming due to acquired resistance in the parasite against antimalarial drugs in the circulation. Resistance can be prevented, or its onset slowed considerably, by combining antimalarials with different mechanisms of action and ensuring very high cure rates through full adherence to correct dose regimens [7]. The disadvantages of this combination are its cost, adverse drug reactions and pharmacokinetic interactions of each drug. It has been found that the parasite has also developed resistance for ACTs, the current chemotherapy for malaria. As the resistance to known antimalarials is increasing, there is a need to expand the antimalarial drug discovery efforts for new classes of molecules to combat malaria.

The current demand for new pharmacophores and novel molecular targets to tackle emerging resistance to antimalarials has stimulated new interest in natural product drug discovery. Natural products represent a source of potential new pharmacophores that are needed for killing the parasite.

Medicinal plants represent an extremely rich source of potential antimalarial agents, with the antimalarial drugs quinine and artemisinin being outstanding examples of therapeutic natural products. The diversity of chemicals found in nature continues to be an important source of molecular templates in the search for novel antimalarial drugs [8]. Natural products can be viewed as an inexhaustible reservoir of molecules that can be optimized to be efficient, well tolerated, and safe to use as antimalarial drugs. Even though plant-derived natural products are used as traditional herbal remedies, most of them have not been explored for the discovery of new targets for malaria parasite [9]. For this reason, more research on new antimalarial compounds from natural products is needed to develop new therapeutic agents with novel mechanisms of action against *Plasmodium falciparum*.

However, it is noteworthy that most antimalarial compounds isolated from natural sources are usually only moderately active, or possess challenging physicochemical and biological properties, and as such represent ‘hits’ rather than actual lead drug candidates [Figure 1.1]. Plant extracts contain large numbers of different chemical constituents making it difficult to ascertain their antimalarial activity before isolation of the bioactive compounds. The conventional approach to natural product development has been the bioassay-guided fractionation of extracts derived from such material, and the subsequent isolation and characterization of pure, active compounds. A suitable tool to speed up natural product drug discovery is the application of UF-LC-MS based binding assays [10] to screen complex mixtures

from plant origins for their binding affinity towards *Plasmodium falciparum* thioredoxin reductase (*PfTrxR*) followed by MS based structure elucidation and confirmation of the identity of new ligands.

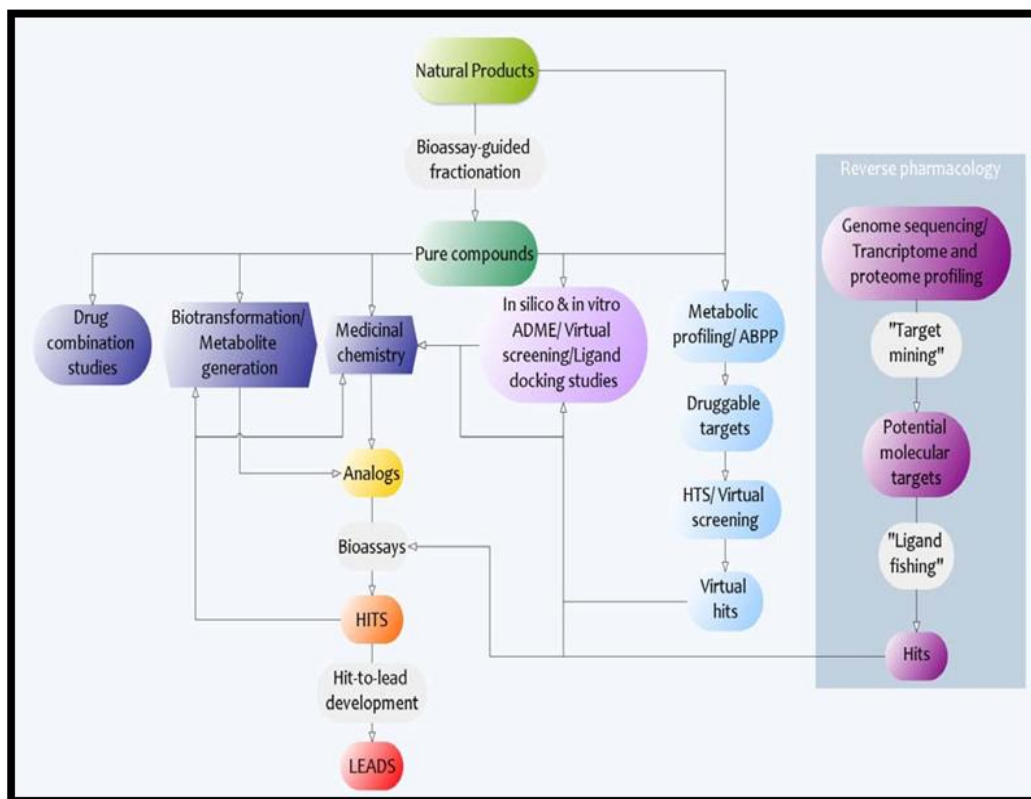


**Figure 1.1** Development of leads from natural products [7].

## 1.2 *Plasmodium falciparum* thioredoxin reductase and glutathione reductase

Malaria infection with *P. falciparum* leads to increased oxidative stress in red blood cells. This is caused by exogenous reactive oxidant species (ROS) and reactive nitrogen species (RNS) produced by the immune system of the host, and by endogenous production of ROS generated during the digestion of host cell hemoglobin and concomitant biochemical reactions [11]. Therefore the parasite requires efficient antioxidant and redox systems to protect itself from

damage caused by reactive oxygen species. In recent years, it has been shown that *P. falciparum* (*Pf*) possesses functional thiol thioredoxin (Trx) and glutathione systems [12]. Thioredoxin reductase (TrxR) and glutathione reductase (GR) are important enzymes of these redox systems that help parasites to maintain adequate intracellular redox environment. The biochemistry and molecular biology of antioxidant defense-related enzymes and intermediates are shown schematically in Figure 1.2. TrxR from *Plasmodium falciparum* (*PfTrxR*) is a homodimer with a subunit Mr of 59,000. Each monomer contains one FAD and one redox active disulfide. *PfTrxR* is a flavoprotein which belongs to a class of pyridine dinucleotide oxidoreductases, catalyzes the NADPH dependent reduction of *Plasmodium falciparum* thioredoxin (*PfTrx*) protein [13]. *PfTrx* contains two redox-active half-cystine residues in an exposed active center, having the CysGly-Pro-Cys sequence. Trx exists either in reduced form (Trx-(SH)<sub>2</sub>) with a dithiol, or in oxidized form (Trx-S<sub>2</sub>). The S-S bond of Trx-S<sub>2</sub> is reduced to Trx-(SH)<sub>2</sub> by NADPH and *PfTrxR* enzyme. Trx-(SH)<sub>2</sub> regulates the activity of *P. falciparum* by reducing the cellular environment [14]. Trx-(SH)<sub>2</sub> acts as a hydrogen donor to ribonucleotide reductase and methionine sulfoxide reductase, involved in DNA synthesis and protein repair. Trx-(SH)<sub>2</sub> can directly reduce hydrogen peroxide and can function as both single oxygen quencher and hydroxyl radical scavenger. These functions of Trx-(SH)<sub>2</sub> are in response to oxidative stress of the parasite (Figure 1.2). Despite the high degree of similarity between *PfTrxR* and the human TrxR, their primary structures present a striking difference in the C-terminus. *PfTrxR* has two cysteine residues near the C-terminal Gly, while the human TrxR contains a Cys-SeCys dipeptide penultimate to the C-terminal Gly [15].

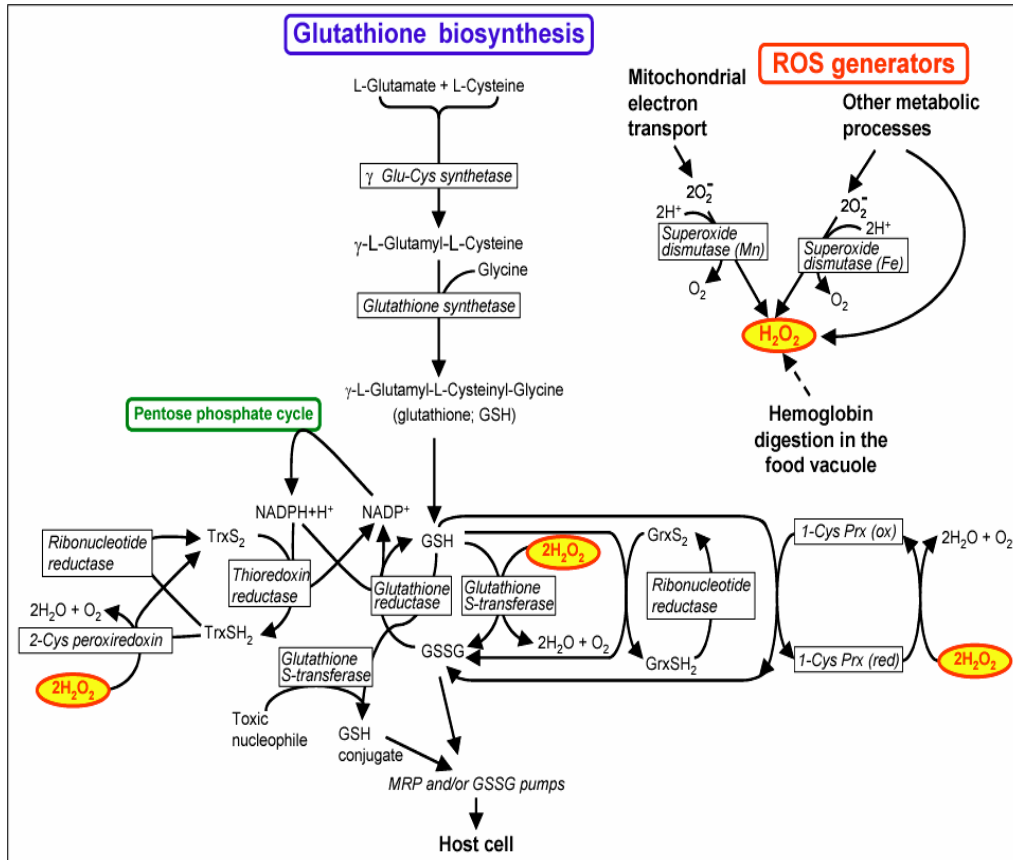


**Figure 1.2** A general scheme showing the various biochemical processes of antioxidant defense. Trx-S<sub>2</sub> and Trx-(SH)<sub>2</sub> are oxidized and reduced thioredoxin, respectively. Plasmodium falciparum glutathione reductase (*PfGR*) catalyzes the reduction of oxidized glutathione (GSSG) to reduced glutathione GSH [11].

The central enzyme of anti-oxidative defense is glutathione reductase (GR) which provides high intracellular concentrations of the reducing tripeptide glutathione by catalyzing the reaction  $GSSG + NADPH + H^+ \rightarrow 2 GSH + NADP^+$  [16]. Glutathione (gamma-glutamyl-cysteinyl-glycine or GSH) is a cysteine-containing tripeptide with reducing and nucleophilic properties which play an important role in cellular protection from oxidative damage of lipids, proteins and nucleic acids and helps in maintaining the reduced environment of the cytosol [17]. Both *P. falciparum* GR and human erythrocyte GR play crucial roles for the

intraerythrocytic growth of the parasite. Glutathione reductase (GR) is an ubiquitous flavoenzyme of disulphide reductase family catalyzing the nicotinamide adenine di-nucleotide phosphate reduced (NADPH) dependent reduction of oxidized glutathione (GSSG) to reduce glutathione, which permits glutathione to function as an intracellular reducing agent [18]. The feature distinguishing high molecular weight TrxR from GR is an additional C-terminal redox center. In contrast to glutathione reductases that specifically reduce glutathione disulfide, many high molecular weight TrxR's have a broad substrate spectrum including low molecular weight compounds as well as proteins; glutathione disulfide (GSSG) is, however, not accepted as a substrate [18]. There are three major features distinguishing *Pf*GR from human GR (hGR) that are thought to be of relevance for selective inhibitor design. The first is an insertion of 34 residues within the central domain (residues 314–347) of *Pf*GR that is known to be highly antigenic, but has an unknown effect on catalytic function. The second involves the amino acid residues lining the wall of the cavity at the dimer interface, where only nine out of 21 residues are conserved in *Pf*GR. The third difference is the pair of helices (H11/H11') at the core of the dimer interface. These helices are regarded as a dimerization and folding center of GR and it has been shown that synthetic peptides can bind to these helices to interfere with the dimerization of hGR [19].

Due to these facts the glutathione and the thioredoxin system have been considered to work independently from each other. Antioxidant enzymes (*Pf*TrxR and *Pf*GR) are essential for the survival of *Plasmodium* parasites for combating the intraerythrocytic oxidative stress. Recent genetic manipulations carried out by Krnajski et al. (2002) have revealed that TrxR is essential for the survival of *P. falciparum*, making it an attractive target for the development of new drugs against malaria. The fact that *Pf*TrxR is essential for the survival of erythrocytic stages of

parasites was demonstrated in knock-out experiments where no parasite with a disrupted *trxR* gene was viable [20]. It has also been reported that *P. falciparum*-infected erythrocytes contain higher GR activity compared to normal erythrocytes, which indicates that GR is highly expressed in parasite infected cells and is essential for its defence mechanism [21]. Disruption of these enzymes is a feasible way to interfere with the erythrocytic development of malaria parasites.

### **1.3 Rapid resolution liquid chromatography**

Chromatography is the most powerful technique available to analytical chemists in which components to be separated are selectively distributed between stationary phase and mobile phase. Liquid chromatography is particularly suitable for separation of compounds having high polarity, high molecular weight, thermal instability and those which can be ionized in solution. The stationary phase used to separate the components is generally a reversed phase column composed of non-polar aliphatic hydrocarbon chains bonded to the silica. Mobile phase which flow through the stationary phase is a polar aqueous solvent or aqueous solvent mixtures such as methanol/water and acetonitrile/water mixtures. Most commonly used bonded phases in reverse phase liquid chromatography are C4, C8 and C18 with respective aliphatic chains attached to silica. The C18 phases are mainly used to separate relatively low molecular weight components whereas the C4 phases are used for separation of biomolecules [22]. These columns are used repeatedly; the sample is injected directly by a syringe or a valve onto the column. The separated solutes are detected as they emerge from the column by a detector and the signal is recorded to give a chromatographic separation.

Rapid resolution liquid chromatography (RRLC) has been introduced as both very efficient and a fast tool for complex sample analysis. RRLC is a new separation technique which uses small particles (sub-2 micron) packed into a short column with increased speed, sensitivity and resolution. Higher flow rates can be used in RRLC. Recently, RRLC has become a routine analysis method in the pharmaceutical industry.

Short rapid resolution HT (RRHT) columns can be used for two main reasons: (1) to dramatically reduce analysis time by increasing the flow rate without losing separation performance, and (2) to achieve higher efficiency and therefore higher resolution, which is required for the separation of complex samples [22]. The performance of a column can be measured in terms of the height equivalent to the theoretical plates (HETP or H) which is calculated from the column length (L) and the column efficiency, or number of theoretical plates (N). N is calculated from an analyte's retention time ( $t_R$ ) and the standard deviation of the peak ( $\sigma$ ).

$$H = L/N \quad \text{Equation 1}$$

$$N = (t_R/\sigma)^2 \quad \text{Equation 2}$$

The van Deemter equation (Equation 3) is the empirical formula that describes the relationship between linear flow velocity ( $\mu$ ) and column efficiency, where A, B, and C are constants related to the mechanistic components of dispersion.

$$H = L/N = A + B/\mu + C\mu \quad \text{Equation 3}$$

According to the van Deemter plot (Figure 1.3), column efficiency is inversely proportional to the particle size (dp) (Equation 4), so by decreasing the particle size there is an increase in

efficiency. Since resolution is proportional to the square root of  $N$  (Equation 5), decreasing particle size increases resolution.

$$N \propto 1/d_p \quad \text{Equation 4}$$

$$R = \sqrt{N/4(\alpha-1/\alpha)(k/k+1)} \quad \text{Equation 5}$$

Also, by using smaller particles, analysis time can be decreased without sacrificing resolution, because as particle size decreases, column length can also be reduced proportionally to keep column efficiency constant. By using the same HPLC mobile phase and flow rate, RRLC reduces peak width and produced taller peaks which increased the S/N 1.8 to 8 fold, improving both sensitivity and resolution. Also according to the van Deemter plot, use of particles smaller than 2  $\mu\text{m}$  produces no loss in column efficiency with increasing flow rates [24]. However, by increasing flow rates to decrease analysis time, there is a corresponding increase in system pressure. A binary pump is used to push the solvent or mobile phase through the stationary phase at high pressure and at a controlled flow rate.

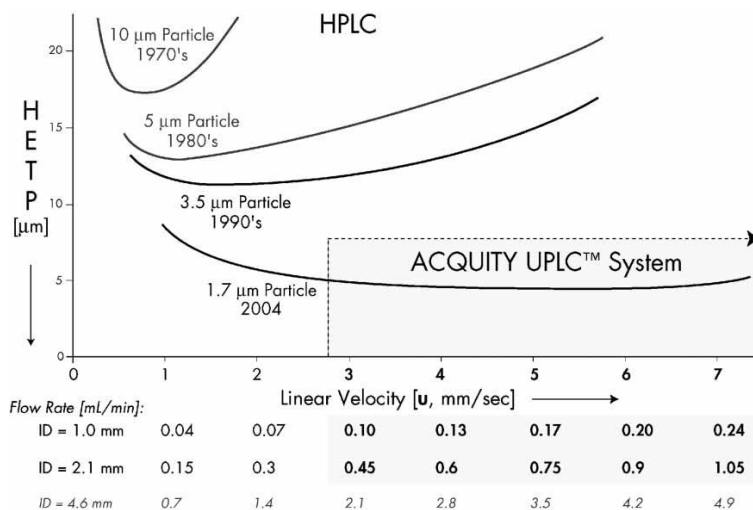


**Figure 1.3** van Deemter plot, illustrating the evolution of particle sizes over the last three decades [24].

#### 1.4 Quadrupole Time of Flight Mass spectrometry

Mass spectrometry has emerged as a popular technique for the analysis of organic compounds and biologics. Mass spectrometers employ distinct types of mass analyzers such as quadrupole, ion trap, time-of-flight (TOF), Fourier transform ion cyclotron resonance and orbitrap each of which provides unique features capable to identify, quantify, and resolve ambiguities by selecting appropriate ionization and acquisition parameters. These mass analyzers differ from each other in resolution, mass accuracy and speed at which they produce mass spectra but possess specific analytical advantage.

Quadrupole mass analyzers are widely used mass spectrometers as they are easy to use and calibrate. The drawback of these mass analyzers is that they work at unit resolution and lack the accuracy in discriminating the large amounts of co-extracted compounds in the case of complex mixture analysis. As a result the quantitative response is affected and confirmation cannot be assured. Quadrupole MS has low sensitivity in full scan mode therefore its identification capabilities are very low [25]. However, novel hybrid instruments with different mass analyzers have rapidly been embraced by the analytical community as powerful and robust instruments due to their higher sensitivity, mass accuracy and mass resolution. Recently, a hybrid Q-TOF mass spectrometer was successfully applied for comprehensive analysis of natural products. Contrary to quadrupole mass spectrometers which only allow the acquisition of a single precursor ion scan at the time, Q-TOF mass spectrometers can acquire a virtually unlimited number of precursor ion spectra due to the TOF analyzer. The selectivity of precursor ion scans is very high on Q-TOF

instruments because the high resolving power of the reflectron-TOF mass analyzers provides high accuracy fragment ions without compromising sensitivity [26].

The basic components of the Q-TOF mass spectrometers are (a) quadrupole mass analyzers, (b) a reflecting TOF analyzer, and (c) a multiple anode detector combined with multichannel time-to-digital converters which are aligned consecutively (Figure 1.4). The configuration of the mass analyzers can be regarded as the replacement of the third quadrupole mass analyzer in a triple quadrupole mass spectrometer by a TOF analyzer. The three quadrupoles of the Q-TOF MS perform different functions from each other. The first quadrupole ( $Q_0$ ) serves to focus and transfer ions originating from the ion source, the second ( $Q_1$ ) is a mass filter quadrupole that can separate ions, and the third quadrupole ( $Q_2$ ) function as a collision cell where ions can be fragmented by collision-induced dissociation through collision with neutral gas molecules (i.e.  $N_2$  or Ar). Ions entering from  $Q_2$  are detected in the TOF analyzer. The basic components of the TOF analyzer are an ion accelerator, an ion mirror, and the ion detector. The ion accelerator serves to accelerate ions, which are then separated in the drift tube based on difference in velocity. The ion reflector functions to reverse the direction of the ion. This instrumental feature improves the mass resolution by reducing variation in the kinetic energy ions pulsed out of the ion accelerator. The Q-TOF mass spectrometer can be operated in three acquisition modes: (i) TOF mass spectrometry (TOF MS) mode, (ii) tandem mass spectrometry (MS/MS) mode, and (iii) product ion scan (PIS) mode [27].

In TOF MS mode, the mass filter quadrupole ( $Q_1$ ) is operated as a transmission element, i.e. all ions having a broad range of  $m/z$  are transmitted simultaneously, and the TOF analyzer records the mass spectrum. This yields a mass spectrum of all ionized molecules present in the electrosprayed solvent. The TOF MS spectrum provides information regarding molecular mass

( $m/z$ ) and number of charges of a given analyte ion. Limited information about the molecular structure of the analyte ion can be derived.

In MS/MS mode, the  $Q_1$  is operated in the mass filter mode to transmit only a precursor ion of interest within a certain mass window (typically of 1-3 Da). Precursor ions are then accelerated into the collision cell ( $Q_2$ ) where they undergo collision-induced dissociation through multiple collisions with gas molecules. Resulting product ions (and remaining precursor ions) then pass into the TOF analyzer for detection. The recorded MS/MS spectrum reflects a set of structure specific fragment ions that provide structural information about the precursor ion. Multiple reaction monitoring (MRM) and data-dependent acquisition are two additional acquisition modes based on MS/MS analysis [27]. By data-dependent acquisition an initial survey TOF MS spectrum is recorded, which is used to automatically select abundant precursor ions for subsequent MS/MS analysis. The MS/MS analysis of each selected precursor ion is performed only once during the sample acquisition, and typically requires 30 seconds for recording each MS/MS. MRM analysis allows the targeted MS/MS analysis of a defined set of precursor ions. This acquisition mode is independent of the abundance of the precursor ions detected by TOFMS, and is performed by the repeated 1 second MS/MS analysis of each of the targeted precursor ions for several minutes. Quantitative analysis of targeted precursor ions is readily performed by monitoring the intensities of fragment ions [27].

In product ion scan (PIS) mode, precursor ions that generate one or a set of specific fragment ions are detected. In this mode, the  $Q_1$  scans over a defined mass range in small steps (0.1 or 0.2 Da). Precursor ions with increasing  $m/z$  values are sequentially transmitted and accelerated into the collision cell where they undergo collision-induced dissociation. The fragment ions generated at the defined precursor  $m/z$  are transmitted into the TOF analyzer for

detection. By this technology a  $Q_1$  mass spectrum is generated that specifically shows only the precursor ions producing the monitored fragment ions. Importantly, the TOF analyzer allows a virtually unlimited number of PIS to be simultaneously recorded and monitored with high mass accuracy (0.1 Da). In comparison, conventional triple quadrupole mass spectrometers only allow the monitoring of a single fragment ion with a relatively poor mass accuracy (1 Da).

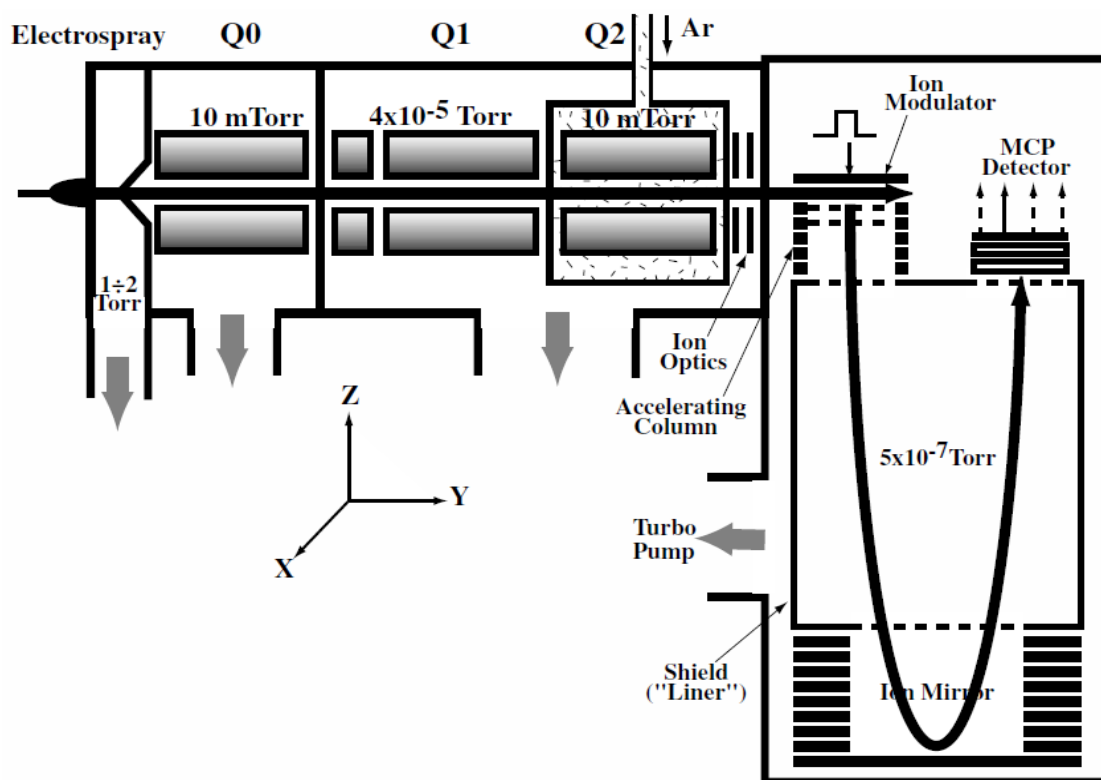


**Figure 1.4** Schematic diagram of the tandem QqTOF mass spectrometer [25].

## 1.5 Electrospray ionization

Electrospray Ionization (ESI) is an atmospheric pressure ionization (API) technique. ESI is the most widely used spray ionization technique. The introduction of electrospray has proven to

be a great tool in biochemistry, allowing the mass spectrometric characterization and sequencing of peptides, proteins and other biopolymers of great importance to human life and medicine. The ESI system is basically the interface between analyte molecules present in a sample solution and their presence as ions in the gas phase. Electrospray ionization was first presented by Dole in 1968 [28]. The basic principles of electrospray have been used in many different fields of application, such as spray painting of cars, drug delivery by inhalation and electrostatic spray deposition of pesticides on crops [29, 30]

From the 1980's and onwards, ESI has grown to become extensively used as an ion source for MS. The successful combination of ESI with MS was initially shown by Fenn and co-workers [31, 32, 33]. Fenn et al. 1989, showed that non-fragmented multiply charged ions could be generated with electrospray ionization, thereby allowing mass determination of heavy biomolecules within the range of a few thousand  $m/z$ . The soft ionization without fragmentation of the analyte molecules is a key feature for the extensive use of electrospray in the analysis of non-volatile and thermally labile bio-molecules that are not amenable to analysis by other conventional techniques [34]. Fenn shared a Nobel Prize for his work on ESI in 2002. In conventional electrospray, a conductive hollow emitter containing a solution of solvents, electrolyte ions as well as charged analyte molecules is used. The open end of the emitter is positioned facing a counter electrode containing the inlet hole of the mass spectrometer. By applying a voltage difference between the emitter and the counter electrode, an electric field is experienced by the sample solution at the tip of the emitter [35, 36]. The electric field polarizes the liquid dielectrically at the emitter tip and distribution of anions and cations is obtained. The essential features of the experimental arrangement are shown in Figure 1.5. For positive ESI mode, i.e. when the potential at the emitter tip is exceeding that of the counter electrode, positive

ions are attracted towards the counter electrode. When the applied voltage exceeds a certain threshold voltage, repulsions between the accumulated cations at the liquid surface cause the meniscus of the liquid to establish a “Taylor cone” (Figure. 1.6). At a high enough imposed field, the cone is drawn to a filament which produces positively charged droplets via a “budding” process when the surface tension is exceeded by the applied electrostatic force. The diameter of the droplets formed is influenced by a number of parameters, including the applied potential, the solution flow rate and solvent properties.

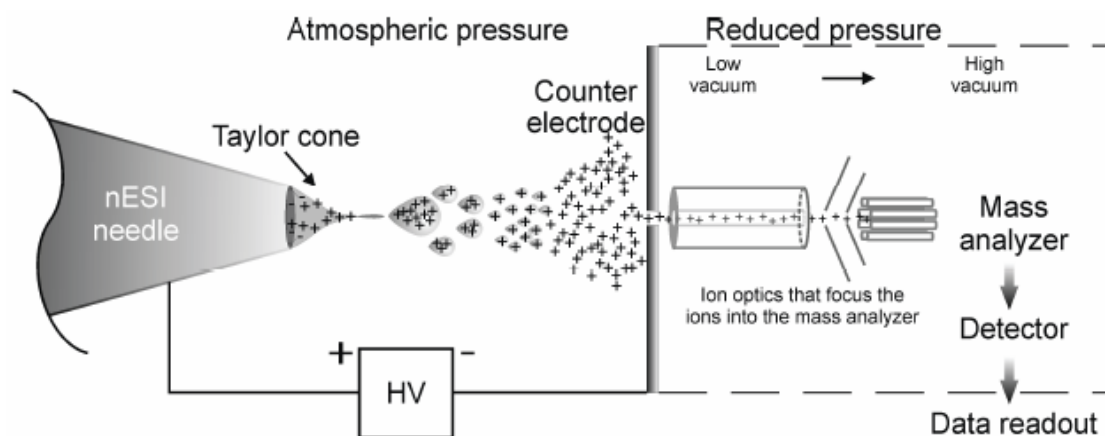


**Figure 1.5** Schematic of the electrospray ionization process and the general MS instrument [36].

Evaporation of solvent from the initially formed droplets, as they traverse a pressure gradient towards the analyzer of the mass spectrometer, leads to a reduction in diameter, with collisional warming preventing freezing. Fission (“Coulomb explosion”) will occur at the point (the “Rayleigh limit”) at which the magnitude of the charge is sufficient to overcome the surface tension holding the droplet together [37].

Finally, gas-phase ions are formed from the very small droplets. Two different models have been proposed for this process: The charged residue model (CRM) presented by Dole and the ion evaporation model (IEM) by Iribarne and Thomson [38, 39]. In the charge residue model, the gas-phase ions are suggested to be formed as a result of continuous droplet fission until each droplet only contains one excess ion (Figure 1.6). The ion evaporation model predicts that gas phase ion emission occurs directly from small droplets. The exact process of gas-phase ion formation has been studied extensively and is still under debate, but generally the IEM has been suggested to be valid for small inorganic ions and the CRM for large ions such as proteins. Disregarding the exact mechanism, the gas phase ions then traverse through the inlet hole of the MS to the mass analyzer where the ions are separated by their mass-to-charge ratio ( $m/z$ ). Subsequently, the ions are detected and the signal from the detector is then transferred to the data system for conversion into a mass spectrum, where the signal intensity versus  $m/z$  is presented.

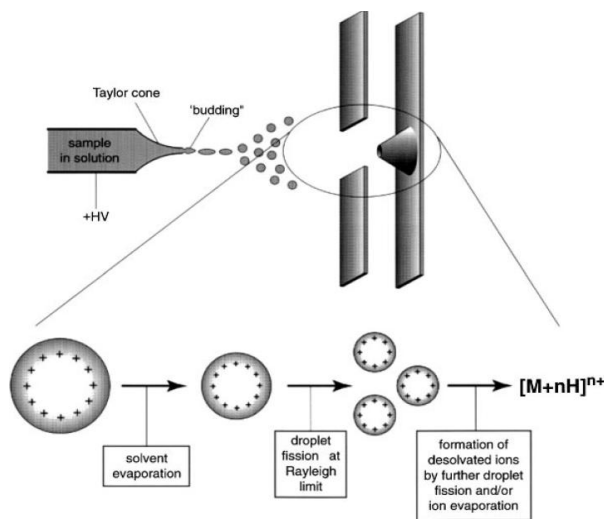


**Figure 1.6** Droplet production in the electrospray interface [36].

## 1.6 Project rationale

Malaria caused by *Plasmodium falciparum* is one of the major threats to human health in the world. This parasite has developed resistance to the majority of the most commonly used antimalarial drugs such as artemisinin combinational therapy (ACT's), chloroquine, sulfadoxin-pyrimethamine etc. Therefore there is an urgent need to identify or discover new targets in the parasite and new drug molecules with potential antimalarial activity. Although the most relevant antimalarial drugs come from natural sources, current reality is that there are no other lead molecules in natural product drug discovery for optimization projects and preclinical development for malaria. Many natural products have shown potent anti-plasmodial effects but, for a variety of reasons, including chemical tractability issues, these have not been pushed forward into hit-to-lead drug discovery projects. Pharmaceutical industries have placed low emphasis on natural-product-based drug discovery efforts because of an increasing reliance on newer technologies, such as combinatorial synthesis and high-throughput screening, and their associated approaches to drug discovery. In an effort to identify new lead molecules, we have emphasized our research on natural product drug discovery for malaria using mass spectrometry. An important factor in the success of natural product drug discovery is to minimize the time required to identify the active component from complex mixtures. Mass spectrometry based bioassays can solve a wide variety of structural identification issues of unknown active principles in plant extracts and complex mixtures with high speed and accuracy. Mass spectrometry based proteomic approaches have the potential to provide insights into the molecular actions of the ligands. We have selected *Plasmodium falciparum* thioredoxin reductase (*PfTrxR*) as our main

target and *Plasmodium falciparum* glutathione reductase (*PfGR*) as an alternative target and these are validated drug targets for malaria drug discovery.

## 1.7 Objectives of Research

The purpose of our research work is to develop mass spectrometry based bioassays to screen a library of natural products and plant extracts to identify inhibitor compounds to *Plasmodium falciparum* thioredoxin reductase (*PfTrxR*). This was accomplished by:

1. Screening natural compounds for ligands to *PfTrxR* by ultrafiltration and LC-MS based binding assay.
2. LC-MS based identification and structure elucidation of oleamide as a ligand of *Plasmodium falciparum* thioredoxin reductase in *Guatteria recurvisepala*
3. Characterization of *PfTrxR* inhibitors using mass spectrometry and *in silico* molecular modeling

We had screened 133 structurally diverse natural compounds from the MEGx® collection of AnalytiCon Discovery and three synthetic hispolone analogs for binding affinity to *Plasmodium falciparum* thioredoxin reductase (*PfTrxR*) using UF-LC-MS based ligand-binding assay. Nine compounds (yohimbine (**1**), catharanthine (**2**), vobasine (**3**), gnetifolin E (**4**), quinidine N-oxide (**5**), 11-hydroxycoronaridine (**6**), hispolone (**7**), hispolone methyl ether (**8**), and hernagine (**9**)) displayed binding affinity for *PfTrxR* at 1  $\mu$ M. The ranking order of compound's binding affinities for *PfTrxR* is **7** > **6** > **2** > **4** > **5** > **8** > **1** > **9** > **3**. On the other hand, compounds **6**, **7**, **2** and **8** demonstrated binding to the active site of *PfTrxR*, when ligands were

tested in an equimolar mixture of 1  $\mu$ M. Detannified methanol extracts of *Guatteria recurvisepala* (Annonaceae), *Topobea watsonii* (Melastomataceae) and *Licania kallunkiae* (Chrysobalanaceae) were also screened for ligands to *PfTrxR*. As a result, protonated molecule  $m/z$  282.2792  $[M+H]^+$  with molecular ion formula  $C_{18}H_{36}NO$ , and DBE of 2 with an error of 1.13 ppm from *Guatteria recurvisepala* displayed binding affinity to the enzyme. Tandem MS analysis of a ligand from *Guatteria* led to its identification as oleamide.

As a key feature, we have developed an LC-MS based functional assay to identify inhibitors of *PfTrxR* in high throughput format by quantifying the intact Trx-SH<sub>2</sub>. Here we demonstrated the separation and identification of the product formed (Trx-SH<sub>2</sub>) in the enzymatic reaction using LC-MS. Relative quantitation of intact Trx-SH<sub>2</sub> was carried out using an Agilent 6520 QTOF MS equipped with positive mode ESI. To validate the functional assay, we screened reference compounds (2,4-dinitrophenylsulfide, 4-nitrobenzothiadiazole and 3-(dimethylamino)-propiofenone (3-DAP)) which were earlier identified as inhibitors of *PfTrxR*. The developed LC-MS based functional assay for identification of inhibitors of *PfTrxR* is a sensitive and reliable method that is amendable for HT. This is the first representation of a relative quantitation of intact Trx-SH<sub>2</sub> using LC-MS. These identified ligands are also being tested for their selectivity towards human glutathione reductase.

Further, our goal was to carry out a joint experimental and computational study to identify natural products, which can selectively target these two enzymes of the parasite distinct from the host enzymes. In this work, the binding affinities of natural products towards *PfTrxR*, *PfGR*, human TrxR and human GR were determined using a mass spectrometry based ligand binding assay. *In silico* molecular modeling was used to ascertain and further confirm the binding

affinities of these ligands towards *Pf*TrxR, *Pf*GR and human isoforms of these enzymes as well as deduce the key interactions between the ligands and proteins.

## 1.8 References

1. World malaria report. WHO. **2012**. Factsheet 2012.
2. J. L. Gallup, J. D. Sachs. The Economic Burden of Malaria. *Am. J. Trop. Med. Hyg.* **2001**, 64, 85–96.
3. D. A. Jerrard, J. S. Broder, J. R. Hanna, J. E. Colletti, K. A. Grundmann, A. J. Geroff, A. Mattu. Malaria: A rising incidence in the united states. *J. Emerg. Med.* **2002**, 23, 23-33.
4. F. W. Muregi and A. Ishih. Next-generation antimalarial drugs: Hybrid molecules as a new strategy in drug design. *Drug Dev. Res.* **2010**, 71, 20 – 32.
5. A. Mannan, I. Ahmed, W. Arshad, M. F. Asim, R. A. Qureshi, I. Hussain, B. Mirza. Survey of artemisinin production by diverse *Artemisia* species in northern Pakistan. *Malaria J.* **2010**, 310, 1 – 9.
6. G. Padmanaban, V. A. Nagaraj, P. N. Rangarajan. Artemisinin-based combination with curcuminoids a new dimension to malaria therapy. *Curr. Sci.* **2012**, 102, 704-711.
7. E. Guantai, K. Chibale. How can natural products serve as a viable source of lead compounds for the development of new/novel anti-malarials? *Malaria J.* **2011**, 10, 1-8.
8. T. N. C.Wells. Natural products as starting points for future antimalarial therapies: going back to our roots? *Malaria J.* **2011**, 10, 2-12.
9. M. J. Balunas, A. D. Kinghorn. Drug discovery from medicinal plants. *Life Sci.* **2005**, 78, 431-441.
10. V. Mulabagal, A. I. Calderón, Development of binding assays to screen ligands for *Plasmodium falciparum* thioredoxin and glutathione reductases by ultrafiltration and liquid chromatography/mass spectrometry. *J. Chromatogr. B.* **2010**, 878, 987-993.

11. Z. Bozdech, H. Ginsburg. Antioxidant defense in *Plasmodium falciparum* – data mining of the transcriptome. *Malaria J.* **2004**, 3 (23), 1–10
12. S. Müller. Thioredoxin reductase and glutathione synthesis in *Plasmodium falciparum*. *Redox. Rep.* **2003**, 8 (5), 251–5.
13. S. Müller, T.W. Gilberger, Z. Krnajski, K. Luersen, S. Meierjohann, R.D. Walter. Thioredoxin and glutathione system of malaria parasite *Plasmodium falciparum*. *Protoplasma.* **2001**, 217, 43–49.
14. A. Holmgren. Thioredoxin. *Ann. Rev. Biochem.* **1985**, 54, 237.
15. P. F. Wang, L. D. Arscott, T. W. Gilberger, S. Müller, C. H. Williams. Thioredoxin reductase from *Plasmodium falciparum*: Evidence for interaction between the c-terminal cysteine residues and the active site disulfide-dithiol. *Biochemistry.* **1999**, 38, 3187–3196.
16. S. Müller, K. Becker, B. Bergmann, R. H. Schirmer, R. D. Walter. *Plasmodium falciparum* glutathione reductase exhibits sequence similarities with the human host enzyme in the core structure but differs at the ligand-binding sites. *Mol. Biochem. Parasit.* **1995**, 74, 11–18.
17. V. Wiwanitkit. *Plasmodium* and host glutathione reductase: molecular function and biological process. *Afr. J. Biotechnol.* **2006**, 5 (21), 2009–2013.
18. M. K. Stefan, R. H. Schirmer, I. Turbachova, R. Iozef, K. Becker. The thioredoxin system of the malaria parasite *Plasmodium falciparum*. *J. Biol. Chem.* **2000**, 275, 51, 40180–40186.
19. G. N. Sarma, S. N. Savvides, K. Becker, M. Schirmer, R. H. Schirmer, P. A. Karplus. Glutathione reductase of the malarial parasite *Plasmodium falciparum*: Crystal structure and inhibitor development. *J. Mol. Biol.* **2003**, 328, 893–907.
20. Z. Krnajski, T. W. Gilberger, R. D. Walter, A. F. Cowman, S. Müller, Thioredoxin reductase is essential for the survival of *Plasmodium falciparum* erythrocytic stages. *J. Biol. Chem.* **2002**, 277, 25970-25975.

21. K. Buchholz, E. D. Putrianti, S. Rahlfs, R. H. Schirmer, K. Becker, K. Matuschewski. Molecular genetics evidence for the *in vivo* roles of the two major NADPH-dependent disulfide reductases in the malaria parasite. *J. Biol. Chem.* **2010**, 285, 37388–37395.
22. P. W. S. Raymond. Principles and practice of chromatography. *Chrom-Ed book series*, 2003. Accessed on 01 November **2012**. Chrom Ed Book 2003.
23. M. I. Churchwell, N. C. Twaddle, L. R. Meeker, D. R. Doerge. Improving LC-MS sensitivity through increases in chromatographic performance: Comparisons of UPLC-ES/MS/MS to HPLC-ES/MS/MS. *J. Chromatogr. B.* **2005**, 825, 134-143.
24. M. E. Swartz. UPLC: An introduction and review. *J. Liq. Chromatogr. Related Technol.* **2005**, 28, 1253-1263.
25. I. V. Chernushevich. Duty cycle improvement for a quadrupole time-of-flight mass spectrometer and its use for precursor ion scans. *Eur. J. Mass Spectrom.* **2000**, 6, 471– 479.
26. S. Lacorte, A. R. Fernandez-Alba. Time of flight mass spectrometry applied to the liquid chromatographic analysis of pesticides in water and food. *Mass Spectrom. Rev.* **2006**, 25, 866– 880.
27. I. V. Chernushevich, A. V. Loboda, B. A. Thomson. An introduction to quadrupole–time-of-flight mass spectrometry. *J. Mass. Spectrom.* **2001**, 36, 849–865.
28. M. Dole, L. L. Mack, R. L. Hines, R. C. Mobley, L. D. Ferguson, M. B. Alice. Molecular beams of macro ions. *J. Chem. Phys.* **1968**, 49 (5), 2240-2249.
29. M. Wilm. Principles of electrospray ionization. *Mol. Cell Proteomics.* **2011**, 10 (7), 1- 8.
30. O. V. Salata. Tools of nanotechnology: Electrospray. *Curr. Nanosci.* **2005**, 1 (1), 25-33.
31. M. Yamashita, J. B. Fenn. Electrospray ion source. Another variation on the free-jet theme. *J. Phys. Chem-US.* **1984**, 88 (20), 4451-4459.

32. J. B. Fenn, M. Mann, C. K. Meng, S. F. Wong, C. M. Whitehouse. Electrospray ionization for mass-spectrometry of large biomolecules. *Science*. **1989**, 246 (4926), 64-71.
33. M. Yamashita, J. B. Fenn. Negative ion production with the electrospray ion source. *J. Phys. Chem-US*. **1984**, 88 (20), 4671-4675.
34. C. S. Ho, C. W. K. Lam, M. H. M. Chan, R. C. K. Cheung, L. K. Law, L. C. W. Lit, K. F. Ng, M. W. M. Suen, H. L. Tai. Electrospray ionisation mass spectrometry: Principles and clinical applications. *Clin. Biochem. Rev.* **2003**, 24, 3-12.
35. R. J. Pfeifer, C. D. Hendricks. Parametric studies of electro hydrodynamic spraying. *AIAA. J.* **1968**, 6 (3), 496-502.
36. L. B. Loeb, A. F. Kip, G. G. Hudson, W. H. Bennett. Pulses in negative point-to-plane corona. *Phys. Rev.* **1941**, 60 (10), 714-722.
37. S. J. Gaskell. Electrospray: Principles and Practice. *J. Mass Spectrom.* **1997**, 32, 677-688.
38. J. V. Iribarne, B. A. Thomson. On the evaporation of small ions from charged droplets. *J. Chem. Phys.* **1976**, 64 (6), 2287-2294.
39. P. Kebarle, U. H. Verkerk. Electrospray: from ions in solution to ions in the gas phase, what we know now. *Mass Spectrom. Rev.* **2009**, 28(6), 898-917.

## 2. Screening of natural compounds for ligands to *PfTrxR* by ultrafiltration and LC-MS based binding assay

### 2.1 Abstract

In this study, we have screened 133 structurally diverse natural compounds from the MEGx<sup>®</sup> collection of AnalytiCon Discovery and three synthetic hispolone analogs for binding affinity to *Plasmodium falciparum* thioredoxin reductase (*PfTrxR*) using an ultrafiltration (UF) and liquid chromatography (LC-MS) based ligand-binding assay newly developed in our laboratory. Nine compounds (yohimbine (1), catharanthine (2), vobasine (3), gnetifolin E (4), quinidine N-oxide (5), 11-hydroxycoronaridine (6), hispolone (7), hispolone methyl ether (8), and hernagine (9)) displayed binding affinity for *PfTrxR* at 1 μM. The ranking order of compound's binding affinities for *PfTrxR* is 7 > 6 > 2 > 4 > 5 > 8 > 1 > 9 > 3. On the other hand, compounds 6, 7, 2 and 8 displayed binding to *PfTrxR*, when ligands were tested in an equimolar mixture of 1 μM.

### 2.2 Introduction

Of malarial parasites, *Plasmodium falciparum* is the most lethal species due to its increased drug resistance towards current antimalarial drugs. Therefore, there is an urgent need to know more about the sites in the parasite which can be potential targets for antiplasmodial activity [1]. It has been found that *Plasmodium falciparum* is susceptible to oxidative stress [2]. Two antioxidant systems, thioredoxin reductase and glutathione reductase counteract the oxidative

stress in *Plasmodium falciparum* [2]. *Plasmodium falciparum* (*Pf*) thioredoxin reductase (TrxR), a 59 kDa flavoprotein which belongs to a class of pyridine dinucleotide oxidoreductases, catalyzes the NADPH dependent reduction of *Plasmodium falciparum* thioredoxin (*Pf*Trx) protein [2]. Reduced thioredoxin regulates the activity of the enzyme by reducing the cellular environment. Reduced *Pf*Trx acts as hydrogen donor to ribonucleotide reductase and methionine sulfoxide reductase, involved in DNA synthesis and protein repair. They can directly reduce hydrogen peroxide and can function as both single oxygen quencher and hydroxyl radical scavenger. These functions of Trx are in response to oxidative stress of the parasite [3]. Because of the involvement of *Pf*TrxR in redox regulation of the parasite, *Pf*TrxR is considered a novel target in the parasite metabolism for antiplasmodial intervention.

Other different combination therapies available to treat malaria are found to be more expensive, not readily available to people in developing countries, and accompanied with adverse effects. As our contribution to address these problems, we are emphasizing the search for bioactive natural products, since these can be viewed as an inexhaustible reservoir of molecules that can be optimized to be efficient, well tolerated, and safe to use as antimalarial drugs [4, 5]. Natural products provide leads for the development of novel therapies for the treatment of malaria. For any compound to intervene with the activity of the enzyme, it has to interact with the target enzyme.

### **2.2.1 *Pf*TrxR and *Pf*GR enzymes binding assay using ultrafiltration (UF) and liquid chromatography mass spectrometry**

Natural product drug discovery programs employ many screening methods for hit identification and lead optimization. Over time there has been a decline in interest of

pharmaceutical companies in natural products approach to drug discovery due to many factors such as incompatibility of crude extracts with high throughput assays (HTS), cost of sample collection, problems with lack of reproducibility and presence of artifacts in some extracts and difficulty in isolating active principles [6]. However, it is well established that the new chemical constituents identified from natural sources is the single most successful strategy for the discovery of new drugs. Advances in analytical methods and bioassay development have helped to push forward the research in natural products [7]. Several natural product drug discovery screening assays such as cell based, cytotoxicity, receptor/enzyme binding, cell membrane permeability assays and assays based on optical detection have been reported which were found to be slow, time consuming, resource intensive, suffer from matrix interference and cannot provide structural information regarding the active compounds that might be present, which is a disadvantage when plant extracts/mixtures are screened [8, 9]. Determination of an enzyme's affinity for small molecules using mass spectrometry is among the more recently developed method that can be a valuable addition to traditional drug discovery techniques. We have employed an ultrafiltration LC-MS based enzyme ligand binding assay to screen vast number of natural products and plant extracts to determine their selective binding affinity towards isolated *PfTrxR* and *PfGR* enzymes. The ultrafiltration step facilitates the separation of ligand-receptor complexes from unbound compounds, and then LC-MS is used to characterize and identify the ligands. This method is advantageous over other methods in that the MS measures only the actual compounds that have affinity for the enzyme and has very high sensitivity and selectivity that is inherent to mass spectrometric detection [10]. Plant extracts contain a large number of different chemical constituents, making it difficult to ascertain their antimalarial activity before isolation of the bioactive compounds. A suitable tool to speed up natural product drug discovery

is the application of UF-LC-MS based binding assays which can screen complex mixtures from plant origins for their binding affinity towards *PfTrxR* followed by MS-based structure elucidation and confirmation of the identity of new ligands.

## **2.3 Materials and methods**

### **2.3.1 Chemicals and enzymes**

Solvents used for LC-MS analysis were purchased from Fischer Scientific International (Atlanta, GA). One hundred and thirty-three compounds from AnalytiCon Discovery GmbH (Germany) natural products library (MEGx) (Table 2.1) were purchased based on compound classes that have reported either antimalarial activity or inhibition of TrxR [12, 13]. Out of 133 natural products, 28 have been identified as novel plant-derived compounds by AnalytiCon Discovery (Table 2.1). Three hispolone analogues were kindly provided by Dr. G. V. Subbaraju, AptuitLauras, Hyderabad, India. Buffer salts and bis-2, 4-dinitrophenyl sulfide were purchased from Sigma-Aldrich (Allentown, PA). Deionized water generated by a Milli-Q water system (Millipore, MA) was used in the experiments. *PfTrxR* ( $M_r$  59 kDa) enzyme was provided as a gift by Prof. Katja Becker, Justus-Liebig University, Giessen, Germany. The recombinant *PfTrxR* was prepared and purified using silver-stained SDS page according to the procedure published by Kanzok et al [14]. The specific activity of *PfTrxR* (1.9 U/mg) was determined by DTNB [5, 5'-dithiobis (2-nitrobenzoic acid)]. Protein concentration of enzymes was determined by Bradford method [15].

### 2.3.2 UF-LC-MS binding assay

In this method, 4  $\mu\text{L}$  of test compound (10  $\mu\text{M}$ ) and 192  $\mu\text{L}$  of incubation buffer containing 20.5 mM  $\text{KH}_2\text{PO}_4$ , 26.5 mM  $\text{K}_2\text{HPO}_4$ , 200 mM  $\text{KCl}$  and 1 mM  $\text{EDTA}$  with pH 6.9, were placed into a micro centrifuge. To this, 4 $\mu\text{L}$  of *Pf*TrxR/*Pf*GR enzyme (1  $\mu\text{M}$ ) was added and incubated at 25°C for 60 min. The incubation mixture was then filtered through a 30 kDa molecular weight cut-off ultrafiltration membrane filter made of regenerated cellulose (Microcon YM-30, Millipore, Billerica, MA) according to the modified method of Liu. et al. [11] and then centrifuged at 13,000  $\times$  g at 4°C for 20 min. The enzyme–ligand complex trapped in the filter was washed with assay buffer (200  $\mu\text{L}$  3 $\times$ ) and centrifuged at 13,000  $\times$  g at 4°C for 20 min each time. The ultrafiltration membrane was placed into a new microcentrifuge tube and the ligands were dissociated from *Pf*GR enzyme by treatment with 200  $\mu\text{L}$  of methanol for 20 min. The ligand ultrafiltrate obtained was centrifuged at 20°C, 13,000  $\times$  g for 20 min. The ultrafiltrate was then dried under nitrogen using N-VAP 116 Nitrogen Evaporator (Organomation Associates, Inc., Berlin, MA) and the released ligands were reconstituted in 100  $\mu\text{L}$  of methanol/water (v/v, 90:10). Assays were carried out in duplicate and the control experiments were performed in a similar way with denatured enzyme. The released ligands were then analyzed by LC-MS. Assays were carried out in duplicate and the control experiments were performed in a similar way with denatured enzyme.

### 2.3.3 LC-MS analysis

All the test compounds for LC-MS analysis were prepared using  $\text{MeOH} - \text{H}_2\text{O}$  (90:10, v/v). Prior to screening, the compounds were divided into batches based on their physicochemical

properties that determine ionization efficiency and electrospray ionization mode. Liquid chromatography analysis was performed using a ZORBAX Eclipse plus C18 column (2.1 mm x 100 mm, 1.8  $\mu$ m) at a flow rate of 0.2 mL/min. An Agilent (Little Falls, DE) 6520 accurate-mass quadrupole time of flight (Q-TOF) mass spectrometer equipped with a 1220 rapid resolution liquid chromatography (RRLC) system was used for separation of batch compounds. Detailed information on LC conditions for separation of batch compounds is provided in Table 2.2.

#### **2.3.3.1 LC-MS analysis of ligands 1, 2, 3, 5, 6, 7, 8 and 9 in equimolar mixture of 1 $\mu$ M**

Compounds were analyzed at 1  $\mu$ M (5  $\mu$ L inj. vol.) using gradient mobile phase (0 min 5% B to 95% B in 20 min) consisting of (A) 0.1% formic acid in H<sub>2</sub>O (v/v) and (B) 0.1% formic acid in 50:50 MeOH-ACN (v/v/v) as solvent system for a run time of 20 min with post run 3 min at a flow rate of 0.2 mL/min. The eight compounds (**1, 2, 3, 5, 6, 7, 8 and 9**) were detected in positive ion electrospray. All the test compounds were detected by MS at a capillary voltage of 3200 V for ESI negative mode and 3500 V for ESI positive mode. Nitrogen was supplied as nebulizing and drying gas at flow rates of 25 and 600 l/h, respectively. The drying gas temperature was 350 °C. The fragmentor voltage was optimized to 175-180 eV. Data were acquired and analyzed using Agilent MassHunter Workstation Qualitative Analysis software, version B.02.00.

**Table 2.1** List of one hundred and thirty-three natural products from Analyticon Discovery library tested for binding to *Pf*TrxR

CAS Number	Common/Chemical name	Novelty <sup>a</sup>
94-62-2	Piperin	N
3155-53-1	7,8-Dihydro-5,6-dehydromethysticin	N
66648-43-9	Moupinamide	N
64363-86-6	1H-Indole-3-ethanaminium	N
89946-11-2	3,3',5,5'-Tetrahydroxy-4-methoxystilbene	N
1083200-79-6	NA	Y
960509-38-0	2,5-Piperazinedione, 3-[[2-(1,1-dimethyl-2-propen-1-yl)-1H-indol-3-yl]methylene]-6-methyl-, (3Z,6R)-	N
158569-73-4	(-)-Talaumidin methyl ether	N
1212329-33-3	NA	N
152543-09-4	Dihydroconiferyldihydro-p-coumarate	N
182056-19-5	4(1H)-Quinolinone, 1-methyl-2-(7-tridecenyloxy)-	N
188113-99-7	4(1H)-Quinolinone, 1-methyl-2-(6,9-pentadecadien-1-yl)-	N
36417-86-4	Paprazine	N
38759-91-0	(±)-Eudesmin	N
220862-05-5	Thunalbene	N
41137-87-5	Hirsutenone	N
886226-15-9	Muricarpone B	N
1083197-74-3	NA	Y
130008-79-6	Phenol, 4-[4-(1,3-benzodioxol-5-yl)-2,3-dimethylbutyl]-2-methoxy-, (R*,R*)- (9CI)	N
1158019-66-9	2-Propen-1-one, 1-(2,4-dihydroxyphenyl)-3-[4-[(3-methyl-2-buten-1-yl)oxy]phenyl]-, (2E)-	Y
76496-57-6	6H-[1,3]Dioxolo[5,6]benzofuro[3,2-c][1]benzopyran-3-ol, 6a,12a-dihydro-	N
112501-42-5	Piperolactam A	N
116086-93-6	Piperolactam D	N

118245-30-0	1,3-Benzodioxole, 5-[(2R,3R)-4-(3,4-dimethoxyphenyl)-2,3-dimethylbutyl]-, rel-	N
886060-78-2	1-(3,4-Dihydroxyphenyl)-7-(4-hydroxyphenyl)-4-hepten-3-one	N
444930-12-5	1,3-Benzodioxole, 5,5'-[(2S,3S)-2,3-dimethyl-1,4-butanediyl]bis-(9CI)	N
78510-20-0	N-trans-Feruloyl-4-O-methyl-dopamine	N
122-69-0	Styracin	N
65026-58-6	Laurolitsine; Norboldine	N
120693-53-0	4(1H)-Quinoline, 1-methyl-2-(4Z, 7Z)-4,7-tridecadienyl	N
485-61-0	Graveoline	N
36062-05-2	3-Heptanone, 5-hydroxy-1,7-bis(4-hydroxy-3-methoxyphenyl)-Hexahydrocurcumin	N
2134-83-0	Vobasine	N
109428-81-1	Cafestol	N
1136618-10-4	Phenol, 3-[(1E)-2-(3-hydroxy-4-methoxyphenyl)ethenyl]-5-methoxy-2-(3-methyl-2-buten-1-yl)-	Y
125564-68-3	2-Propenoic acid, 3-(3,4-dihydroxyphenyl)-, 2-hydroxy-3-[[[(2E)-3-(4-hydroxyphenyl)-1-oxo-2-propen-1-yl]oxy]propyl ester, (2E)-	Y
156788-67-9	3-Hydroxy-4',5-dimethoxy-2-prenylstilbene	N
22313-89-9	1H,3H-Furo[3,4-c]furan, tetrahydro-1,4-bis(3,4,5-trimethoxyphenyl)-	N
212515-38-3	1,3-Benzodioxole, 5,5'-(tetrahydro-1H,3H-furo[3,4-c]furan-1,4-diyl)bis-, (3aR,6aR)-rel- (9CI)	N
71364-33-5	(±)-Tetrahydropalmitine-9-(methoxy-14-C)	N
23095-44-5	Girinimbine	N
56021-85-3	Lyaloside	N
15990-55-6	Bruceolline F	N
139219-98-0	Citracidone III	N
81525-61-3	Citracidone I	N
4339-71-3	Piceatannol	N
146-48-5	Yohimbine	N
100432-87-9	Glucoside, 3-hydroxy-5-(p-hydroxyphenethyl)phenyl (7CI)	Y
859747-99-2	1,3-Benzodioxole, 5-[tetrahydro-4-(3,4,5-trimethoxyphenyl)-1H,3H-furo[3,4-c]furan-1-yl]-	N
2468-21-5	Catharanthine	N
633-65-8	Berberinchlorid	N

1217689-07-0	1H,3H-Furo[3,4-c]furan-1-one, 3-(1,3-benzodioxol-5-yl)tetrahydro-6-(4-hydroxy-3-methoxyphenyl)-	Y
98681-44-8	4H-Dibenzo[de,g]quinolin-2-ol, 5,6,6a,7-tetrahydro-1-methoxy-	N
139101-68-1	$\beta$ -D-Glucopyranoside, 3-hydroxy-5-[2-(4-hydroxy-3-methoxyphenyl)ethyl]phenyl	Y
140671-07-4	Gnetifolin E	N
56973-65-0	1,7-Bis(4-hydroxyphenyl)-4-hepten-3-one	N
288141-04-8	Platyphyllonol 5-xylpyranoside	N
6871-44-9	Echitamine	N
456-12-2	Aegeline	N
58762-96-2	Pinostilbenoside	N
38963-95-0	Resveratrolsoid	N
876659-81-3	Ajmalicine	N
79559-61-8	3-Heptanone, 5-hydroxy-7-(4-hydroxy-3-methoxyphenyl)-1-phenyl-	N
79559-59-4	1,7-Diphenyl-4-hepten-3-one	N
845655-40-5	1(2H)-Isoquinoline, 3,4-dihydro-6-hydroxy-7-methoxy	Y
884495-94-7	1,2-Benzenediol, 4-[3,5-dihydroxy-7-(4-hydroxy-3-methoxyphenyl)heptyl]-	Y
132216-13-8	Amaniensine	Y
25924-78-1	Trichostachine	N
34371-47-6	5 $\beta$ -Carboxystrictosidine	N
798569-00-3	D-Tyrosine, N-[3-(3,4-dihydroxyphenyl)-1-oxo-2-propen-1-yl]-3-hydroxy-	N
104821-27-4	Lyalosidic acid	N
91000-14-5	2-Propenamide, N-[4-(acetylamino)butyl]-3-(4-hydroxy-3-methoxyphenyl)-, (E)- (9CI)	Y
21451-50-3	Deoxycordifoline	Y
479-43-6	Canthin-6-one	N
908094-05-3	3-Heptanone, 5-hydroxy-7-(4-hydroxy-3-methoxyphenyl)-1-(4-hydroxyphenyl)-	N
1212137-68-2	[1,3]Dioxolo[4,5-h]-1,3-dioxolo[7,8][2]benzopyrano[3,4-a][3]benzazepine, 5b,6,7,8,13b,15-hexahydro-15-methoxy-6-methyl-	N
79559-60-7	7-(4-Hydroxy-3-methoxyphenyl)-1-phenyl-4-hepten-3-one	N
33626-08-3	3,5-Dihydroxy-4'-methoxystilbene	N
74133-19-0	Hernagine	N

32507-66-7	Isorhapontigenin	N
NA	Centrolol-3-rutenoside	Y
1083195-05-4	Benzenepropanol, 4-hydroxy- $\alpha$ -[4-(4-hydroxyphenyl)-3-buten-1-yl]-	Y
79120-40-4	Hannokinol	N
29700-22-9	Oxyresveratrol	N
103188-48-3	N-trans-caffeoyltyramine	N
35387-16-7	Vasicinone	N
19902-91-1	Dihydromethysticin	N
60263-07-2	Jacaranone	N
NA	Indol-3-(6-O-b-D-Apiofuranosyl-b-D-glucopyranoside)	Y
1212171-97-5	1,3-Benzodioxole-5-butanol, $\alpha$ -(4-hydroxy-3-methoxyphenyl)- $\beta,\gamma$ -dimethyl-	N
7154-01-0	3-(3,4-Methylenedioxyphenyl)-1,2-propanediol	N
1083192-75-9	2-Buten-1-ol, 4-[4-[2-(7-methoxy-1,3-benzodioxol-5-yl)ethyl]phenoxy]-2-methyl-	Y
48216-02-0	Homochelidonine, $\beta$ - (3CI)	N
23141-27-7	Vincosamide	N
23512-46-1	Piperanine	N
537-42-8	Pterostilbene	N
517-73-7	Melicopicine	N
130233-83-9	Acerogenin G	N
1083192-76-0	Benzene, 1,2,3-trimethoxy-5-[2-[4-[(3-methyl-2-buten-1-yl)oxy]phenyl]ethyl]-	Y
83-95-4	Skimmianine	N
133-03-9	(+)-Episesamin	N
93559-25-2	( $\pm$ )-7-(3'',4''-Dihydroxyphenyl)-5-hydroxy-1-(4'-hydroxyphenyl)-3-heptanone	Y
1174388-79-4	NA	Y
1212227-01-4	NA	N
190271-90-0	$\beta$ -D-Glucopyranoside, 5-(4-hydroxyphenyl)-1-[2-(4-hydroxyphenyl)ethyl]pentyl	N
126722-26-7	Pumiloside	N
104420-85-1	(+)-N-Methylaurotetanine N-oxide	N
58-08-2	Coffeine	N

24192-01-6	Dihydroyashabushiketol	N
4829-55-4	Hetisinone	N
607-91-0	Myristicin	N
105317-66-6	Moskachan D	N
76202-23-8	11-Hydroxycoronaridine	N
70116-00-6	Quinidine N-oxide	Y
115587-58-1	1-Hepten-3-one, 5-hydroxy-1,7-diphenyl-, (1E)-	Y
2051-07-2	Dianisalacetone	N
75821-37-3	5-Hydroxyarborinine	N
149732-51-4	1-(3,4-Dihydroxyphenyl)-7-(4-hydroxy-3-methoxyphenyl)-1,6-heptadiene-3,5-dione	N
30278-29-6	1,7-Diphenylheptane-3,5-diol	N
83161-95-9	3-Heptanone, 7-(4-hydroxy-3-methoxyphenyl)-5-methoxy-1-phenyl-	N
88660-10-0	Pipernonaline	N
66280-26-0	Pregomisin	N
52617-31-9	Haplamine	N
312608-32-5	Furo[2,3-b]quinolin-7-ol, 5,6,7,8-tetrahydro-4,8-dimethoxy-8-(3-methyl-2-buten-1-yl)-	N
1174387-98-4	NA	Y
1174387-99-5	NA	Y
1174389-03-7	NA	Y
58436-29-6	3-Hydroxy-4',5-dimethoxystilbene	N
284463-38-3	3,5-Heptanediol, 1-(4-hydroxy-3-methoxyphenyl)-7-phenyl-	Y
10091-84-6	Triacanthin	N
913692-05-4	NA	N
123648-56-6	Germanaism B	N
467-77-6	Coronaridine	N

<sup>a</sup>NA: Common/chemical name not assigned in the literature.

<sup>b</sup>Novelty: Y: novel compound, N: known compound.

**Table 2.2** LC-MS conditions for detection of the one hundred and thirty-three natural products

Batch	Compound class	Test conc. /Inj. vol.	M.P	Mobile phase A	Mobile phase B	Proportion A:B		Positive/Negative Electrospray	Run time
1 <sup>st</sup> , 2 <sup>nd</sup> , 6 <sup>th</sup> , 7 <sup>th</sup> , 10 <sup>th</sup> , 11 <sup>th</sup>	amides, alkaloids, curcuminoids, coumarins, lignans, quinines, stilbenes	5 µM/5 µl	Gradient	0.1 % formic acid in H <sub>2</sub> O	95% ACN, 5% H <sub>2</sub> O, 0.1% formic acid	<b>min</b> 0 2 4 7 8	<b>% B</b>  20 50 90 90 20	ESI-positive	10 min
3 <sup>rd</sup>	amides	10 µM/2 µl	Isocratic	0.1% formic acid in H <sub>2</sub> O	0.1% formic acid in MeOH	90:10 (A: B)		ESI-negative	8 min
4 <sup>th</sup>	alkaloids, amides, coumarins, lignans	1 µM/1 µl	Isocratic	0.1% formic acid in H <sub>2</sub> O	95% ACN, 5% H <sub>2</sub> O, 0.1% formic acid	5: 95 (A: B)		ESI-positive	10 min
5 <sup>th</sup>	alkaloids	5 µM/5 µl	Gradient	0.1% formic acid in H <sub>2</sub> O	95% ACN, 5% H <sub>2</sub> O, 0.1% formic acid	<b>min</b> 0 2 4 5	<b>% B</b>  20 90 90 20	ESI-positive	7 min

8 <sup>th</sup>	stilbenes	5 $\mu$ M/5 $\mu$ l	Gradient	0.1% formic acid in H <sub>2</sub> O	95% ACN, 5% H <sub>2</sub> O, 0.1% formic acid	<b>min</b> 0 2 4 7 8	<b>% B</b> 20 40 90 90 20	ESI-negative	10 min
9 <sup>th</sup>	curcuminoids alkaloids, diterpenes	1 $\mu$ M/5 $\mu$ l	Gradient	0.1% formic acid in H <sub>2</sub> O	95% ACN, 5% H <sub>2</sub> O, 0.1% formic acid	<b>min</b> 0 2 4 7 8	<b>% B</b> 20 40 90 90 20	ESI-positive	10 min

## 2.4 Results and Discussion

*PfTrxR* plays an important role in the pathophysiology of malaria disease, regulating the oxidative stress in the enzyme. Considering the significance of *PfTrxR* as a novel target in the parasite metabolism for therapeutic intervention, UF and LC-MS binding assay [16] were used to screen one hundred and thirty three various classes of natural compounds (alkaloids, amides, coumarins, curcuminoids, diterpenes, lignans, stilbenes) and three synthetic compounds which can be bound by *PfTrxR*. Out of the one hundred and thirty six compounds screened, nine compounds showed affinity to the enzyme. These compounds were found to be yohimbine (**1**), catharanthine (**2**), vobasine (**3**), gnetifolin E (**4**), quinidine N-oxide (**5**), 11-hydroxycoronaridine (**6**), hispolone (**7**), hispolone methyl ether (**8**), and hernagine (**9**) (Figure 2.1). To screen the ligands for the enzyme, the binding assay was performed by incubating the test compounds with 1  $\mu$ M *PfTrxR* at 25 °C for 1 hr [16] in a total volume of 200  $\mu$ l of assay buffer. The bound ligands in the enzyme-ligand complex trapped on the membrane filter were dissociated using MeOH and the dissociated ligands were dried, reconstituted and then analyzed using both positive and negative ESI-MS experiments.

All ligands were detected by LC-MS within an error of < 1.5 ppm. The relative binding affinities of ligands are shown in Table 2.3. The binding affinity was ascertained by calculating the ratio between the average peak area of compound incubated with active enzyme and the average peak area of compound incubated with denatured enzyme  $\pm$  standard deviation. According to the binding affinity data obtained in the screening of the 136 compounds against *PfTrxR* and binding affinity of our reference compound (bis-2,4-dinitrophenyl sulfide) [16], compounds that specifically bind the enzyme and displayed binding affinity of more than 1.5

were considered ligands. The binding affinity was ranked in the following fashion: non-ligand less than 2, moderate between 2.0 - 3.0 and strong when more than 3.0. The ranking order of compounds binding affinities for *PfTrxR* is **7 > 6 > 2 > 4 > 5 > 8 > 1 > 9 > 3**. Yohimbine (**1**) has moderate binding affinity of 2.0-fold when incubated with 1  $\mu$ M *PfTrxR*. Compound **1**, an indole alkaloid, was first isolated from the seeds and bark of a large Venezuelan tree *Aspidosperma excelsum* Benth [17]. Catharanthine (**2**) and gnetifolin E (**4**) both displayed moderate binding affinity of 2.5-fold to *PfTrxR*. Compound **2**, an indole alkaloid, was isolated from the dried leaves of *Catharanthus roseus* (L.) [18].

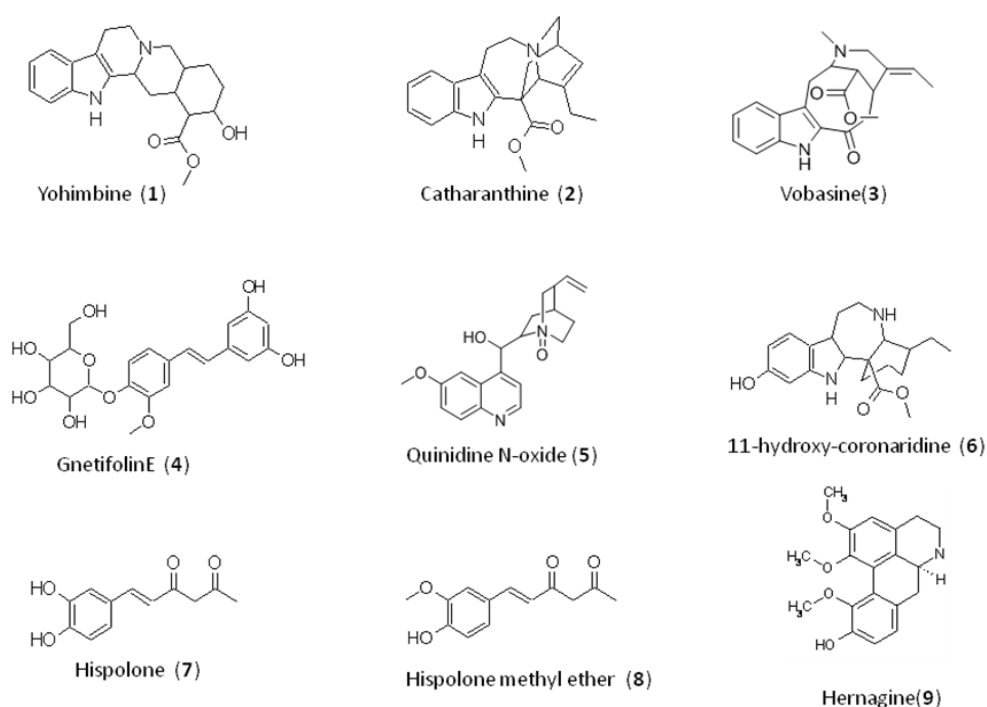


**Figure 2.1** Structures of active compounds screened for *PfTrxR*.

**Table 2.3** Relative binding affinities for ligands **1-10** tested UF-LC-MS screening against *PfTrxR*

Compound	MS detected parent ion <sup>a</sup>	Binding affinity of each ligand 1 $\mu$ M	Binding affinity of equimolar mixture of ligands, 1 $\mu$ M each
Yohimbine ( <b>1</b> )	355.2013 [M+H] <sup>+</sup>	2.0 $\pm$ 0.13	2.2 $\pm$ 0.78
Catharanthine ( <b>2</b> )	337.1910 [M+H] <sup>+</sup>	2.5 $\pm$ 0.05	3.6 $\pm$ 0.59
Vobasine ( <b>3</b> )	353.1865 [M+H] <sup>+</sup>	1.6 $\pm$ 0.87	1.9 $\pm$ 0.56
Gnetifolin E ( <b>4</b> )	419.1351 [M-H] <sup>-</sup>	2.45 $\pm$ 0.16	ND
Quinidine N-oxide ( <b>5</b> )	341.1856 [M+H] <sup>+</sup>	2.6 $\pm$ 0.23	2.6 $\pm$ 0.64
11-hydroxy-coronaridine ( <b>6</b> )	355.2019 [M+H] <sup>+</sup>	3.8 $\pm$ 0.38	3.7 $\pm$ 0.94
Hispolone ( <b>7</b> )	221.0803 [M+H] <sup>+</sup>	7.51 $\pm$ 0.52	3.6 $\pm$ 0.17
Hispolone methyl ether ( <b>8</b> )	235.0961 [M+H] <sup>+</sup>	2.05 $\pm$ 0.24	3.4 $\pm$ 0.42
Hernagine ( <b>9</b> )	328.1534 [M+H] <sup>+</sup>	1.8 $\pm$ 0.61	2.9 $\pm$ 0.70
Dehydroxyhispolone ( <b>10</b> )	205.0855 [M+H] <sup>+</sup>	0.95 $\pm$ 0.43	ND
2,4-Dinitrophenylsulfide (reference compound) [10]	366.9992 [M-H] <sup>+</sup>	3.2 $\pm$ 0.27	ND

<sup>a</sup>Parent ions detected for ligands (**1-10**) in the UF-LC-MS screening when incubated with 1  $\mu$ M of active and denatured *PfTrxR*. ND: not determined, Compound **4** and **10** were not tested in the equimolar mixture because **4** should be detected in ESI negative mode and **10** was not considered a ligand.

Compound **4**, a stilbene glucoside was first isolated from lianas of *Gnetum parvifolium* (Warb.) [19]. Vobasine (**3**) displayed relatively low binding affinity of 1.6-fold to *PfTrxR*. Quinidine N-oxide (**5**) showed moderate binding affinity of 2.6-fold to *PfTrxR*. Compound **5** was identified as novel structure from plant sources by AnalytiCon Discovery. The 11-hydroxycoronaridine (**6**) has relatively high binding affinity of 3.8-fold compared to yohimbine (**1**). Compound **6**, an indole alkaloid, was isolated from seeds and root-bark of *Pterotabema inconspicua* Stapf [20]. Hernagine showed 1.8-fold binding affinity to *PfTrxR*. Hernagine (**9**), an aporphinoid alkaloid, was first isolated from stem bark of *Hernandia nymphaefolia* Presl [21] and later isolated from other *Hernandia* species like *Hernandia cordigera* Vieill [22]. The extracts of *Hernandia cordigera* displayed antiparasitic activity against other than *Plasmodium* species such as *Leishmania donovani*, *Trypanosoma brucei*, *Trichomonas vaginalis* and *Caenorhabditis elegans* [23]. Compounds **1**, **2** and **6** belong to indole alkaloids and displayed moderate binding affinity to *PfTrxR*. Indole alkaloids isolated from natural sources including artemisinin and quinine (and atovaquone, semi-synthetic) showed high selectivity to *Plasmodium* species and are reported to have high antiplasmodial activity both *in vitro* and *in vivo* [24].

In addition to the one hundred and thirty three natural products, we also screened 3 synthetic compounds: hispolone (**7**), hispolone methyl ether (**8**), and dehydroxyhispolone (**10**). These compounds were selected due to their structural resemblance to curcuminoids (bis-demethoxycurcumin, demethoxycurcumin and curcumin) which are already reported to have high binding affinity for *PfTrxR* [16]. Moreover these compounds have significant anti-inflammatory and anti-proliferative activities when tested on human myeloid leukemia cell line KBM-5 and other human cell lines [25]. For these reasons these compounds were tested for

binding affinity to *PfTrxR*. Hispolone (**7**) showed the highest binding affinity of 7.5-fold among all the compounds screened, whereas hispolone methyl ether (**8**) showed moderate binding affinity of 2.5-fold and dehydroxyhispolone (**10**) displayed no affinity (less than 1-fold) for *PfTrxR*. The high binding affinity of hispolone (**7**) can be attributed to the presence of the hydroxyl groups on the phenyl ring. When one of the hydroxyl groups was replaced by a methoxy group in hispolone methyl ether (**8**), there was a 3-fold reduction in the binding affinity for *PfTrxR*. When one of the hydroxyl groups was absent from the ring, as in case of dehydroxyhispolone (**10**) (Figure. 2.1), there was no binding to *PfTrxR*. It can be assumed that 3-hydroxyl group in hispolone might be involved in binding to the active site or at the dimer interface of the enzyme to result in high binding affinity to *PfTrxR*. In hispolone methyl ether, the methoxy group can form an intramolecular hydrogen bond with 4-phenolic hydrogen making the phenolic hydroxyl group unavailable for interaction at active sites or at dimer interface. Therefore it can be hypothesized that hydroxyl groups in hispolone may form a hydrogen bond with the enzyme active site or dimer interface. The role of methoxy group as in the case of hispolone methyl ether (**8**) appears optional.

When compounds ionizable by ESI in positive mode were assayed with 1  $\mu$ M of *PfTrxR* in 1  $\mu$ M equimolar solution, compounds **1**, **2**, **3**, **5**, **6**, **7**, **8**, **9** were identified as ligands (Table 2.3 and Figure 2.2). The ranking order of compound's binding affinities in equimolar mixture for *PfTrxR* is **6** > **7** > **2** > **8** > **9** > **5** > **1** > **3**. Because the amount of *PfTrxR* available for binding was the same as assayed individually, the ligands **6**, **7**, **2** and **8** competed more effectively for the binding site than compounds **9**, **5**, **1** and **3**. No previous work related to ligand-binding affinity to *PfTrxR* or any other *in-vitro* antiparasitic activity was found to be reported on compounds **1-10**, except for compound **1**, where antiparasitic activity (> 200  $\mu$ M) against *P. falciparum*

and antileishmanial activity (23.8  $\mu\text{M}$ ) against *L. major* was reported by Staerk et al. [26].

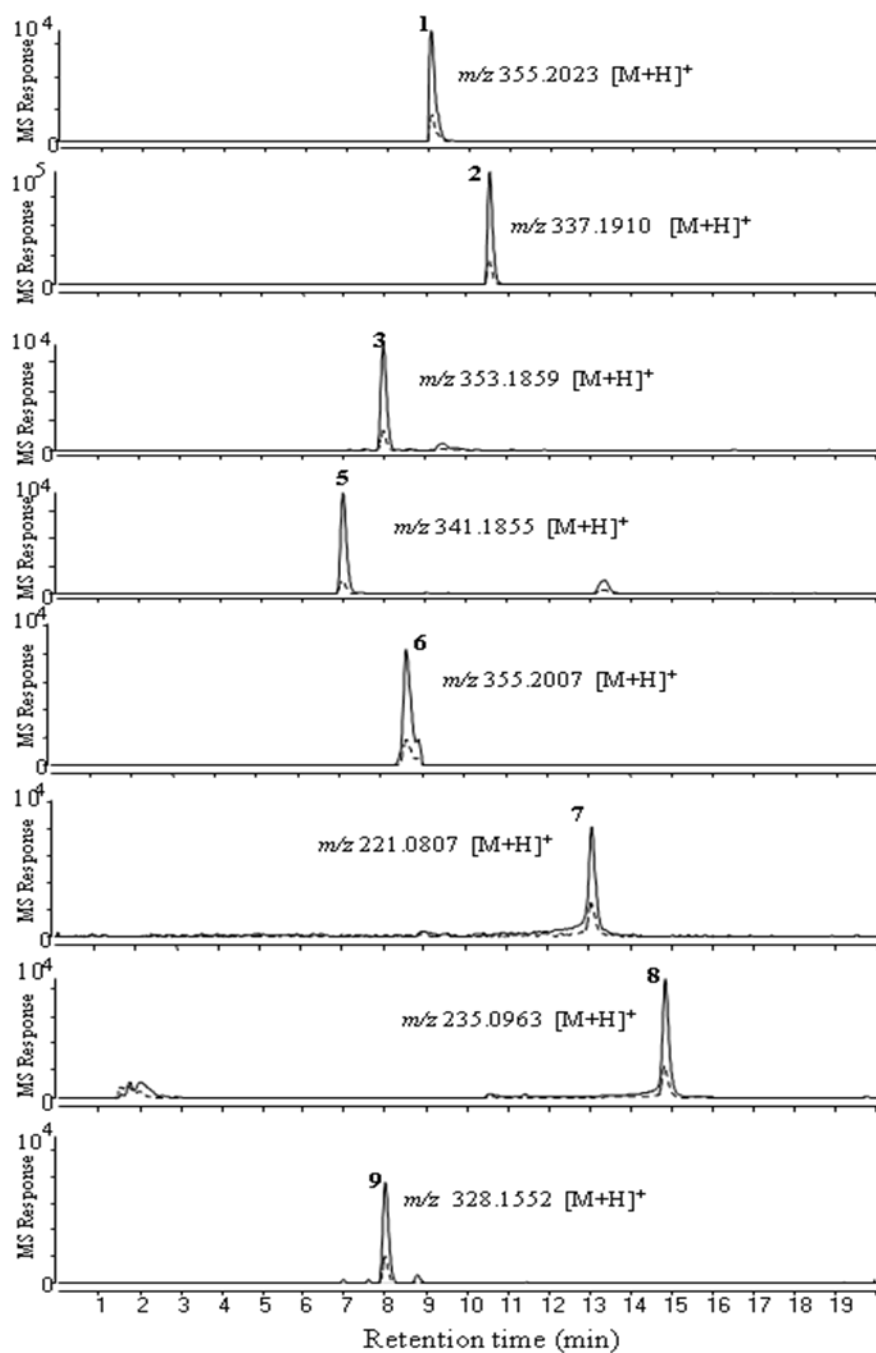


**Figure 2.2** UF and LC-MS screening of equimolar mixture of compounds 1, 2, 3, 5, 6, 7, 8 and 9 incubated with 1  $\mu\text{M}$  *Pf*TrxR.

## 2.5 Conclusions

Screening of natural compounds for ligand binding affinity to *PfTrxR* by UF and LC-MS based approach can be used to address the challenges in the discovery of innovative and cost effective broad spectrum antimalarial agents from plants. LC-MS conditions were developed for all the test compounds prior to the binding assay. Among compounds screened, we found nine compounds (**1**, **2**, **3**, **4**, **5**, **6**, **7**, **8** and **9**) bound to the enzyme. Hispolone (**7**) showed highest binding affinity when tested individually. When the selected eight ligands (**1**, **2**, **3**, **5**, **6**, **7**, **8** and **9**) were tested in equimolar mixture, compounds **6**, **7**, **2** and **8** displayed good binding to *PfTrxR* in comparison to the rest of the ligands. Compounds with strong binding affinity to the enzyme will be subjected to further functional assay studies to test their inhibitory activity.

## 2.6 References

1. P. Olliaro. Mode of action and mechanisms of resistance for antimalarial drugs. *Pharmacol. Ther.* **2001**, 89, 207 – 219.
2. S. Müller, T. W. Gilberger, Z. Krnajski, K. Liersen, S. Meierjohann, R. D. Walter. Thioredoxin and glutathione system of malaria parasite *Plasmodium falciparum*. *Protoplasma*. **2001**, 217, 43-49.
3. T. Zeller, G. Klug, Thioredoxins in bacteria: functions in oxidative stress response and regulation of thioredoxin genes. *Naturwissenschaften*. **2006**, 93, 259-266.
4. C. W. Wright. Recent developments in research on terrestrial plants used for the treatment of malaria, *Nat. Prod. Rep.* **2010**, 27, 961–968.
5. S. Schwikkard, F. R. van Heerden. Antimalarial activity of plant metabolites. *Nat. Prod. Rep.* **2002**, 19 675-692.
6. D. D. Baker, M. Chu, U. Oza, V. Rajgarhia. The value of natural products to future pharmaceutical discovery. *Nat. Prod. Rep.* **2007**, 24, 1225–1244.
7. J. L. Wolfender, P. J. Eugster, N. Bohni, M. Cuendet. Advanced methods for natural product drug discovery in the field of nutraceuticals. *Chimia (Aarau)*. **2011**, 65 (6), 400-6.
8. Y. Choi, R. B. van Breemen. Development of a screening assay for ligands to the estrogen receptor based on magnetic microparticles and LC-MS. *Comb. Chem. High T. Scr.* **2008**, 11, 1–6.
9. X. Cheng, R. B. van Breemen. Mass Spectrometry-Based Screening for Inhibitors of  $\beta$ -Amyloid Protein Aggregation. *Anal. Chem.* **2005**, 77(21), 7012–7015.
10. N. Jonker, J. Kool, H. Irth, W. M. A. Niessen. Recent developments in protein-ligand

- affinity mass spectrometry. *Anal. Bioanal. Chem.* **2011**, 399, 2669–2681.
11. D. Liu, J. Guo, Y. Luo, D. J. Broderick, M. I. Schimerlik, J. M. Pezzuto, R. B. van Breemen. Screening for ligands of human retinoid X receptor- $\alpha$  using ultrafiltration mass spectrometry. *Anal. Chem.* **2007**, 79, 9398 - 9402.
  12. Z. Liu, Z. Y. Du, Z. S. Huang, K.S. Lee, L. Q. Gu. Inhibition of thioredoxin reductase by curcumin analogs. *Biosci. Biotechnol. Biochem.* **2008**, 72, 2214-2218.
  13. C. Morin, T. Besset, J. C. Moutet, M. Fayolle, M. Bruckner, D. Limosin, K. Becker, E. Davioud-Charvet. The aza-analogues of 1, 4-naphthoquinones are potent substrates and inhibitors of plasmodial thioredoxin and glutathione reductases and of human erythrocyte glutathione reductase. *Org. Biomol. Chem.* **2008**, 6, 2731-2742.
  14. S. M. Kanzok, R. H. Schirmer, I. Turbachova, R. Iozef, K. Becker. The Thioredoxin system of the malaria parasite *Plasmodium falciparum*. *J. Biol. Chem.* **2000**, 275, 40180-40186.
  15. M. M. Bradford. A rapid and sensitive method for the quantitation of microgram quantities of proteins utilizing the principle of protein-dye binding. *Anal. Biochem.* **1976**, 72, 248-254.
  16. V. Mulabagal, A. I. Calderón. Development of binding assays to screen ligands for *Plasmodium falciparum* thioredoxin and glutathione reductases by ultrafiltration and liquid chromatography/mass spectrometry. *J. Chromatogr. B.* **2010**, 878, 987-993.
  17. P. R. Benoin, R. H. Burnell, J. D. Riedin. Alkaloids of *Aspidosperma excelsum* Benth. *Can. J. Chem.* **1967**, 45, 725-730.
  18. J. H. Renault, J.-M. Nuzillard, G. Le Crouérou, P. Thépenier, M. Zèches-Hanrot, L. Le Men-Olivier. Isolation of indole alkaloids from *Catharanthus roseus* by centrifugal partition chromatography in the pH-zone refining mode. *J. Chromatogr. A.* **1999**, 849, 421- 431.
  19. M. Lin, J. B. Li, S. Z. Li, D. Q. Yu, X. T. Liang. A dimeric stilbene from *Gnetum*

- parvifolium*. *Phytochemistry*. **1992**, 31, 633-638.
20. A. M. Morfaux, T. Mulamba, B. Richard, C. Delaude, G. Massiot, L. Le Men-Olivier. Alkaloids of *Pterotaberna inconspicua*. *Phytochemistry*. **1982**, 7, 1767-1769.
  21. B. Jean. Alkaloids from *Hernandia cordigera*: Isolation of (+)-hernagine and synthesis of (+)-N methylhernagine. *C. R. Acad. Sci.* **1980**, 291, 187-189.
  22. K. Yakushijin, S. Sugiyama, Y. Mori, H. Murata, H. Furukawa. Hernagine, a new aporphine alkaloid, and 3-cyano-4-methoxypyridine from *Hernandia nymphaefolia*. *Phytochemistry*. **1980**, 19, 161-162.
  23. J. Desrivot, J. Waikedre, P. Cabalion, C. Herrenknecht, C. Bories, R. Hocquemiller, A. Fournet. Antiparasitic activity of some new caledonian medicinal plants, *J. Ethnopharmacol.* **2007**, 112, 7-12.
  24. M. Frederich, M. Tits, L. Angenot. Potential antimalarial activity of indole alkaloids, *T. Roy. Soc. Trop. Med. H.* **2008**, 102, 11-19.
  25. J. Ravindran, G. V. Subbaraju, M. V. Ramani, B. Sung, B. B. Aggarwal. Bisdemethylcurcumin and structurally related hispolon analogues of curcumin exhibit enhanced prooxidant, anti-proliferative and anti-inflammatory activities *in vitro*. *Biochem. Pharmacol.* **2010**, 79, 1658-1666.
  26. D. Staerk, E. Lemmich, J. Christensen, A. Kharazmi, C.E. Olsen, J.W. Jaroszewski. Leishmanicidal, antiplasmodial and cytotoxic activity of indole alkaloids from *Corynanthe pachyceras*. *Planta. Med.* **2000**, 66, 531-536.

### 3. LC-MS based identification and structure elucidation of oleamide as a ligand of *Plasmodium falciparum* thioredoxin reductase in *Guatteria recurvisepala*

#### 3.1 Abstract

In this section we screened plant extracts for new ligands to *Plasmodium falciparum* thioredoxin reductase (*PfTrxR*) followed by their identification and structure elucidation. The detannified methanol extracts from *Guatteria recurvisepala*, *Licania kallunkiae*, *Topobea watsonii* were screened for ligands to *PfTrxR* using ultrafiltration and liquid chromatography-mass spectrometry based binding experiments. The *PfTrxR* ligand identified in the extract of *Guatteria recurvisepala* displayed binding affinity of 3.5-fold when incubated with 1  $\mu\text{M}$  *PfTrxR*. The ligand corresponding to the protonated molecule  $m/z$  282.2792  $[\text{M}+\text{H}]^+$  was eluted at a retention time of 17.95 min in a 20 min gradient of 95% B consisting of (A) 0.1% formic acid in 95%  $\text{H}_2\text{O}$ -5% ACN, and (B) 0.1% formic acid in 95% ACN-5%  $\text{H}_2\text{O}$  in an LC-QTOF-MS. Tandem MS of the protonated molecule  $m/z$  282.2792  $[\text{M}+\text{H}]^+$ ,  $\text{C}_{18}\text{H}_{36}\text{NO}$  (DBE: 2; Error: 1.13 ppm) resulted in two daughter ions  $m/z$  265.2516  $[\text{M}+\text{H}-\text{NH}_3]^+$  (DBE: 3; Error: 0.35 ppm) and  $m/z$  247.2405  $[\text{M}+\text{H}-\text{NH}_3-\text{H}_2\text{O}]^+$ , (DBE: 4, Error: 2.26 ppm). This *PfTrxR* ligand was identified as oleamide and confirmed by comparison of the retention time, molecular formula, accurate mass and double bond equivalence with a standard of oleamide. This is the first report on the identification of oleamide as a *PfTrxR* ligand from *Guatteria recurvisepala* R.E. Fr. (Annonaceae) and the corresponding *in vitro* activity against *P. falciparum* strain K1 ( $\text{IC}_{50}$  4.29  $\mu\text{g}/\text{mL}$ ).

### 3.2 Introduction

Drug discovery for treatment of malaria has been challenging because of the emergence of parasites resistant to the conventional antimalarial drugs. Natural products have historically been important sources of antimalarial agents such as artemisinin and quinine [1]. Even though plant-derived natural products are used as traditional herbal remedies; most of them have not been explored for the discovery of new targets for malaria parasite [2]. For this reason, more research on new antimalarial compounds from natural products is needed to develop new therapeutic agents with novel mechanisms of action against *Plasmodium falciparum*. *Plasmodium falciparum* thioredoxin reductase (*PfTrxR*) plays a significant role in antioxidant defense and redox regulation of the parasite and has been previously validated by knock-out studies as a potential drug target for malaria chemotherapy [3].

Plant extracts contain large numbers of different chemical constituents making it difficult to ascertain their antimalarial activity before isolation of the bioactive compounds. A suitable tool to speed up natural product drug discovery is the application of UF-LC-MS based binding assays [4] to screen complex mixtures from plant origins for their binding affinity towards *PfTrxR* followed by MS based structure elucidation and confirmation of the identity of new ligands.

In this study, extracts from three Panamanian plants *Guatteria recurvisepala* R.E. Fr. (Annonaceae), *Topobea watsonii* Cogn. (Melastomataceae) and *Licania kallunkiae* Prance (Chrysobalanaceae), previously shown to be active in antimalarial screening program of Panamanian plants were examined to identify new ligands for *PfTrxR* using our in house *in vitro*

binding experiments. *Guatteria recurvisepala* is a tree 25 m high that grows in evergreen forests. It is characterized taxonomically by young ferruginous-tomentose branches and various flowers in the axila of the leaves [5]. Genus *Guatteria* is the largest genus of Neotropical trees with 265 species wide spread throughout central and tropical America. *Guatteria* species are known for their use in traditional medicine to treat dyspepsia, stomach-ache and uterine pain and also as febrifuges [6].

During the course of our antimalarial screening program using *in vitro* PfTrxR UF-LC-MS based binding experiments for natural products, the detannified methanol extract of *Guatteria recurvisepala* was found to contain a ligand for PfTrxR. This led us to examine the identity of the chemical constituent responsible for binding to PfTrxR. In this chapter we report the *in vitro* antiplasmodial activity of the tested plant extracts, the identification of ligands to PfTrxR by UF-LC-MS based assay and structure elucidation confirmation of the PfTrxR ligand by using high resolution mass spectrometry.

### **3.2.1 Mass spectrometry for identification and structure elucidation of natural products**

A mass spectrometry based approach is an attractive technique for HTS in drug discovery because they provide the accurate mass of the molecule and specific information on the analyte which is used to determine the elemental formulae. Hyphenated techniques such as LC-MS have played a key role in identification of active principles from plant extracts and other complex mixtures which otherwise is a laborious and slow process involving isolation, purification, and structural elucidation steps, which are usually expensive and time-consuming [7]. These techniques combine the separation method with a structural identification technique, usually MS

and NMR. Although NMR is the most powerful technique for the structural elucidation of organic compounds, drawbacks of coupling NMR to LC limits its use as readout compared to MS which has higher sensitivity. Whereas LC-UV alone does not provide complete data for structural elucidation, development of the diode array detector (DAD) has increased its detection power and effectiveness. UV-DAD has been more and more often applied as a first detection method in identification studies using LC because it is rapid and inexpensive, as compared to the other techniques [7].

In LC-MS, complex mixtures and plant extracts are separated in an LC column and sent to the mass spectrometer where they are ionized and further separated in the mass analyzer according to their mass-to-charge ( $m/z$ ) ratio. In tandem mass spectrometry (MS/MS), an ion (called precursor ion) from the first stage of MS is selected and activated, to produce fragment ions, which are then analyzed in the second stage of MS. The most widely employed ion activation method is the collision induced dissociation (CID), which consists in promoting the energy-controlled collision of a chemically inert gas, (e.g. Ar, He, N<sub>2</sub>, or CO<sub>2</sub>) with the precursor ion (Figure 3.1). The collision energy may be chosen, in order to optimize the MS/MS spectrum. Low collision energy values promote soft fragmentation and produce few fragments, whereas high collision energy values prompt extensive fragmentation, so the produced fragment ions can be used to obtain structural information. On the other hand, important structural information can be obtained and eventual comparison with spectral libraries may be made when moderate collision energy values are utilized. MS spectrometers that are used in MS/MS experiments can be of two main types: i) instruments that are able to store the ions, thus allowing for selection of

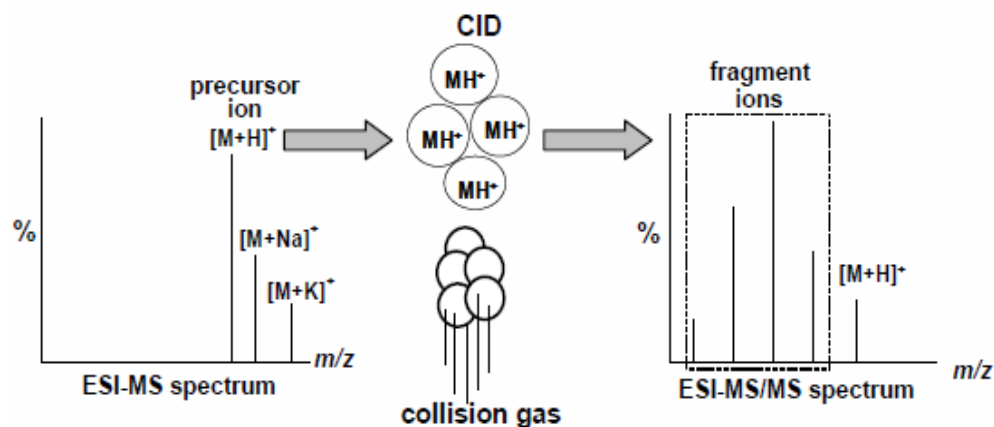


**Figure 3.1** Representation of the CID process in tandem mass spectrometry (MS/MS) [8].

the target ions by injection with authentic patterns, followed by fragmentation, hence generating the mass spectra (e.g. ion cyclotron resonance (ICR), quadrupole ion trap (IT)) and ii) instruments that use a sequence of mass spectrometers in space consisting of quadrupole mass analyzers in sequence (e.g. triple quadrupole, QqQ), or a hybrid MS with quadrupole in sequence e.g., quadrupole-time-of-flight (QTOF) [8].

### 3.2.2 Dereplication of natural products by mass spectrometry

Plant extracts and microorganisms contain a vast number of chemical constituents that may be biologically active and need to be prioritized for the discovery of new drug molecules. For instance, most of the anticancer and antimalarial drugs have been discovered directly from natural products (NPs) or are semi-synthetic derivatives of these natural products. Discovery of novel bioactive compounds from plants is a challenging, laborious, expensive process and requires long time to isolate and characterize an active compound. If the isolated bioactive is known compound then the time and resources spent on it will be a wasted effort [9]. To

overcome these issues, the scientific community has introduced new techniques for the direct identification of bioactive natural products from extracts, thus avoiding re-isolation of already known compounds. Recent HTS technologies to assay plant extracts for biological activity has intensified the need for appropriate dereplication strategies.

Dereplication is the process that allows for the rapid identification of bioactive metabolites in crude extracts by distinguishing previously identified compounds from novel ones. This technique avoids repetitive work of isolation of already known NPs. The dereplication process involves separation of single metabolites by chromatographic methods, identification of these compounds by spectroscopic methods, bioassays for evaluation of the biological activity, and searches in databases for verification of the novelty of these compounds. Liquid chromatography, which enables the analysis of about 60% to 80% of all the existing compounds, has been the most useful tool for the separation of complex mixtures of small molecules [10]. HPLC allows the analyst to identify known compounds by comparison of their retention time and UV spectra which requires the compilation of an internal database because these parameters are not present as searchable fields in most databases. Since UV is not an specific detector, dereplication of unknowns is difficult. Over the past few years, LC-MS combined with DAD has become a widely used tool for dereplication of natural products because of the advantage of using the nominal molecular weight as a search query in nearly all databases along with the UV data to narrow down the answer set. Liquid chromatography mass spectrometry (LC-MS) is a highly sensitive and selective method for identification of NPs in complex mixtures. Compounds separated in the LC column are directed to the mass spectrometer, where they are ionized and separated in the mass analyzer according to their mass-to-charge ( $m/z$ ) ratio. Structure elucidation of the unknown ionized analyte can be achieved by tandem mass spectrometry. In

tandem mass spectrometry (MS/MS), an ion (called precursor ion) from the first stage of MS is selected and activated, to produce fragment ions, which are then analyzed in the second stage of MS to produce fragment ions that can be used to obtain structural information. Dereplication of NPs by means of LC-MS and ESI-MS/MS has often been accomplished on the basis of retention times, UV-DAD spectra, and MS/MS data obtained for each peak of the chromatogram of the crude plant extract as compared to those of previously analyzed authentic standards [10]. MS/MS data of the authentic standards are obtained using the same collision energy value, which is also employed in LC-MS/MS experiments involving the crude extract. The presence of structure diagnostic fragment ions (DFI) is very important for distinction between structural features or for characterization of a class of NPs.

### **3.3 Materials and Methods**

#### **3.3.1 Chemicals and enzymes**

Solvents used for LC-MS and tandem MS analysis were purchased from Fischer Scientific International (Atlanta, GA). Buffer salts, chloroquine (purity  $\geq 98\%$ ) and oleamide (purity 99%) used as standard compounds were purchased from Sigma-Aldrich (Allentown, PA). Deionized water generated by a Milli-Q water system (Millipore, MA) was used in the experiments. *PfTrxR* ( $M_r$  59 kDa) enzyme was provided as a gift by Prof. Katja Becker, Justus-Liebig University, Germany. The recombinant *PfTrxR* was prepared and purified using silver-stained SDS page according to the procedure published by Kanzok et al [7, 11]. The specific activity of *PfTrxR* (1.9 U/mg) was determined by DTNB [5, 5'-dithiobis (2-nitrobenzoic acid)]. Protein concentration of enzymes was determined by Bradford method [8, 12].

### 3.3.2 Plant material

Plants were collected mainly from tropical forests in Panama. Taxonomical information, date and place of collection are provided in Table 3.1. Plants were collected by botanists Carlos Guerra and Alex Espinosa from CIFLORPAN, University of Panama. Taxonomic identification of the plants was performed by Alex Espinosa. Voucher specimens are deposited at the Herbarium of the University of Panama (PMA), Panama.

**Table 3.1** Taxonomic information on the studied plants.

Scientific name	Family	Voucher no.	Collection place / Date of collection
<i>Topobea watsonii</i> Cogn.	Melastomataceae	FLORPAN 6984	El Cope, Cocle. N 08° 36' 52.4" W 080° 09' 09.2". 740 m.a.s.l. April 12, 2007.
<i>Guatteria recurvisepala</i> R.E. Fr.	Annonaceae	FLORPAN 7018	Cerro Azul, Panama. N 09° 11' 47.5" W 79° 23' 53.3". 694 m.a.s.l. April 20, 2007.
<i>Licania kallunkiae</i> Prance	Chrysobalanaceae	FLORPAN 7100	Cerro Azul, Panama. N 09° 11' 59.4" W 079° 23' 39.5". 740 m.a.s.l. June 7, 2007.

m.a.s.l.:meters above sea level.

### **3.3.3 Extraction and isolation**

The extracts were prepared according to the published method [9, 13]. Plant material was extracted with dichloromethane-methanol (1:1 v/v, 600 mL x 2) for 24 h. The extracts were filtered and concentrated *in vacuo* at < 40 °C in a rotary evaporator. The dried extract was redissolved in 100 mL of 90% methanol in water and was partitioned with n-hexane (30 mL, x 3). The aqueous methanol extract portion was collected, concentrated *in vacuo* and the concentrate was treated with 200 mL of a mixture of 20% methanol in chloroform-water (1:1). The resulting extract was washed three times with 50 mL of 1% NaCl. The aqueous phase was discarded and the organic phase was concentrated *in vacuo*. The plant extracts were stored at -80 °C until testing.

## **3.4 Antiplasmodial assays**

### **3.4.1 Antiplasmodial screening of plant extracts**

Antiplasmodial activity was determined in a chloroquine resistant *P. falciparum* strain (W2 Indochina) utilizing a novel microfluorimetric assay to measure the inhibition of parasite growth based on detection of parasitic DNA by intercalation using Pico Green [8, 14]. The IC<sub>50</sub> values were calculated from relative fluorescence units as compared with untreated controls. The parasites were maintained at 2% hematocrit in flat bottom flasks (75 mL) in human red blood cells from O positive blood type donors with RPMI 1640 medium (Gibco BRL) supplemented

with 10% O positive human serum. Chloroquine was used as a standard antimalarial drug and showed an IC<sub>50</sub> value of 85.75 µg/mL.

### **3.4.2 Antiplasmodial activity and IC<sub>50</sub> value of oleamide**

Antiplasmodial activity was determined using the K1 strain of *P. falciparum* (resistant to chloroquine and pyrimethamine). A modification of the [<sup>3</sup>H]-hypoxanthine incorporation assay was used [15]. Briefly, infected human red blood cells in RPMI 1640 medium with 5% Albumax were exposed to serial drug dilutions in microtiter plates. After 48 h at 37 °C in reduced oxygen atmosphere, 0.5 µCi [<sup>3</sup>H]-hypoxanthine was added to each well. Cultures were incubated for a further 24 h before they were harvested onto glass-fiber filters and washed with distilled water. The radioactivity was counted using a Betaplate TM liquid scintillation counter (Wallac, Zurich, Switzerland). The results were recorded as counts per minute (CPM) per well at each drug concentration and expressed as percentage of the untreated controls. From the sigmoidal inhibition curves, IC<sub>50</sub> values were calculated. Assays were run in duplicate and repeated once. Chloroquine was used as a reference antimalarial drug and showed an IC<sub>50</sub> value of 0.069 µg/mL.

### **3.5 PfTrxR enzyme binding assay using ultrafiltration (UF) and LC-MS**

All the plant extracts were tested for their binding affinity at 100 µg/mL. The binding assay was performed according to the published method [4]. The ligands were reconstituted in 100 µL of MeOH- H<sub>2</sub>O (80:20, v/v) and were analyzed by LC-MS. Denatured enzyme was used for

controlled experiment and assays were carried out in duplicate. Bis-2, 4-dinitrophenyl sulfide was used as a reference compound.

### 3.6 LC-MS and tandem MS analysis

Plant extracts for LC-MS analysis were prepared using MeOH - H<sub>2</sub>O (80:20, v/v). Liquid chromatography analysis of plant extracts was performed using a ZORBAX Eclipse plus C18 column (2.1 mm x 100 mm, 1.8 μm) at a flow rate of 0.2 mL/min. The plant extracts were analyzed at 25 μg/mL using gradient mobile phase (5% B → 95% B in 15 min, 95% B from 15 - 18 min and return to 5% B at 20 min) consisting of (A) 0.1% formic acid in 95% H<sub>2</sub>O-5% ACN (v/v/v) and (B) 0.1% formic acid in 95% ACN-5% H<sub>2</sub>O (v/v/v) at a flow rate of 0.2 mL/min for a run time of 20 min. The LC-MS analysis was carried out in an Agilent (Little Falls, DE) 6520 accurate-mass quadrupole time of flight (Q-TOF) mass spectrometer equipped with a 1220 rapid resolution liquid chromatography (RRLC) system. The chemical constituents in the plant extract were detected using positive ESI. The standard compound oleamide was analyzed at 1 μM under the same conditions mentioned above. All the tested compounds were detected by MS at capillary voltage of 3200-3500 V for ESI positive mode. Nitrogen was supplied as nebulizing and drying gas at flow rates of 25 and 600 L/h, respectively. The drying gas temperature was 350 °C. The fragmentor voltage was optimized to 175-180 eV. In tandem LC-MS/MS analysis, the *PfTrxR* ligand from *Guatteria recurvisepala* plant extract and oleamide were subjected to MS/MS experiments using the following parameters: collision energy 60 v, slope 6 m/z offset 8 v, acquisition rate 1.4 spectra/sec, time 714.3 ms/spectrum to study their fragmentation pattern.

Data were acquired and analyzed using Agilent MassHunter Workstation Qualitative Analysis software, version B.02.00. 2.4.

### 3.7 Results and Discussion

Plant extracts were tested at 100 µg/mL for their antiplasmodial activity against a chloroquine resistant *P. falciparum* strain (W2 Indochina) and the percentage of *P. falciparum* growth inhibition of *Guatteria recurvisepala* (leaves), *Topobea watsonii* (stems and branches) and *Licania kallunkiae* (stems) were 56.8%, 58.0% and 85.8%, respectively. Extracts with percentages of *P. falciparum* growth inhibition of  $\geq 50\%$  were considered active. These plant extracts at a concentration of 100 µg/mL were incubated with 1 µM *PfTrxR* at 25 °C for 1 hr to identify new ligands by UF-LC-MS based binding experiments. After the incubation period, the ligands were separated and reconstituted in 100 µL MeOH: H<sub>2</sub>O (80:20) and submitted to LC-MS analysis (Figure 3.2A). Prior to identification of the ligands, LC conditions for plant extracts were optimized (Figure 3.2C) as described in Materials and Methods. We found that the protonated molecule  $m/z$  282.2792 [M+H]<sup>+</sup> from *Guatteria recurvisepala* extract, eluted at 17.95 min, displayed strong binding affinity of 3.5-fold when incubated with 1 µM *PfTrxR* (Figure 3.2B). No binding was observed for compounds in the other two plant extracts. The MS analysis of the *PfTrxR* ligand, protonated molecule  $m/z$  282.2792 [M+H]<sup>+</sup>, resulted in molecular ion formula of C<sub>18</sub>H<sub>36</sub>NO, and double bond equivalence (DBE) of 2 with an error of 1.13 ppm. Tandem LC-MS analysis was performed on *Guatteria recurvisepala* extract to study the fragmentation pattern of the ligand, which resulted in two daughter ions  $m/z$  265.2516 with molecular ion formula C<sub>18</sub>H<sub>33</sub>O from the loss of ammonia [M+H-NH<sub>3</sub>]<sup>+</sup>, DBE of 3 (error: 0.35

ppm), and  $m/z$  247.2405 with molecular ion formula of  $C_{18}H_{31}$  from the loss of ammonia and water  $[M+H-NH_3-H_2O]^+$ , DBE of 4, (error: 2.26 ppm). Following MS analysis of the ligand, standard compound oleamide was analyzed under similar LC-MS (Figure 3.2D) and tandem MS/MS conditions (Figure 3.3). The exact mass, retention time, DBE and fragmented ions of oleamide [11, 16] were exactly the same as those of the *PfTrxR* ligand from the plant extract. On the basis of the above results, we confirm the identity of *PfTrxR* ligand from *Guatteria recurvisepala* extract as oleamide. Oleamide was submitted to *in vitro* testing against *P. falciparum* K1 and displayed an  $IC_{50}$  of 4.29  $\mu\text{g/mL}$ .

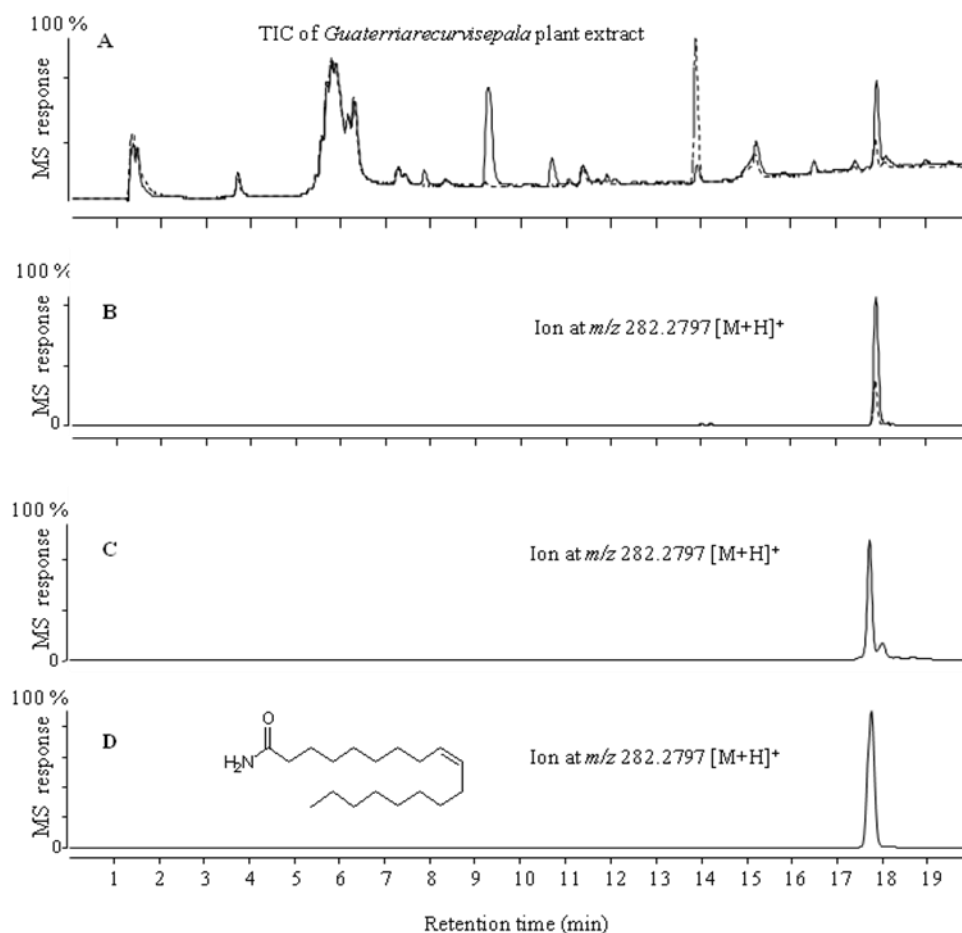


**Figure 3.2** UF-LC-MS based binding experiment of *Guatteria recurvisepala* plant extract incubated with 1  $\mu\text{M}$  *PfTrxR*. Solid line represents the ligand incubated with active enzyme and

the dotted line represents the control experiments using denatured enzyme. (B) Extracted ion chromatogram (EIC) of ligand from binding experiment of *Guatteria recurvisepala* extract. (C) EIC of protonated molecule  $m/z$  282.2792  $[M+H]^+$  from LC-MS analysis of plant extract. (D) EIC of oleamide from LC-MS analysis of standard compound oleamide with its structure

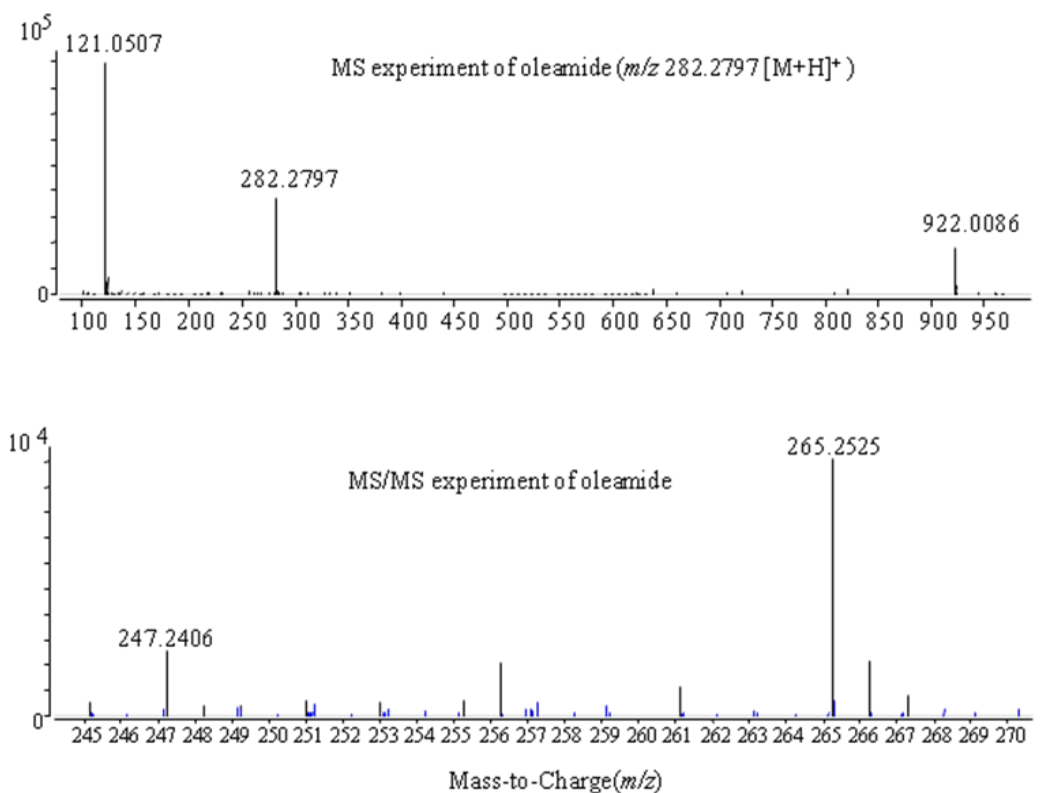


**Figure 3.3** MS analysis of standard compound oleamide with parent ion  $m/z$  282.2792  $[M+H]^+$  (ions at  $m/z$  121.0507 and 922.0086 correspond to reference masses) and MS/MS analysis of oleamide producing two daughter ions  $m/z$  247.2406 and  $m/z$  265.2525.

Detannified methanol extracts of *Guatteria recurvisepala* (Annonaceae), *Topobea watsonii* (Melastomataceae) and *Licania kallunkiae* (Chrysobalanaceae) displayed *in vitro* antiplasmodial activity when tested against *Plasmodium falciparum* W2 Indochina strain. These plant extracts were tested to identify ligands for PfTrxR by UF-LC-MS based binding

experiments. Extracts were initially analyzed in both ESI negative and positive modes with the same LC conditions. The chemical constituents of the plant extracts displayed higher ionization efficiency in ESI positive mode; hence binding experiments were carried out in this mode. Among the three plant extracts, protonated molecule  $m/z$  282.2792  $[M+H]^+$  from *Guatteria recurvisepala* displayed binding affinity to the enzyme. Members of the Annonaceae family such as *Guatteria species* (bark) are known for their antimalarial activity [12, 17]. MS/MS experiments on the ligand from *Guatteria recurvisepala* led to its identification as oleamide. UF-LC-MS based binding experiments can be considered as an alternative technique to identify ligands from plant extracts in contrast to other techniques which otherwise are associated with high cost and time consuming methods to isolate, purify and identify the chemical constituents from plant extracts. We report here the first time oleamide from *Guatteria recurvisepala* plant extract and as a ligand to *PfTrxR*. Oleamide was earlier identified in the plant extract of *Aquilegia vulgaris* L. (Ranunculaceae) [13, 18] and essential oil of fresh mountain celery (*Cryptotaenia japonica* Hassk, Apiaceae) [14, 19].

### 3.8 Conclusions

The LC-MS based *PfTrxR*-ligand binding approach was validated to screen plant extracts by the antiplasmodial activity displayed by oleamide when tested as a pure compound. Herein we suggest that MS based binding experiments with their exceptional selectivity and high sensitivity have greater potential to identify ligands [15, 20] directly from the plant extracts to provide specific information that can be used for isolation and characterization of specific chemical constituents ignoring others.

### 3.9 References

1. M. A. van Agtmael, T. A. Eggelte, C. J. van Boxtel. Artemisinin drugs in the treatment of malaria: from medicinal herb to registered medication. *Trends in Pharmacol. Sci.* **1999**, 20, 199-205.
2. M. J. Balunas, A. D. Kinghorn. Drug discovery from medicinal plants. *Life Sci.* **2005**, 78, 431-441.
3. A. D. Andricopulo, M. B. Akoachere, R. Krogh, C. Nickel, M. J. McLeish, G. L. Kenyon, L. D. Arscott, C. H. Williams, E. Davioud-Charveta, K. Beckerc. Specific inhibitors of *Plasmodium falciparum* thioredoxin reductase as potential antimalarial agents. *Bioorg. Med. Chem. Lett.* **2006**, 16, 2283-2292.
4. V. Mulabagal, A. I. Calderón. Development of binding assays to screen ligands for *Plasmodium falciparum* thioredoxin and glutathione reductases by ultrafiltration and liquid chromatography/mass spectrometry. *J. Chromatogr. B.* **2010**, 878, 987-993.
5. W. D. Douglas. Florade Nicaragua Online. Available at <http://mobot.mobot.org/W3T/Search/Nicaragua/projsf1nic.html>. Accessed on November 11, **2010**.
6. G. S. M. Jose, H. A. A. Eloisa, M. M. C. Lea, O. Jorge, S. A. Josiele. Essential oils of the amazon *Guatteria* and *Guatteriopsis* species. *Flavour Fragr. J.* **2005**, 20, 478-480.
7. K. Tobias, F. Oliver. Advances in structure elucidation of small molecules using mass spectrometry. *Bioanal. Rev.* **2010**, 2, 23-60.

8. J. D. Herbert, I. M. Nathalya, E. M. C. Antônio. Electrospray ionization tandem mass spectrometry as a tool for the structural elucidation and dereplication of natural products: An overview. *Tandem Mass Spectrometry - Applications and Principles*. **2012**, 595-618.
9. A. C. Geoffrey and G. S. Young. Finding the needle in the haystack. The dereplication of natural product extracts. *Pure Appl. Chem.* **1999**, 71 (6), 1089-1094.
10. J. L. Wolfender, K. Ndjoko, K. Hostettmann. Liquid chromatography with ultraviolet absorbance–mass spectrometry detection and with nuclear magnetic resonance: a powerful combination for the on line structural investigation of plant metabolites. *J. Chromatogr. A.* **2003**, 1000, 437-455.
11. S. M. Kanzok, R. H. Schirmer, I. Turbachova, R. Iozef, K. Becker. The thioredoxin system of the malaria parasite *Plasmodium falciparum*. *J. Biol. Chem.* **2000**, 275, 40180-40186.
12. M. M. Bradford. A rapid and sensitive method for the quantitation of microgram quantities of proteins utilizing the principle of protein-dye binding. *Anal. Biochem.* **1976**, 72, 248-254.
13. M. E. Wall, M. C. Wani, D. M. Brown, F. Fullas, J. B. Olwald, F. F. Josephson, N. M. Thornton, J. M. Pezzuto, C. W. W. Beecher. Effect of tannins on screening of plant extracts for enzyme inhibitory activity and techniques for their removal. *Phytomedicine*. **1996**, 3, 281-285.
14. Y. Corbett, L. Herrera, L. Cubilla, T. L. Capson, P. D. Coley, T. A. Kursar, L. I. Romero, E. A. Ortega-Barría. Novel DNA-based microfluorimetric method to evaluate antimalarial drug activity. *Am. J. Trop. Med. Hyg.* **2004**, 70, 119-124.
15. H. Matile, J. R. L. Pink. *Plasmodium falciparum* malaria parasite cultures and their use in immunology. *Immunological Methods*. **1990**, 231-234.

16. F. C. Benjamin, A. L. Richard, L. B. Dale. Structure determination of an endogenous sleep-inducing lipid, cis-9-octadecenamide (oleamide): A synthetic approach to the chemical analysis of trace quantities of a natural product. *J. Am. Chem. Soc.* **1996**, 118, 580-590
17. W. Milliken. Malaria and antimalarial plants in Roraima, Brazil. *Econ. Bot.* **1997**, 51, 212-237.
18. R. Solomonias, N. Kuchiashvili, A. Berulava, V. Pkhakadze, N. Trapaidze, M. Zhvania, I. Abesadze, H. Kojima, N. Dalakishvili. Purification and identification of components of the *Aquilegia vulgaris* extract fraction exhibiting anti-epileptic activity. *J. Biol. Phys. Chem.* **2004**, 4, 185-192.
19. M. C. Cheng, Y. B Ker, T. H. Yu, L. Y. Lin, R. Y. Peng, C. H. Peng. Chemical synthesis of 9(z)-octadecenamide and its hypolipidemic effect: a bioactive agent found in the essential oil of mountain celery seeds. *J. Agric. Food. Chem.* **2010**, 58, 1502-1508.
20. Z. Christine, H. Georg, T. W. Klaus. Expanding the scope of MS binding assays to low-affinity markers as exemplified for mGAT1. *Anal. Bioanal. Chem.* **2008**, 391, 309-316.

#### **4. Development of liquid chromatography/mass spectrometry based screening assay for *Pf*TrxR inhibitors using relative quantitation of intact thioredoxin.**

##### **4.1 Abstract**

We have developed a liquid chromatography/mass spectrometry (LC-MS)-based functional assay to identify inhibitors of *Pf*TrxR by quantifying the product formed (Trx-(SH)<sub>2</sub>) in the enzymatic reaction. Relative quantitation of the reaction product (intact Trx-(SH)<sub>2</sub>) was carried out using an Agilent 6520 QTOF mass spectrometer equipped with a positive mode electrospray ionization (ESI) source. The calibration curve prepared for Trx-(SH)<sub>2</sub> at concentrations ranging from 1.8 to 116.5 mg/mL was linear ( $R^2 > 0.998$ ). The limit of detection (LOD) and limit of quantification (LOQ) of Trx-(SH)<sub>2</sub> were at 0.45 and 1.8 mg/mL respectively. To validate the developed functional assay we have screened reference compounds **1**, **2** and **3** for their *Pf*TrxR inhibitory activity and ten natural compounds (at 10 mM) which were earlier identified as ligands of *Pf*TrxR by a UF-LC-MS based binding assay. The developed LC-MS-based functional assay for identification of inhibitors of *Pf*TrxR is a sensitive and reliable method that is also amendable for high-throughput format. This is the first representation of a relative quantitation of intact Trx-(SH)<sub>2</sub> using LC-MS.

## 4.2 Introduction

Malaria continues to be a significant health problem of global dimensions. Only a limited number of chemotherapeutic agents for the treatment of malaria are available, and the growing problem of drug resistance makes adequate treatment of malaria increasingly difficult [1]. Screening natural products in enzymatic bioassays remains challenging with resource-intensive steps in the natural product drug discovery process [2]. *P. falciparum* (*Pf*) thioredoxin reductase (TrxR), a 59 kDa flavoprotein catalyzes the NADPH dependent reduction of *P. falciparum* thioredoxin (*Pf*Trx), an 11.7 kDa protein. Thioredoxin (Trx) contains two redox-active half-cysteine residues in an exposed active center, having Cys-Gly-Pro-Cys sequence. Trx exists either in reduced form (Trx-(SH)<sub>2</sub>) with a dithiol, or in oxidized form (Trx-S<sub>2</sub>). The S-S-bond of Trx-S<sub>2</sub> is reduced to Trx-(SH)<sub>2</sub> by NADPH and *Pf*TrxR enzyme [3]. Trx-(SH)<sub>2</sub> regulates the activity of *P. falciparum* by reducing the cellular environment. Trx - (SH)<sub>2</sub> acts as hydrogen donor to ribonucleotide reductase and methionine sulfoxide reductase, involved in DNA synthesis and protein repair. Trx-(SH)<sub>2</sub> can directly reduce hydrogen peroxide and can function as both single oxygen quencher and hydroxyl radical scavenger. These functions of Trx-(SH)<sub>2</sub> are in response to oxidative stress of the parasite [4]. Inhibition of *Pf*TrxR enzyme is likely to affect the parasite at several vulnerable points resulting in enhanced oxidative stress, ineffective DNA synthesis and cell division, and disturbed redox regulatory processes. Disruption of the Trx/TrxR balance would have pleiotropic effects on cellular function making it an attractive target for disease control [5]. Enzymatic assays like NADPH, 5,5'-dithiobis(2-nitrobenzoate) (DTNB) and insulin reduction assays have been developed for testing a variety of compounds for their inhibitory activity towards *Pf*TrxR. These assays do not measure product formed (reduced

*PfTrx*) in the reaction; they instead measure inhibitory activity based on UV detection at 340 nm of decreased NADPH levels, 412 and 405 nm of reduced DTNB levels during the enzymatic reaction, respectively [6–8]. Application of liquid chromatography/mass spectrometry (LC-MS) in the identification and relative quantitation of intact Trx–(SH)<sub>2</sub> from the enzymatic reaction based not only on significant differences in protein mass but also on variations in levels of protein formation in the reaction can be a useful tool in the analysis and identification of specific inhibitors for *PfTrxR* [9].

#### **4.2.1 Role of mass spectrometry for detection of enzyme inhibition**

Enzymes are one of the most important classes of drug targets because of the essential roles played by enzymes in life processes and pathophysiology. In the drug discovery process a macromolecule such as an enzyme whose activity is essential for pathogenic species is selected and a library of pure compounds or mixtures of compounds are screened to identify inhibitors. It is of utmost importance to develop rapid and sensitive methods for the study of enzymatic catalysis mechanisms and the characterization of enzymatic activities. Many screening methodologies like UV, radioactivity and fluorescence detection techniques have been employed to identify inhibitors and to study kinetic parameters. Many of the biochemical assays for detection of enzyme inhibition are based on the change of the spectroscopic properties during the conversion of the substrate or cofactor [10]. The major drawback of these techniques is that most natural substrates do not possess the fluorescent or chromophoric moieties; therefore it is necessary to introduce those functionalities synthetically into the molecular structure. These modifications might alter the enzyme recognition of the substrate compound, thus changing the

kinetic behavior significantly. The use of radioisotope substrates in enzymatic reactions is advantageous but unfortunately, the availability of radioactive-labeled substrate compounds were often limited.

Therefore, the demand for a label-free, non-radioactive biochemical assays like MS based enzymatic assays can be a viable alternative to established detection methods. There are several advantages of using MS for screening over other techniques. MS based screening assays can be performed in label free mode, can detect a range of compounds such as substrate, product(s), cofactors and coenzymes, and internal standards (ISs) which can be used to monitor the relative enzyme activity and enzyme inhibition. Accurate mass and fragmentation of identified molecule can lead to discovery of selective inhibitors [10]. ESI-MS plays an important role in a wide range of different applications such as analyte quantification, structure elucidation of biomolecules as well as protein-protein- and protein-ligand interaction studies. The enzymatic reaction carried out off-line can be quenched with 0.5% formic acid or methanol after a defined time. Then the crude reaction mixture can be directly injected into an ESI-MS system and the amount of product formed can be quantified using a calibration curve. The inhibitory activity of the library of compounds can be assessed by comparison to the amount of product formed in a reference assay where there is no inhibitor as in Figure 4.1. ESI-MS-based assay schemes have the advantage of being directly compatible to the liquid-phase reaction conditions [11]. Therefore, it is possible to monitor enzymatic conversions on-line by coupling the reaction vessel directly to the ionization interface of the mass spectrometer.

Generally, the application of mass spectrometry for detection in enzymatic bioassays offers very intriguing possibilities. MS-based assay schemes certainly cannot replace the optical or radioactivity-based assay schemes in routine analysis, but they are an extremely valuable

alternative providing access to areas of enzymology, which could not be studied by the established methodologies [11]. Furthermore, MS-detection schemes seem to have a great potential for the application in high-throughput screening procedures in drug development and biocatalysis research.

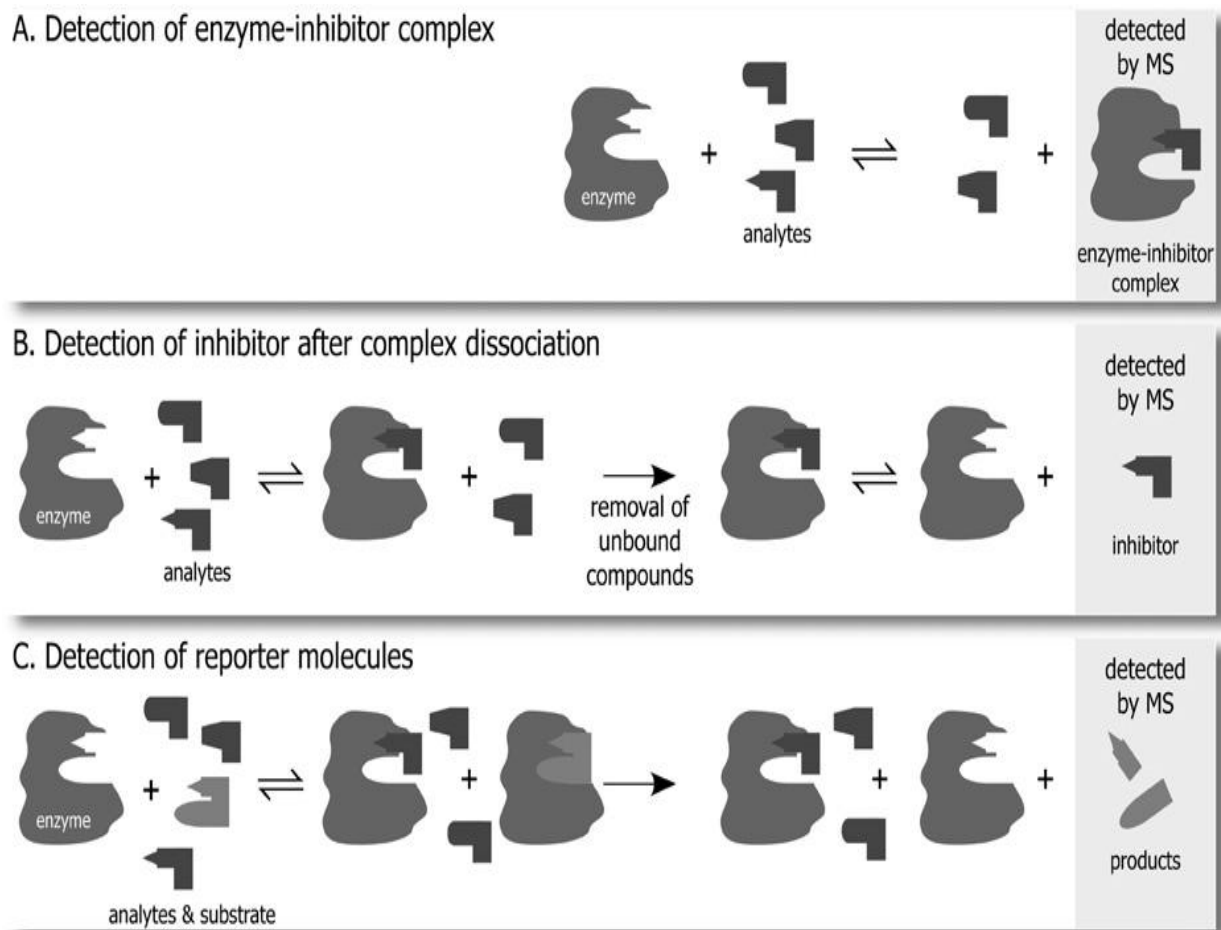


**Figure 4.1** The principles of MS-based screening. (A) Direct screening of the enzyme-inhibitor complex; (B) Direct screening of inhibitor after complex dissociation; and, (C) Indirect screening by reporter molecules [10].

#### 4.2.2 Identification and quantitation of intact proteins

Our goal was to develop a functional assay to screen natural products for *Pf*TrxR inhibitors based on relative quantitation of Trx—(SH)<sub>2</sub> in the enzymatic reaction by LC-MS. There is substantial sample complexity in an enzymatic reaction mixture, which makes it difficult to resolve and accurately quantify proteins of interest. This work represents a method which circumvents the challenge of separating the proteins of interest from the enzymatic reaction mixture and simultaneously quantifying the proteins [12]. Mass spectrometry of proteins can use either the "bottom up" or the "top down" approach. The top-down proteomic techniques in which intact proteins rather than peptides are measured, are advantageous for the detection of post-translational modifications [13]. Signal intensity based relative quantitation approaches are promising alternatives to isotope labeling approaches and have been applied to quantify differentially expressed proteins from complex biological samples [14]. Protein peak intensity measurement is simple and cost effective and has demonstrated high reproducibility and linearity. Several studies have demonstrated that extracted ion chromatograms of selected *m/z* values from MS spectra of the protein correlated well with protein abundance in complex biological samples [14]. It is important to recognize that the top-down method characterizes and measures intact protein without the use of enzymatic digestion and distinguishes between multiple protein isoforms or distinct proteins that share a common peptide sequence. Intact proteins are chromatographically separated and introduced directly into the mass spectrometer, and separated on the basis of their mass-to-charge ratio. Quantitative analysis of intact proteins is commonly addressed using reversed phase chromatography coupled with mass spectrometric-

based approaches [15]. Consequently, the demand for the determination of concentrations of intact proteins in drug development has significantly increased in recent years. The developed method demonstrates that by comparing the peak areas of Trx–(SH)<sub>2</sub> in control with test samples, a relative peak area ratio is obtained. This ratio can then be used to determine the inhibitory activity of the ligands on *PfTrxR* [16]. Mass spectrometry analysis of intact proteins in the *PfTrxR* functional assay demonstrates a high degree of sensitivity, specificity and reliability.

## 4.3 Experimental

### 4.3.1 Chemicals and reagents

NADPH, potassium phosphate (dibasic), formic acid, EDTA and Trx–(SH)<sub>2</sub> (*E. coli*, recombinant) were purchased from Sigma–Aldrich (St. Louis, MO). Solvents were purchased from Fischer Scientific International (Atlanta, GA). Trx–S<sub>2</sub> was purchased from Wako Chemicals USA, Inc. Compounds (**4–13**) were purchased from AnalytiCon Discovery GmbH (Germany). Compounds **1–3** (bis 2,4-dinitrophenyl sulfide (1), 4-nitrobenzothiadiazole (2) and 3-(dimethylamino)-propiophenone (3)) (Figure 4.2), were purchased from Sigma–Aldrich (St. Louis, MO). Double deionized water was generated by a Milli-Q water system (Millipore, MA). Nanosep® 30 kDa MWCO filters were purchased from Pall® Life Sciences, Ann Arbor, MI. *PfTrxR* (Mr, 59 kDa) enzyme was a kind gift from Prof. Katja Becker, Justus-Liebig University, Giessen, Germany. The recombinant *PfTrxR* was prepared and purified using silver-stained SDS page according to the procedure published by Kanzok et al. [17]. The specific activity of *PfTrxR* (1.9 U/mg) was determined by DTNB [5,5-dithiobis(2-nitrobenzoic acid)]. Protein concentration of enzymes was determined by Bradford method [18].

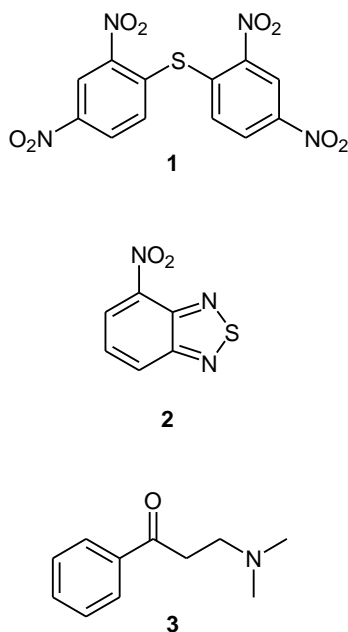


**Figure 4.2** Structures of reference compounds 1, 2 and 3

#### 4.3.2 Functional assay

10  $\mu\text{M}$  test compound (in 1% DMSO) was incubated with 0.5  $\mu\text{M}$  *PfTrxR* enzyme and 200  $\mu\text{M}$  NADPH in the assay buffer (PE buffer: 100 mM potassium phosphate and 2 mM EDTA, pH 7.4). The enzymatic reaction was initiated by addition of 2.5  $\mu\text{M}$  Trx-S<sub>2</sub> and incubated at 25 °C for 30 min. After the incubation, the reaction was quenched by the addition of 0.1% formic acid. The reaction mixture was filtered through a 30 kDa cut-off ultrafiltration membrane centrifuged at 13,000 rpm at 20 °C for 10 min. The enzyme was trapped on the membrane and product (Trx-(SH)<sub>2</sub>) formed in the reaction was recovered in the filtrate and analyzed by LC-MS. Control experiment (without inhibitor) was performed the same way and the amount of Trx-(SH)<sub>2</sub> was used to reference the activity in the test sample. A calibration curve using

known amounts of Trx-(SH)<sub>2</sub> was prepared to quantify the amount of Trx-(SH)<sub>2</sub> produced in the reactions.

### 4.3.3 Sample preparation

Trx (1 mg/mL) stock solutions were prepared in PE buffer. NADPH 2 mg/mL stock solution was prepared in 80% PE buffer. Inhibitor stock solutions were prepared in DMSO. The concentration of DMSO in the assay was kept at 1%.

### 4.3.4 Trx-(SH)<sub>2</sub> calibration curve

Serial dilutions of reduced *Pf*Trx (Trx-(SH)<sub>2</sub>) ranging from 1.8 to 116.5 µg/mL were prepared in PE buffer. Triplicate data points were collected and plotted using the least squares regression (Figure 4.3).

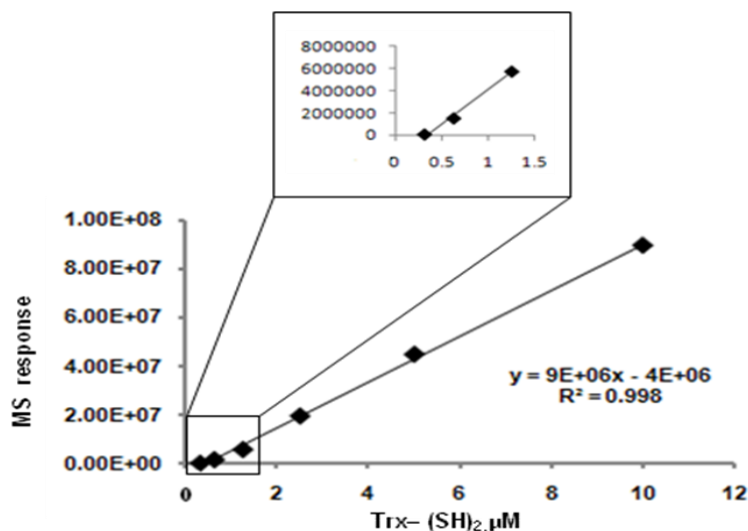


**Figure 4.3.** Calibration curve of intact Trx-(SH)<sub>2</sub>.

#### 4.3.5 LC-MS analysis of intact thioredoxin

An Agilent 1220 Rapid Resolution Liquid Chromatography (RRLC) system (Agilent technologies, Santa Clara, CA) coupled to mass spectrometer was used to separate two intact proteins. A 1:1 mixture comprising 2.5  $\mu\text{M}$  of Trx-S<sub>2</sub> and Trx-(SH)<sub>2</sub> intact proteins were loaded on a 2.1 mm (internal diameter) Poroshell 300 SB C<sub>18</sub> (length 75 mm) column (particle size 5  $\mu\text{M}$ ) with a flow rate of 0.4 mL/min in solution A water (0.1% formic acid) and solution B acetonitrile (0.1% formic acid). The gradient was run as follows: 3% B for 0-2 min, 3-35% B for 2 min and 35-65% B for 6 min, total gradient time is 10 min at column temperature of 60 °C. The retention times of Trx-S<sub>2</sub> and Trx-(SH)<sub>2</sub> were 7.5 min and 6.9 min (Figure. 4.4) with average measured mass of 11673.5278 Da (ppm: 1.3) and 11675.5434 (ppm: 1.27) respectively. Quantitation of relative amount for intact Trx-(SH)<sub>2</sub> used total ion count from ESI<sup>+</sup> spectrum. The MS settings used nebulizer drying gas at 10 L/min, nebulizer pressure at 30 psig, gas temperature at 350 °C, capillary voltage at 4000 V, fragmentor at 250 V, skimmer at 60 V. Acquisition rate was at 1 scan/sec scanning from 300-3200 *m/z*.

#### 4.3.6 Data Analysis

Protein molecular weight analysis software (MassHunter Bioconfirm, Ver. B.02.00) was used to deconvolute multiply charged protein ions to the molecular weight (Figure. 4.5c) that distinguishes Trx-S<sub>2</sub> from Trx-(SH)<sub>2</sub> easily due to mass accuracy at 1/100 of a Dalton.

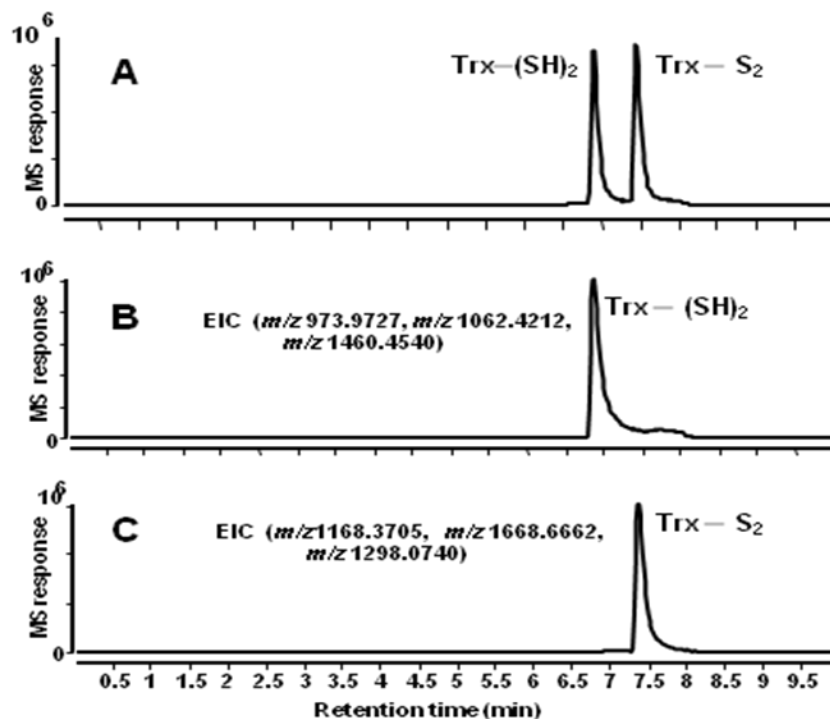


**Figure 4.4** (A) LC-MS analysis of thioredoxin. (B) Extracted ion chromatogram (EIC) of product formed (reduced thioredoxin) in control experiments (without inhibitor). (C) Extracted ion chromatogram (EIC) of substrate (oxidized thioredoxin) in the presence of compound 1 at 10  $\mu$ M where no reduced thioredoxin was formed.

Major  $m/z$  values such as 973.9727, 1062.4212 and 1460.4540 from multiply charged protein envelope in Trx-(SH)<sub>2</sub> spectrum were used for relative quantitation by displaying the extracted ion chromatogram (EIC) (Figure. 4.5b). EICs were integrated to obtain peak areas and then compared in both test and control samples. The  $m/z$  values were kept consistent throughout the analysis of the intact Trx-(SH)<sub>2</sub>. The IC<sub>50</sub> values were calculated by plotting the test compound concentration (log concentration) versus percent inhibition on *Pf*TrxR with respect to the control experiments. The dose-response curves (Figure 4.6) were constructed using graphic software (Prism 5.20, GraphPad Software, Inc., La Jolla, CA) whose IC<sub>50</sub> values are given in Table 4.1.

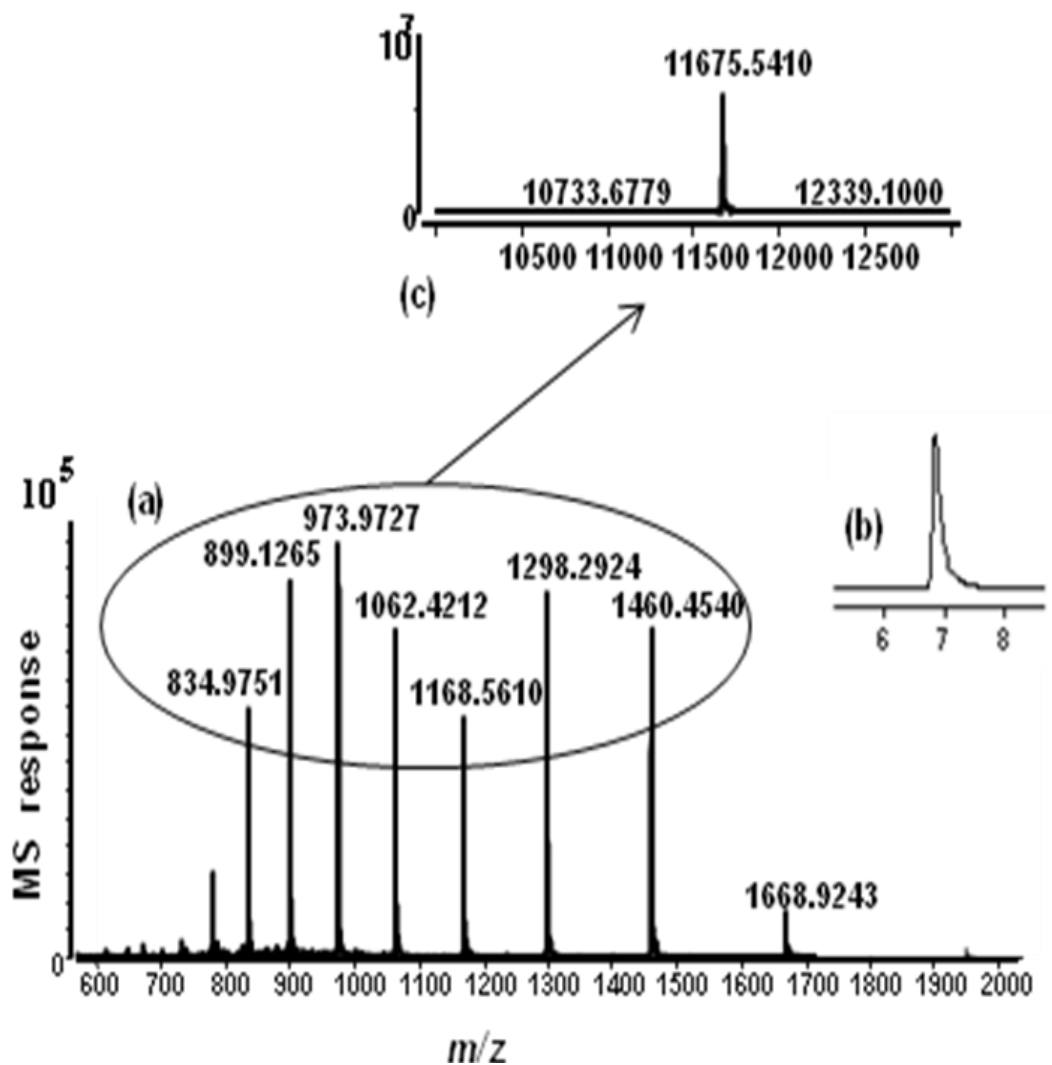


**Figure 4.5** (a) MS spectra of Trx-(SH)<sub>2</sub>. (b) Extracted ion chromatogram (EIC:  $m/z$  973.9727,  $m/z$  1062.4212,  $m/z$  1460.4540) of Trx-(SH)<sub>2</sub>. (c) MS spectra deconvoluted to obtain molecular weight of Trx-(SH)<sub>2</sub>.

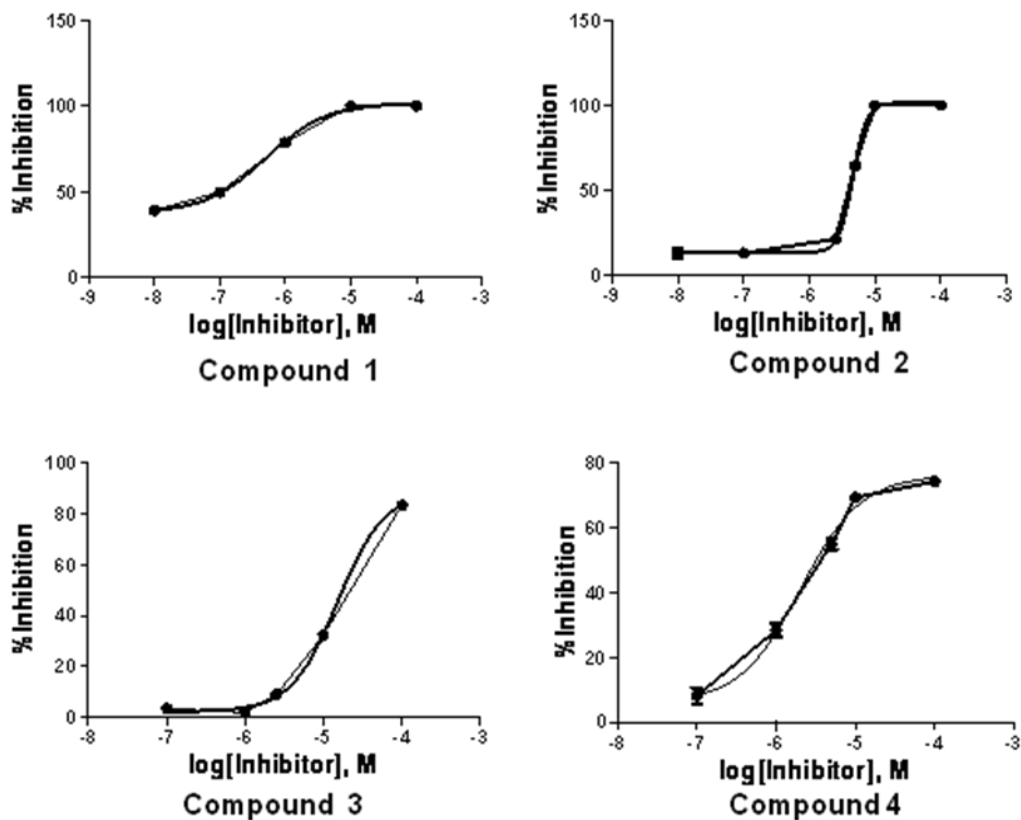


**Figure 4.6** Dose response curves of compounds **1**, **2**, **3** and **4** tested at 0.5  $\mu\text{M}$  *PfTrxR*.

**Table 4.1**  $\text{IC}_{50}$  values of compounds **1** – **4** tested in duplicates and injected in triplicates.

Compound	Log $\text{IC}_{50}$	$\text{IC}_{50}$ ( $\mu\text{M}$ )	R Square
1	-6.29	0.52	0.9963
2	-5.33	4.60	0.9940
3	-4.81	15.21	0.9966
4	-5.69	2.03	0.9856

#### 4.4 Results and Discussion

The assay for the identification of inhibitors for *PfTrxR* consists of the following three key elements: RRLC reversed phase separation, enzymatic assay, and ESI-MS as readout. The enzymatic assay is based on detection of reaction product of a substrate-conversion-based redox reaction. In this study we report the method development of a functional assay for evaluating the inhibitory activity of *PfTrxR* ligands. LC-MS conditions were optimized for Trx-S<sub>2</sub> and Trx-(SH)<sub>2</sub> protein ionization prior to the functional assay (Figure 4.4). The product formed in the functional assay experiments was quantified using the relative peak areas of Trx-(SH)<sub>2</sub> in control and test sample. The response of Trx-(SH)<sub>2</sub> ion intensity to concentration in the calibration curve was linear ( $R^2 > 0.998$ ). The limit of detection (LOD) and the limit of quantitation (LOQ) for Trx-(SH)<sub>2</sub> were found at 0.45 µg/mL (or 4.5 ng with S/N ratio of 9) and 1.8 µg/mL (or 18 ng), respectively. To validate the assay, reference compounds **1–3** (Figure 4.2), known inhibitors of *PfTrxR* from the literature were tested for their inhibitory activity towards the enzyme. Compounds **1** and **2** were reported as uncompetitive inhibitors (where the inhibitors bind to one of the enzyme-substrate intermediate complexes) of *PfTrxR* with IC<sub>50</sub> values 0.5 µM and 2 µM respectively according to Andricopulo et al. [6]. Compound **3**, a saturated Mannich base was found to inhibit the enzyme by electrophilic attack on electron rich thiol groups present on *PfTrxR* with IC<sub>50</sub> 15.4 µM according to Davioud-Charvet et al. [19]. The reference compounds (**1-3**) and compound **4** were initially tested at 10 µM in the newly developed functional assay. Complete inhibition of 0.5 µM *PfTrxR* characterized by no formation of Trx-(SH)<sub>2</sub> was not observed when compounds **1** and **2** were tested at 10 µM. Compound **3**, a

saturated mannich base displayed more than 50% inhibition of *PfTrxR* at 10  $\mu\text{M}$ . A dose-response curve was developed (% inhibition vs concentration) for these reference compounds with concentrations ranging from 0.01  $\mu\text{M}$  to 100  $\mu\text{M}$  by incubating with 0.5  $\mu\text{M}$  *PfTrxR* at 25  $^{\circ}\text{C}$  followed by quantification of  $\text{Trx}-(\text{SH})_2$  by LC-MS. The percent inhibition of the reaction product  $\text{Trx}-(\text{SH})_2$  was calculated using the equation  $100 (c_0 - c)/c_0$ , where  $c_0$  was the amount of  $\text{Trx}-(\text{SH})_2$  produced with no inhibitor and  $c$  was the concentration of  $\text{Trx}-(\text{SH})_2$  with inhibitor. When the  $c$  value was zero (as in case of DNPS), it meant that there was no product formed in the reaction mixture in presence of the inhibitor. Hence it was considered as 100% inhibition of the reaction product. Compounds **1**, **2** and **3** displayed  $\text{IC}_{50}$  values of 0.52, 4.6 and 15.21  $\mu\text{M}$ , respectively (Table 4.1). The  $\text{IC}_{50}$  values determined for compounds **1** and **3** in the newly developed functional assay were in good agreement with reported values in the literature using UV based bioassay [6, 19]. From these results we conclude that our functional assay can be used to screen competitive and uncompetitive inhibitors of *PfTrxR*. In addition to the reference compounds **1** to **3**, we also tested the inhibitory activity of 10 compounds such as demethoxycurcumin (**4**), yohimbine (**5**), catharanthine (**6**), vobasine (**7**), gnetifolin E (**8**), quinidine N-oxide (**9**), 11-hydroxycoronaridine (**10**), hispolone (**11**), hispolone methyl ether (**12**), and hernagine (**13**) at 10  $\mu\text{M}$ . These compounds were identified as ligands with binding affinity more than 2 fold to *PfTrxR* at 1  $\mu\text{M}$  by UF-LC-MS based binding assay [4]. Curcumin analogs were identified as more potent inhibitors of *PfTrxR* than natural curcumin. Therefore compound **4**, a curcumin analog, was tested for the first time for its inhibitory activity in our system. Among these ligands, compounds which displayed more than 50% inhibition at 10  $\mu\text{M}$  were selected to subject for  $\text{IC}_{50}$  determination. Nine ligands showed less than 50% inhibition whereas compound **4** presented more than 50% inhibition. To determine the  $\text{IC}_{50}$  value for

compound **4**, concentrations ranging from 0.01  $\mu\text{M}$  to 100  $\mu\text{M}$  were tested at 0.5  $\mu\text{M}$  *PfTrxR*. The  $\text{IC}_{50}$  value of compound **4** was 2.03  $\mu\text{M}$  (Table 4.1). Control experiments without inhibitor or *PfTrxR* were carried out to test the stability of  $\text{Trx-S}_2$  in the presence of NADPH. In the absence of *PfTrxR*, NADPH alone could not convert  $\text{Trx-S}_2$  to  $\text{Trx-(SH)}_2$ , which indicates that the enzyme along with cofactor is essential to yield the product in the enzymatic reaction.

It is well known that *PfTrxR* is a valid target in drug discovery for malaria since it differs structurally and mechanistically from human thioredoxin reductase. Mass spectrometry is a reliable analytical tool for the identification and quantification of intact proteins. In this study, MS is preferred over optical methods (UV/Vis) for the identification of *PfTrxR* inhibitors because of its specificity derived from the accurate mass measurement especially when the quantification of product formed in the reaction is protein, much bigger than small molecule ligand, which often contributes to the noise signal in the optical method. An MS based functional assay can directly measure and quantify the reaction product and is, thus, a good approach for screening of inhibitors of *PfTrxR* based on the amount of  $\text{Trx-(SH)}_2$  formed in the presence of test compound. Our analytical strategy can identify and quantify the intact  $\text{Trx-(SH)}_2$  directly with high specificity and sensitivity. After the enzymatic reaction, separation of *PfTrxR* from the reaction mixture by chromatography was found to be challenging, as it had the same retention time as the reduced form  $\text{Trx-(SH)}_2$ . The ions of *PfTrxR* were found to interfere with the ions of  $\text{Trx-(SH)}_2$  as they both have the same retention time and hence could not be separated by their respective mass spectra. Therefore, after unsuccessful LC methods and column trials to separate *PfTrxR* and  $\text{Trx-(SH)}_2$ , the ultrafiltration step was used to separate the enzyme from the reaction mixture based on the molecular weight difference between Trx (12 kDa) and the enzyme (59 kDa) as described in the experimental procedure. The concentration of

Trx-S<sub>2</sub> and NADPH used in the reaction were optimized to 2.5 μM and 200 μM, respectively. Under both conditions, the formation of Trx-(SH)<sub>2</sub> was higher when control experiments (without inhibitor) were run at different concentrations of substrate (1.25, 2.5, 5 and 10 μM) and cofactor (200, 400, 600 and 800 μM). To optimize incubation time for the functional assay, control experiments (without inhibitor) were carried out at different time points (0, 30, 60, and 90 min) for maximum production of Trx-(SH)<sub>2</sub>. The maximum product formation in the experiments was observed at an incubation time of 30 min. After 30 min incubation, there was no increase in the amount of Trx-(SH)<sub>2</sub> (Table 4.2).

**Table 4.2** Trx-(SH)<sub>2</sub> time course study in control experiments tested in duplicates and injected in triplicates.

Incubation time (min)	Trx-(SH) <sub>2</sub> (μg /mL)
0	13.49 ± 0.67
30	34.89 ± 0.45
60	31.73 ± 0.41
90	32.30 ± 0.27

Control experiments were carried out at 0.5 μM and 1 μM to optimize the enzyme concentration in the reaction. *PfTrxR* at 0.5 μM yielded more Trx-(SH)<sub>2</sub> (34.89 μg/mL) when compared to *PfTrxR* at 1 μM which resulted in 5.79 μg/mL of Trx-(SH)<sub>2</sub>. Therefore, 0.5 μM *PfTrxR* is considered as the optimum concentration in the functional assay. The enzymatic reaction was carried out at 25 °C according to the method of Andricopulo et al. [6]. We further confirmed the influence of temperature on the product formation. At 37 °C, less product (12.96 μg/mL) was

formed whereas experiments at 25 °C resulted in maximum conversion of Trx-S<sub>2</sub> to Trx-(SH)<sub>2</sub> (34.56 µg/mL). Removal of phosphate buffer salts from the reaction mixture was essential as they interfere with protein detection by competing for ionization thus reducing the sensitivity for protein; they were easily desalted on a C<sub>18</sub> column at the initial time with a high percentage of water and sent to waste by segmenting the LC flow to the MS from 6.2 min to 8 min.

#### **4.5 Conclusions**

In summary, we have demonstrated a convenient and efficient method to separate and identify the product (Trx-(SH)<sub>2</sub>) formed in the enzymatic reaction using LC-MS. Our experiments have shown that Trx-(SH)<sub>2</sub> can be quantified by comparing the peak areas of Trx-(SH)<sub>2</sub> in control and test sample where a relative ratio is obtained to calculate percentage inhibition of *PfTrxR*. This method demonstrates a direct measurement of the Trx-(SH)<sub>2</sub> in the enzymatic reaction with a high degree of specificity, sensitivity and throughput. This assay can be a valuable tool for high-throughput ligand screening, particularly to find potent inhibitors for *PfTrxR*.

## 4.6 References

1. H. L. Ziegler, D. Staerk, J. Christensen, L. Hviid, H. Hagerstrand, J. W. Jaroszewski. *In vitro Plasmodium falciparum* drug sensitivity assay: Inhibition of parasite growth by incorporation of stomatocytogenic amphiphiles into the erythrocyte membrane. *Antimicrob. Agents Chemother.* **2002**, 46, 1441-1446.
2. A. R. de Boer, T. Letzel, D. A. van Elswijk, H. Lingeman, W. M. A. Niessen, H. Irth. On-line coupling of high-performance liquid chromatography to a continuous-flow enzyme assay based on electrospray ionization mass spectrometry. *Anal. Chem.* **2004**, 76, 3155–3161
3. A. Holmgren. Thioredoxin. *Ann. Rev. Biochem.* **1985**, 54, 237–71.
4. R. Munigunti, V. Mulabagal, A. I. Calderón. Screening of natural compounds for ligands to *PfTrxR* by ultrafiltration and LC–MS based binding assay. *J. Pharm. Biomed. Ana.* **2011**, 55, 265–7.
5. H. M. Alger, D. L. Williams. The disulfide redox system of *Schistosoma mansoni* and the importance of a multifunctional enzyme, thioredoxin glutathione reductase. *Mol. Biochem. Parasit.* **2002**, 121, 129–139.
6. A. D. Andricopulo, M. B. Akoachere, R. Krogh, C. Nickel, M. J. McLeish, G. L. Kenyon, L. D. Arscott, C. H. Williams, E. Davioud-Charvet, K. Becker. Specific inhibitors of *Plasmodium falciparum* thioredoxin reductase as potential antimalarial agents. *Bioorg. Medicinal Chem. Lett.* **2006**, 16, 2283–2292.
7. E. D. Chavet, K. Becker, V. Landry, S. Gromer, C. Logé, C. Sergheraert. Synthesis of 5, 5'-Dithiobis (2-nitrobenzamides) as alternative substrates for trypanothione reductase and

- thioredoxin reductase: A microtiter colorimetric assay for inhibitor screening. *Anal. Biochem.* **1999**, 268, 1-8.
8. Z. Liu, Z. Y. Du, Z. S. Huang, K. S. Lee, L. Q. Gu. Inhibition of thioredoxin reductase by curcumin analogues. *Biosci. Biotechnol. Biochem.* **2008**, 72, 2214–2218.
  9. T. L. Williams, J. H. Callahan, S. R. Monday, P. C. H. Feng, S. M. Musser. Relative quantitation of intact proteins of bacterial cell extracts using coextracted proteins as internal standards. *Anal. Chem.* **2004**, 76, 1002–1007.
  10. R. B. Arjen, L. Henk, M. A. N. Wilfried, I. Hubertus. Mass spectrometry-based biochemical assays for enzyme inhibitor screening. *Trends Anal. Chem.* **2007**, 26 (9), 867 – 883.
  11. L. Jingjing, C. Xueheng, F. Lei. LC-MS based assay method for DPP-IV inhibitor screening and substrate discovery. *Anal. Methods.* **2012**, 4, 1797-1805.
  12. S. Julka, J. Folkenroth, S. A. Young. Two dimensional liquid chromatography–ultraviolet/mass spectrometric (2DLC–UV/MS) analyses for quantitation of intact proteins in complex biological matrices. *J. Chromatogr. B.* **2011**, 879, 2057–2063.
  13. Y. Wang, B. M. Balgley, P. A. Rudnick, C. S. Lee. Effects of chromatography conditions on intact protein separations for top-down proteomics. *J. Chromatogr. A.* **2005**, 1073, 35–41.
  14. M. Wang, J. You, K. G. Bemis, T. J. Tegeler, D. P. G. Brown. Label-free mass spectrometry-based protein quantification technologies in proteomic analysis. *Brief. Funct. Genomic. Proteomic.* **2008**, 7, 329–339.
  15. M. T. Mazur, H. L. Cardasis, D. S. Spellmana, A. Liaw, N. A. Yates, R. C. Hendrikson. Quantitative analysis of intact apolipoproteins in human HDL by top-down differential mass spectrometry. *Proc. Natl. Acad. Sci.* **2010**, 107, 7728–7733.

16. J. M. Asara, H. R. Christofk, L. M. Freimark, L. C. Cantley. A label-free quantification method by MS/MS TIC compared to SILAC and spectral counting in a proteomics screen. *Proteomics*. **2008**, 8, 994–999.
17. S. M. Kanzok, R. H. Schirmer, I. Turbachova, R. Iozef, K. Becker. The thioredoxin system of the malaria parasite *Plasmodium falciparum*. *J. Biol. Chem.* **2000**, 275, 40180–40186.
18. M. M. Bradford. A rapid and sensitive method for the quantitation of microgram quantities of proteins utilizing the principle of protein–dye binding. *Anal. Biochem.* **1976**, 72, 248–254.
19. E. D. Charvet, M. J. McLeish, D. M. Veine, D. Giegel, L. D. Arscott, A. D. Andricopulo, K. Becker, S. Müller, R. H. Schirmer, C. H. Williams, G. L. Kenyon. Mechanism-based inactivation of thioredoxin reductase from *Plasmodium falciparum* by Mannich bases. implication for cytotoxicity. *Biochemistry*. **2003**, 42, 13319–13333.

## 5. Characterization of *Pf*TrxR inhibitors using mass spectrometry and *in silico* molecular modeling

### 5.1 Abstract

1,4-Napthoquinone (1,4-NQ), bis-2,4-dinitrophenyl sulfide (2,4-DNPS), 4-nitrobenzothiadiazole (4-NBT), 3-dimethylaminopropiophenone (3-DAP) and menadione (MD) and natural products were tested for *Pf*TrxR inhibitory activity, antimalarial activity against both chloroquine (CQ)-sensitive (D6) and chloroquine (CQ)-resistant (W2) strains of *Plasmodium falciparum* through an *in vitro* assay and non-covalent interactions to *Pf*TrxR through docking studies. The four inhibitors of *Pf*TrxR 1,4-NQ, 2,4-DNPS, 4-NBT and MD displayed antimalarial activity and toxicity to VERO Cell line at IC<sub>50</sub> values of < 20 μM. Docking experiments revealed that 2,4-DNPS, 4-NBT and MD interact non-covalently with the intersubunit region of *Pf*TrxR whereas 1,4-NQ and 3-DAP binds covalently to the target.

In this work, the binding affinities of natural products towards *Pf*TrxR, *Pf*GR, human TrxR and human GR were determined using a new mass spectrometry based ligand binding assay and *in silico* molecular modeling. Curcumin and demethoxycurcumin (DMC) are predicted to bind with close proximity to the dimer interface of *Pf*TrxR at the intersecting helices between the subunits. The current work is intended to prove the feasibility of our approach in finding new lead antimalarial compounds from plants by combining mass spectrometry and computational studies.

## 5.2 Introduction

Malaria, a tropical parasitic disease, continues to be the dominant cause of death in low-income countries especially in Africa and is considered to be one of the top three killers among communicable infectious diseases [1]. With a rapidly growing population in regions with high malaria transmission, it has been estimated that in the absence of effective intervention strategies the number of malaria cases will double over the next 20 years [2]. Malaria caused by *Plasmodium falciparum* is considered to be the most deadly and also the one with highest rate of drug resistance [3].

*P. falciparum* requires efficient antioxidant and redox systems to prevent damage caused by reactive oxygen species. In recent years, it has been shown that *P. falciparum* (*Pf*) possesses functional low molecular weight thiol thioredoxin (Trx) and glutathione systems [4]. Thioredoxin reductase (TrxR) and glutathione reductase (GR) are important enzymes of these redox systems that help the parasite to maintain an adequate intracellular redox environment. These antioxidant enzymes (*Pf*TrxR and *Pf*GR) are essential for the survival of *Plasmodium* parasites for combating the intraerythrocytic oxidative stress. Disruption of these enzymes is a feasible way to interfere with the erythrocyte development of malaria parasites [5]. The current chemotherapy of the malaria as recommended by WHO is based on artemisinin-based combination therapies (ACTs) as the front line of treatment for malaria. The main drawbacks of the combination therapies are high cost, adverse drug reactions, and a high degree of pharmacokinetic mismatch leading to prolonged exposure of parasites to low doses of partner drug and its active metabolites, which may facilitate development of resistant parasites [6].

Development of parasites resistance to the known antimalarials remains a major challenge for the effective management of malaria. Intensive drug discovery programs have aimed at developing new antimalarials or modifying current antimalarials to improve their efficacy and reduce any evidence of resistance. It has been understood that the chemical diversity of natural products is a better source for successful drugs than synthetic compounds, thus shifting the emphasis to natural product drug discovery. Unfortunately natural products other than quinine, artemisinin, hydroxynaphthoquinones, doxycyclin, clindamycin and azithromycin have not been in preclinical development [7]. Since quinine and artemisinin are outstanding examples of therapeutic natural products, there is a need to explore nature, a rich source of antimalarials for new pharmacophores/templates that can guide the design of potentially superior analogs [7].

### **5.2.1 Selective tools for identifying inhibitors of *Pf*TrxR and *Pf*GR**

*In silico* molecular modeling methods, such as docking, can aid in the drug discovery process by ascertaining the binding affinities of existing and novel natural products towards *Pf*TrxR, *Pf*GR, and the human isoforms of these enzymes. Ideally, the simulations can also elucidate the origin behind the observed inhibition. For example, the most common inhibitor binding sites in these reductases are at the active site and at the crystallographic 2-fold axis in the large cavity at the dimer interface. The dimer interface shows non-competitive or uncompetitive behavior and their interaction with the protein is purely non-covalent [8, 9, 10]. Docking calculations are well-suited to explore this interface; however, the simulations are unable to reproduce inhibitors that bind at the active site, as they usually show covalent binding and competitive behavior with respect to both the redox cofactors and the glutathione/thioredoxin substrates. A joint experimental and computational effort should help counterbalance the

deficiencies present in each technique and provide an enhanced avenue for natural product based inhibitor development.

### 5.2.2 Key differences in active sites between parasite and human enzymes

Comparison between the *h*TrxR and *Pf*TrxR structures shows that they have 46 % sequence identity and overlays with an RMSD of 0.91 Å between the 374 monomer atom pairs (Figure 5.1). The most important difference that can be exploited for selective noncompetitive inhibitors between the two enzymes is at the dimer interface. *Pf*TrxR is narrower than in *h*TrxR due to the presence of Tyr 101 and His 104 (Figure 5.2) and can therefore host smaller molecules. Their counterparts in the human isoform are Gln and Leu and this difference can determine the chemical nature of suitable inhibitors [12]. The molecular surfaces of the parasite and the human enzymes also indicate that the charges on the cavity walls are different, with the *h*TrxR's being more negatively charged compared to the *Pf*TrxR's (Figure 5.3) [12].

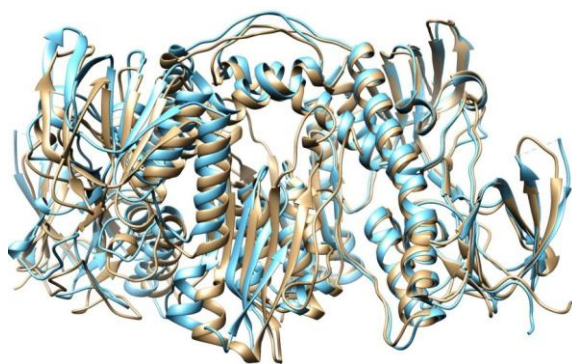


**Figure 5.1** Superposition of *h*TrxR (brown) with *Pf*TrxR (blue).

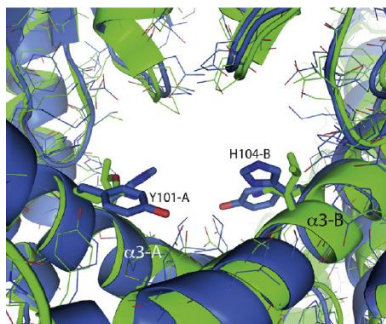


**Figure 5.2** *PfTrxR* (blue) in comparison with *hTrxR* (green) [12].

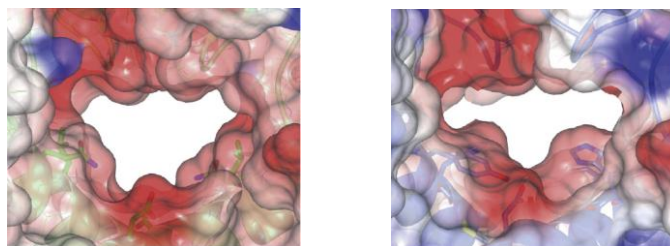


**Figure 5.3** Molecular surfaces of the *PfTrxR* and *hTrxR* cavities [12].

Similar to the thioredoxin reductases, the *hGR* and *PfGR* structures were found to have 45% sequence identity with an RMSD overlay of 1.00 Å between 343 monomer atom pairs (Figure 5.4). For the enzyme/substrate complex structures that have been solved, the structures indicate that one inhibitor binds per enzyme subunit. The dimer cavity connects to both glutathione disulfide (GSSG) binding sites through two channels that also serve as mediators between the bulk solvent and the cavity (Figure 5.5) [8]. Significant differences are found at the dimer interface where the amino acid residues lining the wall of the cavity have very low conservation. Only 9 out of 21 residues are conserved in *PfGR*, which is an important factor for selective inhibitor design, and implies that the binding mode of any inhibitor cannot be extended to be similar between the proteins [13].

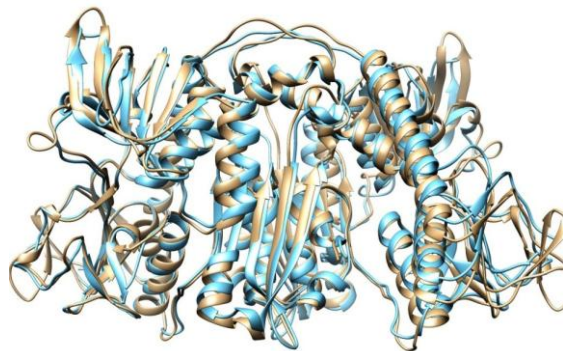


**Figure 5.4** Superposition of *hGR* (brown) with *PfGR* (blue).

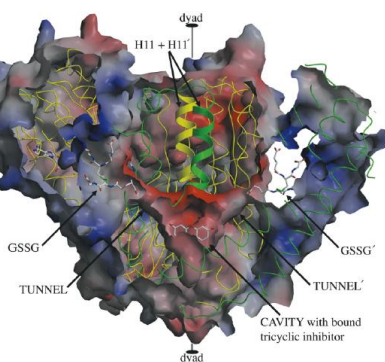


**Figure 5.5** The dimer cavity of *hGR* [13].

The molecular surfaces of the two enzymes also indicate that the charges on the cavity walls are quite different, with the *hGR* cavity being highly negatively charged, and the *PfGR* cavity being quite neutral (Figure 5.6).

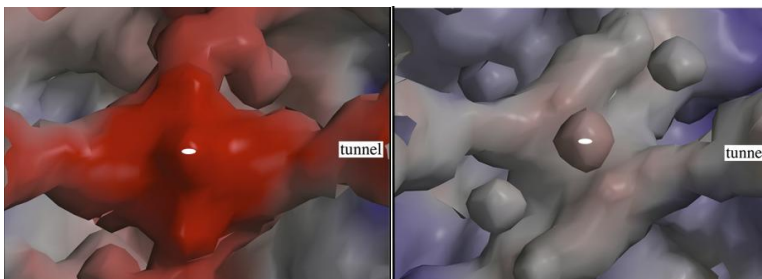


**Figure 5.6** Molecular surfaces of the *PfGR* and *hGR* cavities [13].

The current study aimed to prove the combined approach of LC-MS based *PfTrxR* and *PfGR* binding and functional assays, molecular docking for identification of key interactions of *PfTrxR* and *PfGR* inhibitors to improve selectivity and phenotypic assays for malaria for identification of activity against parasite blood stages and against drug resistant parasites to assure the identification of specific *PfTrxR* and *PfGR* inhibitors as scaffolds for lead optimization.

## **5.3 MATERIALS AND METHODS**

### **5.3.1 Chemicals and enzymes**

Solvents used for LC/MS analysis were purchased from Fischer Scientific International (Atlanta, GA). Seven compounds from AnalytiCon Discovery GmbH (Germany) natural products library (MEGx) were purchased based on compound classes that have reported either antimalarial activity or inhibition of TrxR [14, 15]. Hispolone was kindly provided by Dr. G. V. Subbaraju, AptuitLauras, Hyderabad, India. Buffer salts and bis-2, 4-dinitrophenyl sulfides were purchased from Sigma-Aldrich (Allentown, PA). Deionized water generated by a Milli-Q water system (Millipore, MA) was used in the experiments. *PfTrxR* ( $M_r$  59 kDa) enzyme was provided as a gift by Prof. Katja Becker, Justus-Liebig University, Giessen, Germany. The recombinant *PfTrxR* was prepared and purified using silver-stained SDS page according to the procedure published by Kanzok et al [16]. The specific activity of *PfTrxR* (1.9 U/mg) was determined by DTNB [5, 5'-dithiobis (2-nitrobenzoic acid)]. Protein concentration of enzymes was determined by Bradford method [17].

### 5.3.2 Protocols of experiments

#### 5.3.2.1. *PfTrxR* enzyme binding assay using ultrafiltration and liquid chromatography-mass spectrometry

In this method, 4  $\mu\text{L}$  of test compound (10  $\mu\text{M}$ ) and 192  $\mu\text{L}$  of incubation buffer containing 20.5 mM  $\text{KH}_2\text{PO}_4$ , 26.5 mM  $\text{K}_2\text{HPO}_4$ , 200 mM  $\text{KCl}$  and 1 mM  $\text{EDTA}$  with pH 6.9, were placed into micro centrifuge. To this, 4 $\mu\text{L}$  of *PfTrxR/PfGR* enzyme (1  $\mu\text{M}$ ) was added and incubated at 25°C for 60 min. The incubation mixture was then filtered through a 30 kDa molecular weight cut-off ultrafiltration membrane filter made of regenerated cellulose (Microcon YM-30, Millipore, Billerica, MA) and then centrifuged at 13,000  $\times$  g at 4°C for 20 min. The enzyme–ligand complex trapped on the filter was washed with assay buffer (200  $\mu\text{L}$  3 $\times$ ) and centrifuged at 13,000  $\times$  g at 4°C for 20 min each time. The ultrafiltration membrane was placed into a new microcentrifuge tube and the ligands were dissociated from *PfTrxR* enzyme by treatment with 200  $\mu\text{L}$  of methanol for 20 min. The dissociated ligand obtained was centrifuged at 20°C, 13,000  $\times$  g for 20 min. The ultrafiltrate was then dried under nitrogen using N-VAP 116 Nitrogen Evaporator (Organomation Associates, Inc., Berlin, MA) and the released ligands were reconstituted in 100  $\mu\text{L}$  of methanol/water (v/v, 90:10). Assays were carried out in duplicate and the control experiments were performed in a similar way with denatured enzyme. The released ligands were then analyzed by LC-MS. [15].

#### 5.3.2.2. LC-MS based *PfTrxR* functional assay

The test compound (10 mM in 1% dimethyl sulfoxide [DMSO]) was incubated with 0.5 mM *PfTrxR* enzyme and 200 mM NADPH in the assay buffer (PE buffer: 100 mM potassium phosphate and 2 mM  $\text{EDTA}$ , pH 7.4). The enzymatic reaction was initiated by addition of 2.5

mM Trx-S<sub>2</sub> and incubated at 25 °C for 30 min. After the incubation, the reaction was quenched by addition of 0.1% formic acid. The reaction mixture was filtered through a 30 kDa MWCO ultrafiltration membrane centrifuged at 13 000 rpm at 20 °C for 10 min. The enzyme was trapped on the membrane and product (Trx-(SH)<sub>2</sub>) formed in the reaction was recovered in the filtrate and analyzed by LC/MS. A control experiment (without inhibitor) was performed the same way and the amount of Trx-(SH)<sub>2</sub> was used to reference the activity in the test sample. A calibration curve using known amounts of Trx-(SH)<sub>2</sub> was prepared to quantify the amount of Trx-(SH)<sub>2</sub> produced in the reactions [14].

### **5.3.2.3. Antiplasmodial activity and cytotoxicity against L6 cells of tested natural products**

Antiplasmodial activity was determined using the K1 strain of *P. falciparum* (resistant to chloroquine and pyrimethamine). A modification of the [<sup>3</sup>H]-hypoxanthine incorporation assay was used. Briefly, infected human red blood cells in RPMI 1640 medium with 5% Albumax were exposed to serial drug dilutions in micro titer plates. After 48 h at 37 °C in a reduced oxygen atmosphere, 0.5 µCi [<sup>3</sup>H]-hypoxanthine was added to each well. Cultures were incubated for a further 24 h before they were harvested onto glass-fiber filters and washed with distilled water. The radioactivity was counted using a Betaplate<sup>TM</sup> liquid scintillation counter (Wallac, Zurich, Switzerland). The results were recorded as counts per minute (CPM) per well at each drug concentration and expressed as percentage of the untreated controls. From the sigmoidal inhibition curves, IC<sub>50</sub> values were calculated. Assays were run in duplicate and repeated once. Chloroquine was used as a reference anti-malarial drug and showed an IC<sub>50</sub> value of 0.069 µg/mL.

Cytotoxicity assays were performed in 96-well microtiter plates, each well containing 100  $\mu\text{L}$  of RPMI 1640 medium supplemented with 1% L-glutamine (200 mM) and 10% fetal bovine serum, and  $4 \times 10^4$  L6 cells (a primary cell line derived from rat skeletal myoblasts). Serial drug dilutions of seven 3-fold dilution steps covering a range from 90 to 0.123  $\mu\text{g}/\text{mL}$  were prepared. After 72 h of incubation, the plates were inspected under an inverted microscope to assure growth of the controls and sterile conditions. Ten  $\mu\text{L}$  of Alamar Blue solution was then added to each well and the plates incubated for another 2 h. Then the plates were read with a Spectramax Gemini XS microplate fluorometer using an excitation wavelength of 536 nm and an emission wavelength of 588 nm. Data were analysed using the microplate reader software Softmax Pro. Podophyllotoxin was the reference drug used [18].

#### **5.3.2.4. Assays for *in vitro* antimalarial activity and cytotoxicity of known *PfTrxR* inhibitors**

##### **Antimalarial assay**

Briefly, antimalarial activity of the compounds were determined *in vitro* on chloroquine sensitive (D6, Sierra Leone) and resistant (W2, IndoChina) strains of *P. falciparum*. The 96-well microplate assay is based on the effect of the compounds on growth of asynchronous cultures of *P. falciparum*, as determined by the assay of parasite lactate dehydrogenase (pLDH) activity [19].

##### **Cytotoxicity assay**

Cytotoxicity in terms of cell viability were evaluated using VERO cells by Neutral Red assay [20]. This assay was conducted on compounds designated as active in the *PfTrxR* functional assay and the antimalarial phenotypic screening.

### 5.3.2.5 ROS assay

Accelerated generation and accumulation of reactive oxygen intermediates (superoxide radical, hydroxyl radical and hydrogen peroxide) are mainly responsible for oxidative stress [21]. The intraerythrocytic formation of ROS was monitored in real-time with 2',7'-dichlorofluorescein diacetate (DCFDA), a fluorescent ROS probe [22]. Human erythrocytes collected in citrate phosphate anticoagulant were used. The erythrocytes were washed twice with 0.9 % saline and suspended in PBSG at a hematocrit of 10%. A 60 mM stock of DCFDA was prepared in DMSO and added to the erythrocytes suspension in PBSG (10% hematocrit) to obtain the final concentration of 600  $\mu$ M. Erythrocytes suspension containing 600  $\mu$ M of DCFDA was incubated at 37°C for 20 min and centrifuged at 1000 g for 5 min. The pellet of DCFDA loaded erythrocytes was suspended in PBSG to 50% hematocrit and used for kinetic ROS formation assay. The assay was directly set up in a clear flat-bottom 96 well microplate. The reaction mixture contained 40  $\mu$ L of DCFDA loaded erythrocytes, the test compounds (concentration as mentioned) and potassium phosphate buffer (100 mM, pH 7.4), to make up the final volume to 200  $\mu$ L. The controls without drug were also set up simultaneously. Each assay was set up at least in duplicate. The plate was immediately placed in a microplate reader programmed to kinetic measurement of fluorescence (excitation 488 nm and emission 535 nm) for 2 hours with 5 min time intervals.

### 5.3.2.6 Computational methods

Auto Dock Vina [23] was used to dock inhibitors to the respective targets. Initial Cartesian coordinates for the protein-ligand structures were derived from reported crystal structures of *hGR* (PDB ID: 1XAN) [8], *PfGR* (PDB ID: 1ONF) [13], *hTrxR* (PDB ID: 3QFA) [24] and *PfTrxR* (PDB ID: 4B1B) [12]. The protein targets were prepared for molecular docking simulation by removing water molecules and bound ligands. AutoDockTools (ADT) [25] was used to prepare the docking simulations whereas Chimera was used to analyze the docking poses. All ligands were constructed using PyMol [26] with subsequent geometry optimizations carried out using the semiempirical method PDDG/PM3 [27, 28, 29]. Polar hydrogens were added. Conjugate gradient minimizations of the systems were performed using GROMACS [30]. A grid was centered on the catalytic active site region and included all amino acid residues within a box size set at  $x = y = z = 20 \text{ \AA}$ .

### 5.3.2.7 AutoDockVina details

Standard flexible protocols of AutoDockVina using the Iterated Local Search global optimizer [23] algorithm were used to evaluate the binding affinities of the molecules and interactions with the receptors. All ligands and docking site residues, as defined by the box size used for the receptors, were set to be rotatable. Calculations were carried out with the exhaustiveness of the global search set to 100, number of generated binding modes set to 20 and maximum energy difference between the best and the worst binding modes set to 5. Following completion of the docking search, the final compound pose was located by evaluation of

AutoDock Vina's empirical scoring function where the conformation with the lowest docked energy value was chosen as the best. The experimental binding poses of *hGR* control structures xanthenes (PDB ID: 1XAN) [31] and pyocyanin (PDB ID: 3SQP) [32] were successfully reproduced using the described docking protocols (Figure 5.7).

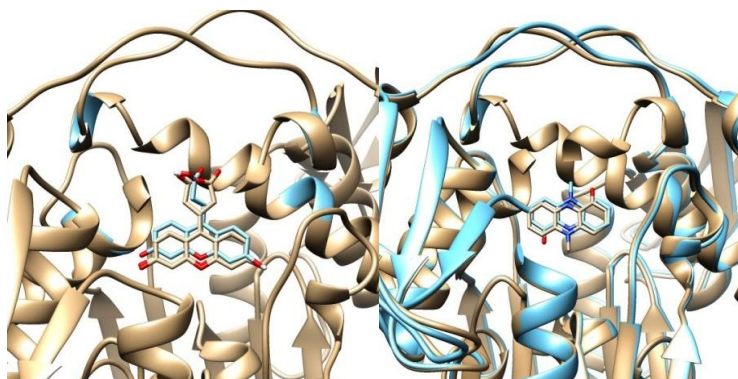


**Figure 5.7** *hGR* inhibitors xanthenes (left) and pyocyanin (right) docked (in blue) and compared to the experimental crystal structures (in brown).

## 5.4. Results and Discussion

### 5.4.1. Evaluation of known inhibitors of *PfTrxR*

Based on the newly developed *PfTrxR* functional assay five known inhibitors of *PfTrxR* [33, 34] and *PfGR* [35], i.e., 1, 4-naphthoquinone (1, 4-NQ), bis-2, 4-dinitrophenyl sulfide (2, 4-DNPS), 4-nitrobenzothiadiazole (4-NBT), 3-dimethylaminopropiophenone (3-DAP) and menadione (MD), (Figure 5.8) showed more than 50% *PfTrxR* inhibition at 10  $\mu\text{M}$  and displayed  $\text{IC}_{50}$  values of 0.75, 0.5, 2.0, 15.4 and 1.6  $\mu\text{M}$ , respectively. The *in vitro* antimalarial activity of five known inhibitors of *PfTrxR* (1, 4-naphthoquinone, 2, 4-DNPS, 4-NBT, 3-DAP, menadione) was evaluated against both CQ-sensitive (D6 clone) and CQ resistant (W2 clone) strains of *P.*

*falciparum*, while cell cytotoxicity was determined against VERO cells (Table 5.1) using the procedure as described earlier.

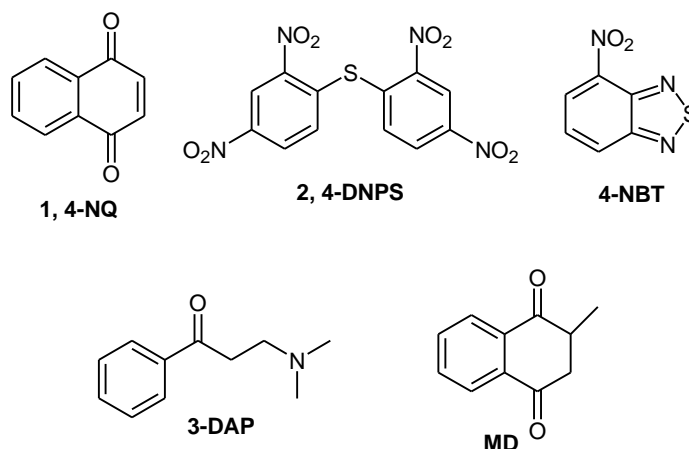


**Figure 5.8** Structures of five known inhibitors of *PfTrxR*.

The five compounds were tested in cell culture against *P. falciparum* displaying the following range of activity ( $IC_{50}$  in  $\mu M$ ): 1, 4-NQ 8.9 D6/16.7 W2, 2, 4-DNPS 91.2 D6/72.3 W2, 4-NBT 8.3 D6/9.8 W2, 3-DAP >100 D6/>100 W2 and menadione 18.5 D6/28.3 W2. The compounds 1, 4-NQ and 4-NBT were found to be the most active against the two strains of *P. falciparum*, menadione and 2,4-DNPS were moderately active and 3-DAP was inactive. In terms of antiparasmodial activity against the W2 strain, 1, 4-NQ and 4-NBT showed  $IC_{50}$  value of < 20  $\mu M$ . The lack of antiparasmodial activity of 3-DAP suggested low permeability of this compound in the absence of active transport to red blood cells and parasites due its high polarity (QP logS - 1.414 (-6.5/0.5)). The correlation between inhibition of *PfTrxR* and antiparasmodial activity in cell culture allows for a proof of concept for our drug discovery approach. Among the most active compounds (1,4-NQ, 2,4-DNPS, 4-NBT and MD) showed toxicity to VERO cell line from concentrations of 41.5 - 85.4  $\mu M$  except for 3-DAP. The selectivity displayed by the tested compounds was considerably low.

In order to test the five *PfTrxR* inhibitors for their ability to induce signs of oxidative stress by accelerated generation and accumulation of reactive oxygen intermediates (superoxide radical, hydroxyl radical and hydrogen peroxide) [21], the intraerythrocytic formation of ROS was monitored in real-time for 120 min with 2',7'-dichlorofluorescein diacetate (DCFDA), a fluorescent ROS probe [22]. Among the *PfTrxR* inhibitors only 4-NBT, MD and 1,4-NQ increased oxidative stress by the production of 100, 50 and 45% ROS respectively over a period of 2 h in the human erythrocytes (Figure 5.9). Whereas 3-DAP and 2,4-DPNS did not increase the production of ROS. The obtained data on 4-NBT, 1,4-NQ and MD suggested that their mechanism of action is through inhibition of *PfTrxR*.

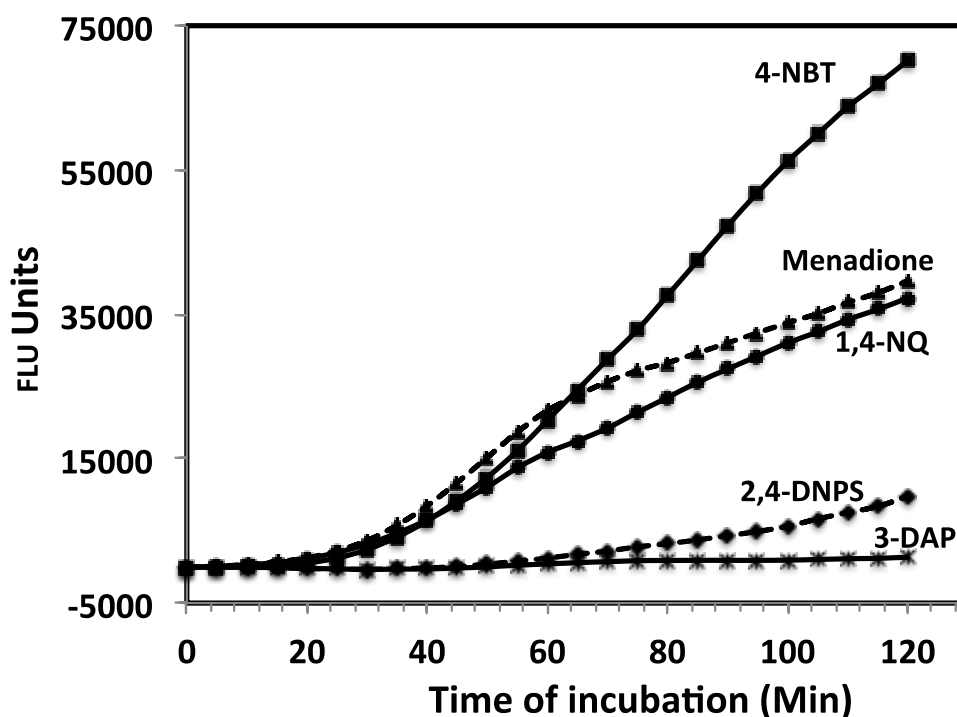


**Figure 5.9** Formation of reactive oxygen species (ROS), as indicated by increase in fluorescence DCFDA loaded human erythrocytes by five *PfTrxR* inhibitors.

The 1, 4-NQ chemical features and the ability to generate OH radical suggest the proficiency in altering intracellular redox status [36]. The antimalarial naphthoquinones (1, 4-NQ and MD) are believed to perturb the major redox equilibria of the targeted *P. falciparum* infected red blood cells, which might be removed by macrophages. This perturbation results in development arrest and death of the malaria parasite at the trophozoite stage [37]. The 1, 4-NQ displayed inhibitory activity against *PfGR* with  $IC_{50}$  value of 2.2  $\mu$ M and 2-fold selectivity toward the parasite isoform whereas menadione showed  $IC_{50}$  value of 42  $\mu$ M and more selectivity toward the human counterpart. To gain further insight into the mode of interaction for these molecules, molecular docking was used to study the interaction of non-covalent reductase inhibitors. MD [38], 2,4-DNPS [33] and 4-NBT [33] have been proposed to bind at the intersubunit region in *PfTrxR*'s and GR's.

However, 1, 4-NQ and 3-DAP bind to the reductases covalently precluding the use of docking calculations. For example, 1, 4-NQ is an inhibitor of GR and TrxR that behaves as a subversive substrate (Morin et al. 2008). 3-DAP inactivates TrxR by alkylating the C-terminal redox active catalytic Cys-Cys pair. This is achieved by the formation of a reactive  $\alpha$ ,  $\beta$ -unsaturated ketone intermediate after it undergoes deamination in solution [34]. As with 3-DAP, it has an  $\alpha$ ,  $\beta$ -unsaturated ketone that acts as the alkylator [39]. The calculations correctly reproduced the activity trend observed in the experimental  $IC_{50}$  values for the non-covalent inhibitors, 2, 4-DNPS, MD, and 4-NBT in *PfTrxR* (Table 5.2).

**Table 5.1** Antiplasmodial activity and inhibition of *Pf*TrxR by known inhibitors

Test compounds	<i>Pf</i> TrxR IC <sub>50</sub> (μM)	<i>Pf</i> (D6) CQ sensitive IC <sub>50</sub> (μM)	SI D6	<i>Pf</i> (W2) CQ resistance IC <sub>50</sub> (μM)	SI W2	VERO IC <sub>50</sub> (μM)
1,4-NQ	0.75	8.9 ± 2.3	4.6	16.7± 3.7	2.4	41.5
2,4-DNPS	0.5	91.2 ± 11.3	0.8	72.3 ± 11.3	1.0	68.7
4-NBT	2	8.3 ± 2.1	10	9.8 ± 1.9	8	85.4
3-DAP	15.4	>100	>1	>100	>1	>100
MD	1.6	18.5 ±1.9	3.8	28.3 ± 5.6	2.5	71.2
CQ		0.055 ± 0.006		0.440 ± 0.045		

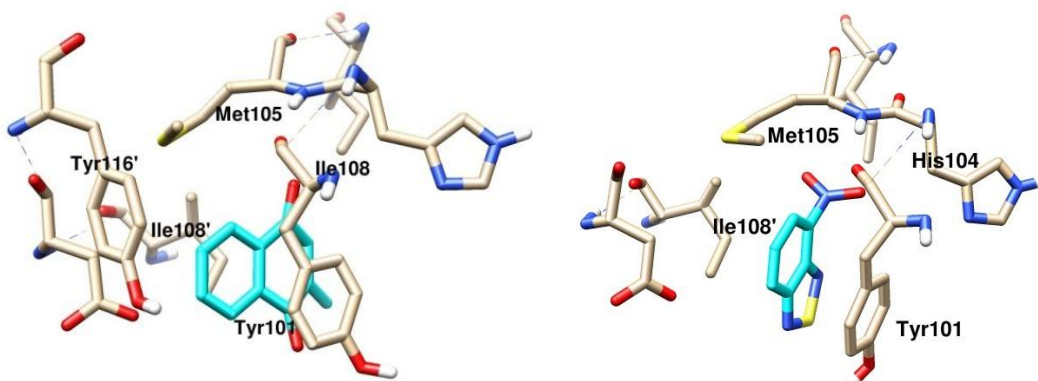
For antiplasmodial, we are using the following activity criteria - Compounds with IC<sub>50</sub> < 20 μM are active. If a compound shows IC<sub>50</sub> < 20 μM and selectivity index (IC<sub>50</sub> VERO cells/ IC<sub>50</sub> parasite >100 it qualifies for *in vivo* testing - Compounds with IC<sub>50</sub> 20 – 100 μM are moderately active. Compounds with IC<sub>50</sub> >100 μM are inactive.

For the *Pf*TrxR/MD complex, pi stacking interactions are predicted to form between the inhibitor's phenyl ring and Tyr 101 side chain ring. The backbone nitrogen of Met105 is in close proximity to the carbonyl group of menadione, however, the predicted angle between N-H and O of 85° impedes hydrogen bonding.

**Table 5.2** Comparison between computed binding affinities (kcal/mol) at the dimer interface in *Pf*TrxR and experimental IC<sub>50</sub> values (μM).

Molecule	Computed Binding Affinity (kcal/mol)	Exptl. <i>Pf</i> TrxR IC <sub>50</sub> (μM)
2,4-DNPS	-8.4	0.5
MD	-7.9	1.6
4-NBT	-6.0	2

The molecule further forms hydrophobic interactions with the phenyl ring of Tyr 116' and the sidechains of Ile 108 from both subunits. Similar to MD, 4-NBT's phenyl ring also has pi-pi stacking with Tyr 101's phenyl ring, but forms hydrophobic interactions only with Ile 108 from subunit B in the large cavity. The nitro group causes the molecule to twist subtly compared to MD in order to better interact with the electrostatic surface created by the peptide bond between His 104 and Met 105's and sulfur on methionine (Figure 5.10). Compared to the size of the cavity, MD and 4-NBT are small molecules and do not fully interact with most of the residues lining the wall of the dimer interface. 2, 4-DNPS forms the only electrostatic interaction at a distance of 3.9 Å with Asn481'. Pi stacking interactions are formed between one of the inhibitor's phenyl ring and Tyr101 side chain ring with the other phenyl ring of the molecule forming a parallel displaced pi stacking interaction with Tyr101' (subunit B). As with MD and 4-NBT, the side chains of Ile 108 from both subunits form hydrophobic interactions too with 2, 4-DNPS. Most of the interactions the 3 molecules are forming with the proteins are with the intersecting helices between the two subunits of the enzymes (Figure 5.10).



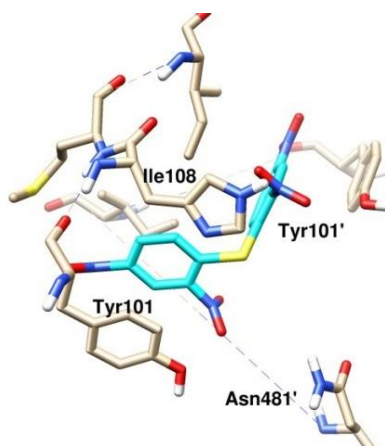


**Figure 5.10** *PfTrxR*/MD, *PfTrxR*/4-NBT, and *PfTrxR*/2, 4-DNPS complexes.

The experimental activities for 2, 4-DNPS and 4-NBT show significant selectivity between the parasite and human isoform of TrxR (Table 5.3). The experimental values for 2, 4-DNPS show an 8-fold selectivity for *PfTrxR*, whereas 4-NBT has a 25-fold selectivity, respectively. While the docking simulations correctly predicted binding trends, the large magnitudes in experimental  $IC_{50}$  values were unexpected.

**Table 5.3** Comparison between computed binding affinities (kcal/mol) at the dimer interface and experimental  $IC_{50}$  values ( $\mu$ M) selectivity in *PfTrxR* and *hTrxR*.

Molecule		<i>PfTrxR</i>	<i>hTrxR</i>
2,4-DNPS	Exptl. $IC_{50}$	0.5	4
	Cal. Binding affinity (kcal/mol)	-8.4	-8.1

4-NBT	Exptl. IC <sub>50</sub>	2	50
	Cal. Binding affinity (kcal/mol)	-6.0	-5.7

The docked poses however have considerable differences within the cavity, which could point to the observed selectivity (Figure 5.11). The presence of Tyr 101 in *Pf*TrxR enables 2, 4-DNPS to form a favorable pi stacking interaction with the phenyl ring of the molecule whereas its counterpart in *h*TrxR is a Gln 72 that orients the molecule to avoid steric clashes. This results in the second ring of the molecule forming a parallel displaced pi stacking interaction with Tyr 101' whereas a hydrogen bond between the nitro group and Gln 72' in the *h*TrxR is realized. The effect of this substitution on 4-NBT seems to be the fact that the presence of Gln 72 pushes the molecule deep into the large cavity precluding the interaction with the residues of the intersecting helices between the subunits.

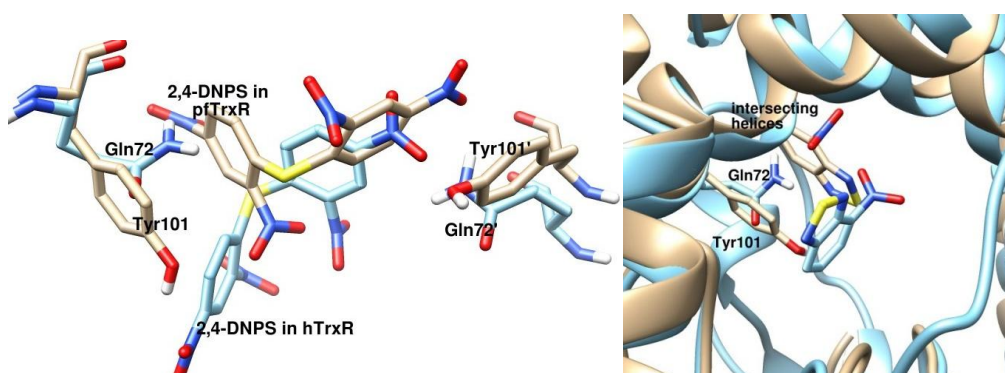


**Figure 5.11** The docking pose differences of 2, 4-DNPS and 4-NBT between the *Pf*- (brown) and *h*-TrxR (blue).

## 5.4.2 Evaluation of natural products as inhibitors of *Pf*TrxR and *Pf*GR

### 5.4.2.1 Curcumin and demethoxycurcumin (DMC)

Based on the report of Mulabagal and Calderon in 2010 [15] about curcumin and DMC as *Pf*TrxR ligands, we tested these compounds for their ability to inhibit *Pf*TrxR. Curcumin and DMC showed more than 2-fold binding affinity for *Pf*TrxR target enzyme but curcumin displayed less than 50% inhibition of *Pf*TrxR at 10  $\mu$ M when tested in the functional assay compared to DMC which displayed more than 50% *Pf*TrxR inhibition at 10  $\mu$ M with an  $IC_{50}$  value of 2.0  $\mu$ M. The fact that curcumin has been shown to inhibit mammalian or rat TrxR by alkylating the cystein/selenocystein catalytic active site residues, supports our data and prediction that curcumin selectively inhibits mammalian TrxR but not the *Pf*TrxR. The *in vitro* antimalarial activity of curcumin and demethoxycurcumin (DMC) was evaluated against both CQ-sensitive (D6 clone) and CQ resistant (W2 clone) strains of *P. falciparum*, while cell cytotoxicity was determined against VERO cells (Table 5.4) using the procedure as described earlier.

**Table 5.4** Antiplasmodial activity and inhibition of *Pf*TrxR by curcuminoids

Test compounds	<i>Pf</i> TrxR $IC_{50}$ ( $\mu$ M)	<i>Pf</i> (D6) CQ sensitive $IC_{50}$ ( $\mu$ M)	SI D6	<i>Pf</i> (W2) CQ resistance $IC_{50}$ ( $\mu$ M)	SI W2	VERO $IC_{50}$ ( $\mu$ M)
Curcumin	NA	15.9 $\pm$ 2.1	4.0	41.2 $\pm$ 6.2	1.6	64.6
DMC	2.03	17.7 $\pm$ 3.1	5.0	82.7 $\pm$ 10.3	1.1	89.7
CQ		0.055 $\pm$ 0.006		0.440 $\pm$ 0.045		

NA: Not active i.e, *Pf*TrxR inhibition was < 50% at 10  $\mu$ M.

The two compounds were active against the D6 strain of *P. falciparum* and moderately active against the resistant W2 strain. The antiplasmodial activity of curcumin ( $IC_{50}$ : 4.21  $\mu$ M) against CQ resistant strain MP-14 of *P. falciparum* has been reported by Mishra et al., 2008 [40]. Furthermore the curcuminoids showed cytotoxicity against VERO cells from 64  $\mu$ M and selectivity index of 4-6-fold and 1-fold against D6 and W2, respectively. This is the first report on the antiplasmodial activity of these two curcuminoids through the target *PfTrxR*. Curcumin and DMC were also tested for production of ROS for human erythrocytes and it was found that they were not able to induce oxidative stress.

Curcumin and demethoxycurcumin (DMC) are predicted to bind to the dimer interface of *PfTrxR* at the intersecting helices between the subunits. It is evident that, the first phenol moiety (demethoxylated in DMC) interacts with the residues on sub-unit A whereas the other moiety extends toward sub-unit B (Figure 5.12). Curcumin contains two phenyl methoxy groups, whereas DMC contains one methoxy group (Figure 5.13) which suggests that the phenyl methoxyl groups may contribute to the difference in inhibition towards *PfTrxR*. In curcumin, the *ortho-methoxy* group can form an intramolecular hydrogen bond with the phenolic hydrogen, making the H-atom abstraction from the *ortho-methoxy* phenols surprisingly easy. How phenyl methoxy groups mediate inhibition of *PfTrxR*, however, is unclear.

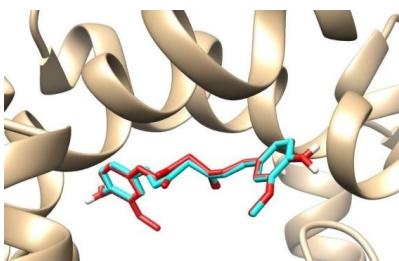


**Figure 5.12** *PfTrxR*/DMC (blue) and –Curcumin (red) complexes.

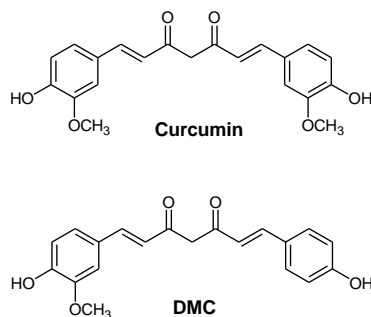


**Figure 5.13** Structures of curcumin and demethoxycurcumin (DMC)

Earlier theoretical studies showed that hydrogen bonding between *ortho*-methoxy oxygen and phenolic hydrogen in curcumin influences the planarity, conformation and ability to undergo oxidation [41]. In both molecules, the phenyl moiety forms a pi-stacking interaction with Tyr101 of the respective sub-unit with the hydroxyl group in DMC donating a hydrogen bond of 2.5 Å to the oxygen of Tyr 116 in sub-unit A. Curcumin's OH group is bent in the opposite direction because of the conformational change and thus the H-bond is not realized. For sub-unit B, the opposite case happens. Curcumin form a 2.4 Å H-bond with the Tyr 101' and DMC's OH group bends avoiding the interaction (Figure 5.14).

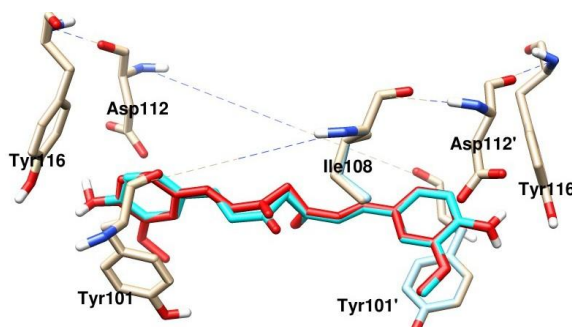


**Figure 5.14** The interactions between DMC (blue) and Curcumin (red) with *PfTrxR*

The hydrophobic  $\alpha$ ,  $\beta$ -unsaturated chain interacts with the side chain of Ile 108 from sub-unit A. The experimental data shows a marked difference between the two compounds with respect to

*PfTrxR* inhibitory activity whereas docking analysis predicted close affinities (Table 5.5). These slight differences in the predicted binding poses of the two molecules could probably point to the differences in experimental values. However it was found that curcumin bind to the mammalian TrxR covalently [39] precluding the use of docking calculations.

**Table 5.5** Comparison between predicted binding affinities and experimental IC<sub>50</sub> values of curcuminoids.

<b>Dimer-interface</b>			
<b>Computed</b>		<b>Exptl.</b>	
<b>Molecule</b>	<b>Affinity (kcal/mol)</b>	<b>Molecule</b>	<b><i>PfTrxR</i> IC-50 (μM)</b>
Demethoxycurcumin	-9.6	Demethoxycurcumin	2.03
Curcumin	-9.4	Curcumin	Not active

Therefore the difference in inhibition towards *PfTrxR* of the two compounds can be attributed to conformational changes in curcumin and DMC, and the availability of phenol hydroxyl group in DMC as key interaction site for inhibition of *PfTrxR*.

#### 5.4.2.2 Subset of *PfTrxR* natural product ligands

In order to complete the biological evaluation of all compounds reported by Munigunti et. al. (2011) as *PfTrxR* ligands, binding affinities were determined towards human isoforms of *PfTrxR* and *PfGR*. Further determination of *PfTrxR* and *PfGR* inhibitory activity and docking studies were also performed on these ligands. Six of these compounds showed binding to *PfTrxR* of >2- fold and no binding to the human isoform of the enzyme (Table 5.6). The 11-

hydroxycoronaridine, quinidine-N-oxide and hernagine showed high selectivity towards *PfTrxR* compared to *PfGR*, whereas yohimbine, vobasine, hispolone and gnetifolin E were selective to both *PfTrxR* and *PfGR* compared to human isoforms of both enzymes. Yohimbine, catharanthine, hernagine, vobasine, hispolone and gnetifolin E (Figure 2.1) displayed less than 50% inhibition of *PfTrxR* in the LC-MS based *PfTrxR* functional assay using relative quantitation of intact proteins, particularly reduced thioredoxin. Here the lack of *PfGR* inhibitory activity of these compounds is reported with binding of 2-fold to *PfGR* and no binding to human isoform. The *in vitro* antimalarial activity and cytotoxicity of yohimbine, quinidine-N-oxide, vobasine and gnetifolin E against *P. falciparum* K1 strain were found to be 7.25, 5.69, 1.54, 31.65  $\mu\text{g/mL}$  and 34.2, 100, 12.2, 24.5  $\mu\text{g/mL}$  respectively (Table 5.7). Three compounds out of eight displayed cytotoxicity against L6 cells from 2.75  $\mu\text{g/mL}$  except by 11-(OH)-coronaridine and hernagine which displayed cytotoxicity at  $>10$   $\mu\text{g/mL}$  (Table 5.7). *In silico* molecular modeling was used to ascertain and further confirm the binding affinities of these ligands towards *PfTrxR*, *PfGR* and human isoforms of these enzymes as well as to deduce the key interactions between the ligands and proteins. However, the results obtained from docking studies did not correlate well with the experimental data. This difference in data from experiments and docking studies was due to nature of different scaffolds. These data suggest that the tested natural products bind non-specifically to the two targets. The antiplasmodial natural products might kill *P. falciparum* through different targets.

**Table 5.6** UF-LC-MS based binding affinities of natural products for *Pf*TrxR and *Pf*GR

<b>Compound</b>	<b>BA for <i>Pf</i> TrxR</b>	<b>BA for H. TrxR</b>	<b>BA for <i>Pf</i> GR</b>	<b>BA for <i>h</i>GR</b>
Yohimbine	2.0	0.75	2.3	1.6
Catharanthine	2.5	0.44	2.1	3.5
11-(OH)- Coronaridine	2.6	1.18	1	1
Quinidine N-oxide	2.5	0.78	1	1
Hernagine	1.8	1.25	1	1
Vobasine	1.6	1.22	3.6	1.7
Hispolone	2.4	1	2.3	1.5
Gnetifolin E	2.5	1.3	2.7	1.8
Demethoxycurcumin	2.2	1.4	3.0	2.1
Curcumin	2.7	2.0	3.2	1
2,4-DNPS	3.2	0.9	6.0	2.7

Compounds are considered as ligands which display binding affinity of > 2-fold.

**Table 5.7** *Pf*TrxR and *Pf*GR inhibitory and antiplasmodial activities by selected natural products

Compound	% Inhib <i>Pf</i> TrxR 10 $\mu$ M	<i>Pf</i> TrxR IC-50 $\mu$ M	<i>Pf</i> GR IC-50 $\mu$ M	<i>H. GR</i> IC-50 $\mu$ M	<i>Pf</i> K1 IC-50 $\mu$ g/mL	Cytotoxicity L6 IC-50 $\mu$ g/mL
Yohimbine	40	> 169.3	> 169.3	> 169.3	7.25	34.2
Catharanthine	47	> 178.3	> 178.3	> 178.3	0.996	3.35
11-(OH)- Coronaridine	0	> 169.3	> 169.3	> 169.3	2.98	> 10
Quinidine N-oxide	0	> 176.3	> 176.3	> 176.3	5.69	> 100
Hernagine	46	95.4	91.6	98.6	3.63	> 10
Vobasine	28.7	90.7	85.1	89.7	1.54	12.2
Hispolone	30	> 272.7	59.1	59.1	2.78	2.75
Gnetifolin E	27	> 142.7	40.04	52.3	31.65	24.5
Chloroquine					0.089	
Podophyllotoxin						0.009

For antiplasmodial, we are using the following activity criteria: - Compounds with  $IC_{50} < 0.5$   $\mu$ g/ml are active. If a compound shows  $IC_{50} < 0.2$   $\mu$ g/ml and selectivity index ( $IC_{50}$  L6 cells/  $IC_{50}$  parasite)  $> 100$  it qualifies for in vivo testing. Compounds with  $IC_{50}$  0.5 – 5  $\mu$ g/ml are moderate active. Compounds with  $IC_{50} > 5$   $\mu$ g/ml are inactive.

## 5.5 Conclusions

In this study, tools for the identification of *Pf*TrxR using mass spectrometry, phenotypic screening and docking studies has been developed and validated for their potential use for

antimalarial drug discovery project. The *in vitro* antiplasmodial activity of five known inhibitors and curcuminoids was reported for the first time in this work. From our experiments it was also evident that curcumin selectively inhibits mammalian TrxR and not *Pf*TrxR owing to the differences in active sites of these two enzymes. Even though the eight natural products displayed binding affinity towards *Pf*TrxR, they failed to inhibit *Pf*TrxR when tested in the LC-MS based *Pf*TrxR functional assay. However, five natural products (catharanthine, 11-(OH)-coronaridine, hernagine, vobasine and hispolone) displayed moderate antimalarial activity when tested *in vitro* against *P. falciparum*.

## 5.7 References

1. K. Becker, Y. Hu, N. Biller-Andorno. Infectious diseases - a global challenge. *Int. J. Med. Microbiol.* **2008**, 296, 179-185.
2. J. Sachs, P. Malaney. The economic and social burden of malaria. *Nature.* **2002**, 415, 680-685.
3. World malaria report. WHO. **2012**. Factsheet 2012.
4. S. Müller. Thioredoxin reductase and glutathione synthesis in *Plasmodium falciparum*. *Redox Rep.* **2003**, 8(5), 251–5.
5. S. Müller, T. W. Gilberger, Z. Krnajski, K. Lüersen, S. Meierjohann, R. D. Walter. Thioredoxin and glutathione system of malaria parasite *Plasmodium falciparum*. *Protoplasma.* **2001**, 217, 43–49.
6. F. Nosten, N. J. White. Artemisinin-based combination treatment of *falciparum* malaria. *Am. J. Trop. Med. Hyg.* **2007**, 77 (6), 181–192.
7. E. Guantai, K. Chibale. How can natural products serve as a viable source of lead compounds for the development of new/novel anti-malarials? *Malaria J.* **2011**, 10, S2-S8.
8. S. N. Savvides, P. A. Karplus. Kinetics and crystallographic analysis of human glutathione reductase in complex with a xanthene inhibitor. *J. Biol. Chem.* **1996**, 271, 8101-8107.
9. P. A. Karplus, E. F. Pai, G. E. Schulz. Crystallographic study of the glutathione binding site of glutathione reductase at 0.3-nm resolution. *Eur. J. Biochem.* **1989**, 178, 693–703.
10. A. Schönleben-Janás, P. Kirsch, P. R. Mittl, R. H. Schirmer, R. L. Krauth-Siegel. Inhibition of human glutathione reductase by 10-arylisalloxazines: crystalline, kinetic, and electrochemical studies. *J. Med. Chem.* **1996**, 39, 1549–1554.

11. K. Becker, R. I. Christopherson, W. B. Cowden, N. H. Hunt, R. H. Schirmer. Flavin analogs with antimalarial activity as glutathione reductase inhibitors. *Biochem. Pharmacol.* **1990**, 39, 59–65.
12. G. Boumis, G. Giardina, F. Angelucci, A. Bellelli, M. Brunori, D. Dimastrogiovanni, F. Saccoccia, A. E. Miele. Crystal structure of *Plasmodium falciparum* thioredoxin reductase, a validated drug target. *Biochem. Biophys. Res. Commun.* **2012**, 425, 806-811.
13. G. N. Sarma, S. N. Savvides, K. Becker, M. Schirmer, R. H. Schirmer, P. A. Karplus. Glutathione reductase of the malarial parasite *Plasmodium falciparum*: crystal structure and inhibitor development. *J. Mol. Biol.* **2003**, 328, 893-907.
14. R. Munigunti, A. I. Calderón. Development of liquid chromatography/mass spectrometry based screening assay for PfTrxR inhibitors using relative quantitation of intact thioredoxin. *Rapid Commun. Mass Spectrom.* **2012**, 26, 1-6.
15. V. Mulabagal, A. I. Calderón. Development of binding assays to screen ligands for *Plasmodium falciparum* thioredoxin and glutathione reductases by ultrafiltration and liquid chromatography/mass spectrometry. *J. Chromatogr. B.* **2010**, 878, 987-993.
16. S. M. Kanzok, R. H. Schirmer, I. Turbachova, R. Iozef, K. Becker. The Thioredoxin system of the malaria parasite *Plasmodium falciparum*. *J. Biol. Chem.* **2000**, 275, 40180-40186.
17. M. M. Bradford. A rapid and sensitive method for the quantitation of microgram quantities of proteins utilizing the principle of protein-dye binding. *Anal. Biochem.* **1976**, 72, 248-254.
18. I. Orhan, B. Şener, M. Kaiser, R. Brun, D. Tasdemir. Inhibitory activity of marine sponge-derived natural products against parasitic protozoa. *Mar. Drugs.* **2010**, 8, 47-58.

19. M. T. Makler, D. J. Hinrichs. Measurement of the lactate dehydrogenase activity of *Plasmodium falciparum* as an assessment of parasitemia. *Am. J. Trop. Med. Hyg.* **1993**, 48, 205-210.
20. H. Babich, E. Borenfreund. Cytotoxicity of T-2 toxin and its metabolites determined with the neutral red cell viability assay. *Appl. Environ. Microbiol.* **1991**, 57(7), 2101-2103.
21. M. L. Sivilotti. Oxidant stress and haemolysis of the human erythrocyte. *Toxicol. Rev.* **2004**, 23, 169-188.
22. S. Ganesan, N. D. Chaurasiya, R. Sahu, L. A. Walker, B. L. Tekwani. Understanding the mechanisms for metabolism-linked hemolytic toxicity of primaquine against glucose 6-phosphate dehydrogenase deficient human erythrocytes: evaluation of eryptotic pathway. *Toxicology.* **2012**, 294(1), 54-60.
23. O. Trott, A. J. Olson. AutoDockVina: improving the speed and accuracy of docking with a new scoring function, efficient optimization and multithreading. *J. Comput. Chem.* **2010**, 31, 455-461.
24. K. Fritz-Wolf, S. Kehr, M. Stumpf, S. Rahlfs, K. Becker. Crystal structure of the human thioredoxin reductase-thioredoxin complex. *Nat. Commun.* **2011**, 2, 383-383.
25. G. M. Morris, R. Huey, W. Lindstrom, M. F. Sanner, R. K. Belew, D. S. Goodsell, A. J. Olson. AutoDock4 and AutoDockTools4: Automated docking with selective receptor flexibility. *J. Comput. Chem.* **2009**, 30, 2785-2791.
26. The PyMOL molecular graphics system, Version 1.5.0.4, Schrödinger, LLC.
27. M. P. Repasky, J. Chandrasekhar, W. L. Jorgensen. PDDG/PM3 and PDDG/MNDO: Improved semiempirical methods. *J. Comput. Chem.* **2002**, 23, 1601-1622.

28. I. Tubert-Brohman, C. R. W. Guimarães, M. P. Repasky, W. L. Jorgensen. Extension of the PDDG/PM3 and PDDG/MNDO semiempirical molecular orbital methods to the halogens. *J. Comput. Chem.* **2003**, 25, 138-150.
29. I. Tubert-Brohman, C. R. W. Guimarães, W. L. Jorgensen. Extension of the PDDG/PM3 Semiempirical molecular orbital method to sulfur, silicon, and phosphorus. *J. Chem. Theory Comput.* **2005**, 1, 817-823.
30. B. Hess, C. Kutzner, D.v. d. Spoel, E. Lindahl. GROMACS 4: Algorithms for highly efficient, load-balanced, and scalable molecular simulation, *J. Chem. Theory Comput.* **2008**, 4, 435–447.
31. S. N. Savvides, P. A. Karplus. Kinetics and Crystallographic Analysis of Human Glutathione Reductase in Complex with a Xanthene Inhibitor. *J. Biol. Chem.* **1996**, 271, 8101–8107.
32. D. M. Kasozi, S. Gromer, H. Adler, K. Zocher, S. Rahlfs, S. Wittlin, K. Fritz-Wolf, R. H. Schirmer, K. Becker. The bacterial redox signaller pyocyanin as an antiplasmodial agent: comparisons with its thioanalog methylene blue. *Redox Rep.* **2011**, 16(4), 154-65.
33. D. Andricopulo, M. B. Akoachere, R. Krogh, C. Nickel, M. J. McLeish, G. L. Kenyon, L. D. Arscott, C. H. Williams, E. Davioud-Charvet, K. Becker. Specific inhibitors of *Plasmodium falciparum* thioredoxin reductase as potential antimalarial agents. *Bioorg. Medicinal Chem. Lett.* **2006**, 16, 2283–2292.
34. E. D. Charvet, M. J. McLeish, D. M. Veine, D. Giegel, L. D. Arscott, A. D. Andricopulo, K. Becker, S. Müller, R. H. Schirmer, C. H. Williams, G. L. Kenyon. Mechanism-based inactivation of thioredoxin reductase from *Plasmodium falciparum* by Mannich bases. Implication for cytotoxicity. *Biochemistry.* **2003**, 42, 13319–13333.

35. T. Morin, J. C. Besset, M. Moutet, M. Fayolle, D. Bruckner, K. Limosin, E. Becker, E. Davioud-Charvet. The aza-analogues of 1, 4-naphthoquinones are potent substrates and inhibitors of *Plasmodial* thioredoxin and glutathione reductases and of human erythrocyte glutathione reductase. *Org. Biomol. Chem.* **2008**, 6, 2731-2742.
36. Y. Shang, C. Chen, Y. Li, J. Zhao, T. Zhu. Hydroxyl radical generation mechanism during the redox cycling process of 1,4-naphthoquinone. *Environ. Sci. Technol.* **2012**, 46 (5), 2935–2942.
37. T. Müller, L. Johann, B. Jannack, M. Brückner, D. A. Lanfranchi, H. Bauer, C. Sanchez, V. Yardley, C. Deregnaucourt, J. Schrével, M. Lanzer, R. H. Schirmer, E. Davioud-Charvet. Glutathione reductase-catalyzed cascade of redox reactions to bioactivate potent antimalarial 1,4-naphthoquinones - A new strategy to combat malarial parasites. *J. Am. Chem. Soc.* **2011**, 133, 11557–11571.
38. P. A. Karplus, G. E. Schulz. Substrate binding catalysis by *Glutathione reductase* as derived from derived enzyme: Substrate crystal structures at 2 Å resolution. *J. Mol. Biol.* **1989**, 210, 163-180.
39. J. Fang, J. Lu, A. Holmgren. Thioredoxin reductase is irreversibly modified by Curcumin. *J. Biol. Chem.* **2005**, 280, 25284-25290.
40. S. Mishra, K. Karmoiya, N. Surolia. Synthesis and expolartion of novel curcumin analogues as antimalarial agents. *Bioorg. Med. Chem.* **2008**, 16(6), 2894-2902
41. S. K. Sandur, M. K. Pandey, B. Sung, K. S. Ahn, A. Murakami, G. Sethi, P. Limtrakul, V. Badmaev, B. B. Aggarwal. Curcumin, demethoxycurcumin, bisdemethoxycurcumin, tetrahydrocurcumin and turmerones differentially regulate anti-inflammatory and anti-

proliferative responses through a ROS-independent mechanism. *Carcinogenesis*. 2007, 28, 1765–1773.